

SORPTIVE REMOVAL OF ARSENIC FROM DRINKING WATER

A DISSERTATION

*Submitted in partial fulfilment of the
requirements for the award of the degree*

of

MASTER OF TECHNOLOGY

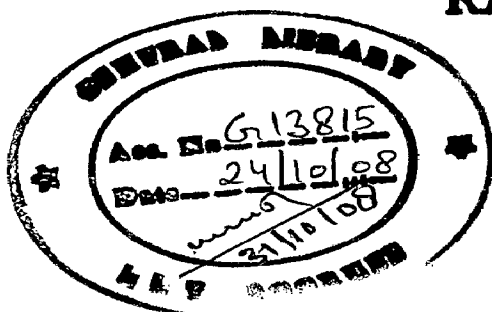
in

CHEMICAL ENGINEERING

(With Specialization in Computer Aided Process Plant Design)

By

RAVI KIRAN VISSA



**DEPARTMENT OF CHEMICAL ENGINEERING
INDIAN INSTITUTE OF TECHNOLOGY ROORKEE
ROORKEE -247 667 (INDIA)
JUNE, 2008**



INDIAN INSTITUTE OF TECHNOLOGY ROORKEE
ROORKEE

CANDIDATE'S DECLARATION

I hereby declare that the work which is being presented in the dissertation report entitled **SORPTIVE REMOVAL OF ARSENIC FROM DRINKING WATER** in partial fulfillment of the requirements for the award of the degree **Master of Technology** with specialization in **Computer Aided Process Plant Design**, to the **Department of Chemical Engineering, Indian Institute of Technology Roorkee, Roorkee** is an authentic record of my own work carried out during a period from July 2007 to June 2008 under the supervision of **Dr. I.M. Mishra**, Professor, Chemical Engineering Department, Indian Institute of Technology Roorkee, Roorkee.


The matter presented in this thesis has not been submitted by me for the award of any other degree of this or any other Institute.

Place: Roorkee

Date: 30 June 2008


(RAVI KIRAN VISSA)

This is to certify that the above statement made by the candidate is correct to the best of my knowledge.


Dr. I. M. Mishra,
Professor,
Department of Chemical Engineering,
Indian Institute of Technology Roorkee,
Roorkee, Uttarakhand (India).

ACKNOWLEDGEMENTS

I express my deep sense of gratitude to Prof. I.M. Mishra, Department of Chemical Engineering, Indian Institute of Technology Roorkee, Roorkee, for his precious guidance, suggestions and supervision at every level of my dissertation. I am obliged forever for his kind inspiration, encouragement and wholehearted support without which it was not possible to complete my work.

I would like to take this opportunity to put on record my respects to Prof. Shri Chand, Head of the Department, for providing me various facilities during the course of the present work. My sincere thanks are also due to Prof. Surendra Kumar, Prof. I. D. Mall, Dr. B. Prasad, Dr. (Mrs.) Shashi Kumar, Dr. Vimal Chandra Srivastava, Dr. Kailash Wasewar, Department of Chemical Engineering, IIT, Roorkee for their kind assistance and encouragement.

I am thankful to Prof. Kailash Chandra, and Prof. A. K. Chaudhary of the Institute Instrumentation Centre for their generous assistance and facilitation in the analysis of the samples.

Special thanks are due to technical staff of the Department; Shri B. K. Arora, Shri Ayodhya Prasad Singh, Shri. Rajendra Bhatnagar, , Shri Jugendra Singh Chaudhary, Shri Satpal Singh, Shri Harbans Singh, Shri Tara Chand, Shri Bhagwan Pal Singh, Shri Bhag Singh, Shri Arun Kumar Chopra, Shri Vipin Ekka, Shri Arvind Kumar, who helped me during the course of my experimental work. Thanks are also due to Mr. Shadab Ali, Shri S.P. Singh, Mrs. Anuradha, Mr. Verma, Shri Sudesh and other ministerial staff of the Department of Chemical Engineering for their assistance.

I would deeply appreciate the encouragement and moral support of my parents and friends without which it was not possible for me to complete my research work.

I thank God for encouraging me in every possible way and providing me strength to withstand the adversities during my past years.

RAVI KIRAN VISSA

ABSTRACT

Consumption of arsenic and its compounds present in the drinking water causes many health problems. High arsenic concentrations have been reported in USA, China, Chile, Bangladesh, Taiwan, Mexico, Argentina, Poland, Canada, Hungary, Japan and India. Epidemiological studies suggest that there are significant health risks, including cancer, associated with prolonged exposure to elevated arsenic concentrations in drinking water even at quite low concentrations. Many removal processes have been in practice for the removal of arsenic from the aqueous solutions viz. adsorption, oxidation, microfiltration, coagulation, etc.

In the present study, iron-coated bagasse fly ash (BFA-Fe) and rice husk ash (RHA-Fe) have been used for the removal of arsenic from synthetic drinking water. The physico-chemical characterization of the adsorbents have been carried out using standard methods e.g. sieving, scanning electron microscopy (SEM), thermo-gravimetric analysis (TGA) and differential thermal analysis (DTA), FTIR spectroscopy, etc. Batch experiments were carried out to determine the effect of various factors such as contact time (t), initial concentration (C_0), pH, adsorbent dose (m) and temperature (T) on adsorption process. Results obtained from these studies have been analyzed by various kinetic and isotherm models. The removal efficiency of BFA-Fe was found to be more than that of RHA-Fe at its natural pH (6.3-6.5). Pseudo-first-order, pseudo-second-order, intraparticle diffusion models and Bangham models have been used to represent the kinetics of the sorption process. The sorption kinetics was best approximated by pseudo-second-order kinetic model. An increase in temperature induced a negative effect on the sorption process. Experimental equilibrium isotherm data have been analyzed using Langmuir, Freundlich, Temkin and Redlich-Peterson (R-P) isotherms, and their parameters have been determined by non-linear regression analysis. Error analysis has been carried out using various error functions. Freundlich isotherms, generally, well-represented the equilibrium adsorption of As onto BFA-Fe and RHA-Fe. Thermal degradation kinetics of spent adsorbents were carried out and found that they are stable upto 400 °C.

CONTENTS

ABSTRACT	i
CONTENTS	ii
LIST OF FIGURES	iv
LIST OF TABLES	vii
NOMENCLATURE	ix
Chapter I	
INTRODUCTION	1
1.1: General	1
1.2: Characteristics of Arsenic	3
1.3: Arsenic Removal Technologies	11
1.4: Baggase Fly Ash and Rice Husk Ash as Adsorbents	11
1.5: Objectives of the Present Study	14
Chapter II	
LITERATURE REVIEW	15
2.1: Adsorption of As(III) from Drinking Waters	15
2.2: Adsorption of As(V) from Drinking Waters	16
2.3: Adsorption of As(III), As(V) and its Compounds from Drinking Waters	17
2.4: Sorption of As by Iron Impregnated Adsorbents	22
Chapter III	
ADSORPTION FUNDAMENTALS	29
3.1: General	29
3.2: Physical Adsorption vs. Chemisorption	29
3.3: Adsorption Kinetics	30

3.4: Controlling Steps in Adsorption Process	34
3.5: Adsorption Isotherms	34
3.6: Factors Effecting Adsorption	38
3.7: Error Analysis	39
Chapter IV	41
EXPERIMENTAL PROGRAMME	
4.1: Materials	41
4.2: Adsorbent Characterization	42
4.3: Batch Experimental Programme	43
4.4: Analysis and Disposal of Spent Adsorbents	45
Chapter V	47
RESULTS AND DISCUSSION	
5.1: General	47
5.2: Characterization of Adsorbents	47
5.3: Batch Adsorption of Arsenic onto BFA-Fe and RHA-Fe	54
5.4: Adsorption Equilibrium Study	72
5.5: Estimation of Thermodynamic Parameters	81
5.6: Thermal Degradation Kinetics of the Spent Adsorbents	85
Chapter-VI	94
CONCLUSIONS AND RECOMMENDATIONS	
6.1: Conclusions	94
6.2: Recommendations	95
REFERENCES	96

LIST OF FIGURES

No.	TITLE	Page No.
5.2.1:	Photograph of FeCl ₃ coated BFA and RHA	48
5.2.2:	SEM of blank, As(III) and As(V) loaded BFA-Fe at 500X and 1000X, respectively	49
5.2.3:	SEM of blank As(III), and As(V) loaded RHA-Fe at 500X and 1000X, respectively	50
5.2.4:	EDAX spectra analysis of adsorbents before and after adsorption	51
5.2.5:	FTIR spectra of blank, As(III) and As(V) loaded BFA-Fe	53
5.2.6:	FTIR spectra of blank, As(III) and As(V) loaded RHA-Fe	53
5.3.1:	Effect of BFA-Fe dose on the removal of As(III) and As(V) ($C_0 = 100 \mu\text{g dm}^{-3}$, $pH_0 = 5.3$ and 5.5 for As(III) and As(V) respectively, $T = 303 \text{ K}$, $t = 5 \text{ h}$).	55
5.3.2:	Effect of RHA-Fe dose on the removal of As(III) and As(V) ($C_0 = 100 \mu\text{g dm}^{-3}$, $pH_0 = 5.3$ and 5.5 for As(III) and As(V) respectively, $T = 303 \text{ K}$, $t = 5 \text{ h}$)	55
5.3.3:	Effect of initial pH on the equilibrium uptake and % removal of As(III) and As(V) ($C_0 = 100 \mu\text{g dm}^{-3}$, $m = 3 \text{ g dm}^{-3}$, $T = 303 \text{ K}$, $t = 5 \text{ h}$, RPM = 150) by BFA-Fe	56
5.3.4:	Effect of initial pH on the equilibrium uptake and % removal of As(III) and As(V) ($C_0 = 100 \mu\text{g dm}^{-3}$, $m = 3 \text{ g dm}^{-3}$, $T = 303 \text{ K}$, $t = 5 \text{ h}$, RPM = 150) by RHA-Fe	56
5.3.5:	Effect of initial concentration on the removal of As(III) and As(V) ($m = 3 \text{ g dm}^{-3}$, $T = 303 \text{ K}$, $pH_0 = \text{Natural (6.3)}$, RPM = 150, Time = 5h) by BFA-Fe	58
5.3.6:	Effect of initial concentration on the removal of As(III) and As(V) ($m = 3 \text{ g dm}^{-3}$, $T = 303 \text{ K}$, $pH_0 = \text{Natural (6.5)}$, RPM = 150, Time = 5h) by RHA-Fe	58
5.3.7:	Effect of contact time on the removal of As(III) and As(V) ($C_0 = 100 \mu\text{g dm}^{-3}$, $m = 3 \text{ g dm}^{-3}$, $T = 303 \text{ K}$, $pH_0 = 6.3-6.5$, RPM = 150) by BFA-Fe and RHA-Fe	60
5.3.8:	Time versus percent removal plot for the removal of As(III) and As(V) by BFA-Fe. $T = 303 \text{ K}$, $C_0 = 100 \mu\text{g dm}^{-3}$, $m = 3 \text{ g dm}^{-3}$, RPM = 150.	60
5.3.9:	Time versus residual concentration plot for the removal of As(III) and As(V) by BFA-Fe. $T = 303 \text{ K}$, $C_0 = 100 \mu\text{g dm}^{-3}$, $m = 3 \text{ g dm}^{-3}$, RPM = 150	61

5.3.10: Time versus percent removal plot for the removal of As(III) and As(V) by RHA-Fe. $T = 303 \text{ K}$, $C_0 = 100 \mu\text{g dm}^{-3}$, $m = 3 \text{ g dm}^{-3}$, RPM = 150	61
5.3.11: Time versus residual concentration plot for the removal of As(III) and As(V) by RHA-Fe. $T = 303 \text{ K}$, $C_0 = 100 \mu\text{g dm}^{-3}$, $m = 3 \text{ g dm}^{-3}$, RPM = 150	62
5.3.12: Equilibrium adsorption isotherms at different temperatures for adsorption of As(III) onto BFA-Fe. ($pH_0 = 6.3$, $C_0 = 20-500 \mu\text{g dm}^{-3}$, $m = 3 \text{ g dm}^{-3}$)	63
5.3.13: Equilibrium adsorption isotherms at different temperatures for adsorption of As(V) onto BFA-Fe. ($pH_0 = 6.5$, $C_0 = 20-500 \mu\text{g dm}^{-3}$, $m = 3 \text{ g dm}^{-3}$)	63
5.3.14: Equilibrium adsorption isotherms at different temperatures for adsorption of As(III) onto RHA-Fe. ($pH_0 = 6.3$, $C_0 = 20-500 \mu\text{g dm}^{-3}$, $m = 3 \text{ g dm}^{-3}$)	64
5.3.15: Equilibrium adsorption isotherms at different temperatures for adsorption of As(V) onto RHA-Fe. ($pH_0 = 6.5$, $C_0 = 20-500 \mu\text{g dm}^{-3}$, $m = 3 \text{ g dm}^{-3}$)	64
5.3.16: Time versus q_t (experimental and calculated) plot for the removal of As(III) and As(V) by BFA-Fe. $T = 303 \text{ K}$, $C_0 = 100 \mu\text{g dm}^{-3}$, $m = 3 \text{ g dm}^{-3}$	67
5.3.17: Time versus q_t (experimental and calculated) plot for the removal of As(III) and As(V) by RHA-Fe. $T = 303 \text{ K}$, $C_0 = 100 \mu\text{g dm}^{-3}$, $m = 3 \text{ g dm}^{-3}$	67
5.3.18: Weber and Morris intra-particle diffusion plot for the removal of As(III) and As(V) by BFA-Fe. $T = 303 \text{ K}$, $C_0 = 100 \mu\text{g dm}^{-3}$, $m = 3 \text{ g dm}^{-3}$	69
5.3.19: Weber and Morris intra-particle diffusion plot for the removal of As(III) and As(V) by RHA-Fe. $T = 303 \text{ K}$, $C_0 = 100 \mu\text{g dm}^{-3}$, $m = 3 \text{ g dm}^{-3}$	69
5.3.20: Bangham plot for the removal of As(III) and As(V) by BFA-Fe. $T = 303 \text{ K}$, $C_0 = 100 \mu\text{g dm}^{-3}$, $m = 3 \text{ g dm}^{-3}$	71
5.3.21: Bangham plot for the removal of As(III) and As(V) by RHA-Fe. $T = 303 \text{ K}$, $C_0 = 100 \mu\text{g dm}^{-3}$, $m = 3 \text{ g dm}^{-3}$	71
5.3.22: F(t) plot for the determination of effective pore diffusivity (D_e) of As(III) and As(V) by BFA-Fe. $T = 303 \text{ K}$, $C_0 = 100 \mu\text{g dm}^{-3}$, $m = 3 \text{ g dm}^{-3}$	73
5.3.23: F(t) plot for the determination of effective pore diffusivity (D_e) of As(III) and As(V) by RHA-Fe. $T = 303 \text{ K}$, $C_0 = 100 \mu\text{g dm}^{-3}$, $m = 3 \text{ g dm}^{-3}$	73

5.5.1: Van't Hoff plot for the adsorption of As(III) onto BFA-Fe	83
5.5.2: Van't Hoff plot for the adsorption of As(V) onto BFA-Fe	83
5.5.3: Van't Hoff plot for the adsorption of As(III) onto RHA-Fe	84
5.5.4: Van't Hoff plot for the adsorption of As(V) onto RHA-Fe	84
5.6.1: TGA analysis of (a) Blank, (b) As(III) and (c) As(V) loaded BFA-Fe in the air atmosphere	90
5.6.2: TGA analysis of (a) Blank, (b) As(III) and (c) As(V) loaded RHA-Fe in the air atmosphere	91
5.6.3: TGA analysis of (a) Blank, (b) As(III) and (c) As(V) loaded BFA-Fe in the Nitrogen atmosphere	92
5.6.4: TGA analysis of (a) Blank, (b) As(III) and (c) As(V) loaded RHA-Fe in the Nitrogen atmosphere	93

LIST OF TABLES

No.	TITLE	Page No.
1.1.1:	Percent of population without access to drinking water in various parts of the world	2
1.1.2:	Percent of population without access to safe drinking water in Asian continent	3
1.2.1:	Characteristics of arsenic	5
1.2.2:	Properties of arsenic	6
1.2.3:	Countries affected by arsenic contamination and maximum with permissible limits for drinking water	9
1.3.1:	Comparison of major arsenic removal technologies	12-13
2.1.1:	Literature review on adsorption of As(III) by various adsorbents	16
2.2.1:	Literature review on adsorption of As(V) by various adsorbents	18
2.3.1:	Literature review on adsorption of As(III) and As(V) by various adsorbents	21
2.4.1:	Literature review on adsorption of arsenic by metal impregnated adsorbents	27-28
3.2.1:	Comparison of physical and chemical adsorption	30
5.2.1:	Physical characteristics of adsorbents	47
5.2.2:	Elemental composition of adsorbents before adsorption	52
5.3.1:	Effect of initial pH of As on % Removal	57
5.3.2:	Kinetic parameters for the removal of As(III) and As(V) by BFA-Fe and RHA-Fe	68
5.3.3:	Comparison of effective pore diffusivities of As(III) and As(V) for BFA-Fe and RHA-Fe	72
5.4.1:	Isotherm parameters for the adsorption of As(III) onto BFA-Fe at different Temperatures	75
5.4.2:	Isotherm parameters for the adsorption of As(V) onto BFA-Fe at different Temperatures	76
5.4.3:	Isotherm parameters for the adsorption of As(III) onto RHA-Fe at different Temperatures	77

5.4.4: Isotherm parameters for the adsorption of As(V) onto RHA-Fe at different Temperatures	78
5.4.5: Error analyses functions for adsorption of As(III) and As(V) onto BFA-Fe	79
5.4.6: Error analyses functions for adsorption of As(III) and As(V) onto RHA-Fe	80
5.5.1: Thermodynamic parameters for the sorption of As(III) and As(V) onto BFA-Fe	82
5.5.2: Thermodynamic parameters for the sorption of As(III) and As(V) onto RHA-Fe.	82
5.6.1: DTA for the blank and loaded adsorbents in the air and nitrogen atmosphere at flow rate 200 ml min ⁻¹	87
5.6.2: Thermal degradation characteristics of blank and loaded adsorbents in air and nitrogen atmosphere at a flow rate of 200 ml min ⁻¹	88
5.6.3: Distribution of volatiles released during thermal degradation of blank and loaded adsorbents in an air and nitrogen atmosphere at a flow rate of 200 ml min ⁻¹	89

INDIAN INSTITUTE OF TECHNOLOGY ROORKEE

ROORKEE - 247 667

No. ACD/ *19* /A-184

Date

30/6/08

Prof. & Head

Chief Off

Enclosed please find herewith *3* copies of dissertation

Submitted by Shri/ Ms. *Ravi Kiran Vissu* for the degree of

M.Tech./ M.Arch./ M.U.R.P./ M.Phil. in the field of *CAPP*

(Batch *2006-07*) for further necessary action at your end please.

Copies of dissertation of above student have been checked and found correct.

Encl. : As Above

[Signature]
For ASSTT. REGISTRAR(ACD.)

NOMENCLATURE

ABBREVIATIONS

As	Arsenic
ARE	Average relative error
BFA	Bagasse fly ash
DTA	Differential thermal analysis
DTG	Differential thermal gravimetry
EDAX	Energy dispersive X-ray analysis
FTIR	Fourier transform infrared spectroscopy
HYBRID	Hybrid fractional error function
ICP-MS	Inductively coupled plasma mass spectrometer
MPSD	Marquardt's percent standard deviation
RHA	Rice husk ash
SAE	Sum of absolute error
SEM	Scanning electron micrograph
SSE	Sum of squares of error
TG	Thermal gravimetry
TGA	Thermo-gravimetric analysis
US EPA	United States Environmental Protection Agency

NOTATIONS

b	Temkin isotherm constant
C_0	Initial concentration of adsorbate in solution, $\mu\text{g dm}^{-3}$
C_e	Equilibrium liquid phase concentration, $\mu\text{g dm}^{-3}$
C_0	Initial concentration of adsorbate in solution, $\mu\text{g dm}^{-3}$

D_e	Effective diffusion coefficient of adsorbate in the adsorbent phase, $m^2 s^{-1}$
h	Initial sorption rate, $\mu g g^{-1} min^{-1}$
k_{0B}	Constant in Bangham equation, g
k_A	Adsorption rate constant for the adsorption equilibrium, min^{-1}
k_D	Desorption rate constant for the adsorption equilibrium, min^{-1}
k_f	Rate constant of pseudo-first-order adsorption model, min^{-1}
k_{int}	Intra-particle diffusion rate constant, $\mu g g^{-1} min^{-1/2}$
k_S	Rate constant of pseudo-second-order adsorption model, $g \mu g^{-1} min$
K_F	Constant of Freundlich isotherm, $(\mu g g^{-1}) (dm^3 \mu g^{-1})^{-1/n}$
K_L	Constant of Langmuir isotherm, $dm^3 \mu g^{-1}$
K_R	Constant of Redlich-Peterson isotherm, $g dm^{-3}$
K_L	Constant of Langmuir isotherm, $dm^3 mg^{-1}$
m	Mass of adsorbent per liter of solution, $g dm^{-3}$
n	Number of data points
p	Number of parameters in the isotherms
pH_0	Initial pH of the solution
q_e	Equilibrium single-component solid phase concentration, $\mu g g^{-1}$
$q_{e,cal}$	Calculated value of solid phase concentration of adsorbate at equilibrium, $\mu g g^{-1}$
$q_{e,exp}$	Experimental value of solid phase concentration of adsorbate at equilibrium, $\mu g g^{-1}$
q_m	Maximum adsorption capacity of adsorbent, $\mu g g^{-1}$
q_t	Amount of adsorbate adsorbed by adsorbent at time t , $\mu g g^{-1}$
t	Time, min
T	Absolute temperature, K
V	Volume of the solution, dm^3
w	Mass of the adsorbent, g
X_{Ae}	Fraction of the adsorbate adsorbed on the adsorbent under equilibrium
ΔG_{ads}^0	Gibbs free energy change of the adsorption process, $kJ mol^{-1}$
ΔH^0	Enthalpy change, $kJ mol^{-1}$

ΔS^0	Entropy change, $\text{kJ mol}^{-1} \text{K}^{-1}$
$1/n$	Mono-component (non-competitive) Freundlich heterogeneity factor of the single component
a_R	Constant of Redlich-Peterson isotherm, $\text{dm}^3 \mu\text{g}^{-1}$
C_s	Adsorbent concentration in solution $\mu\text{g dm}^{-3}$
B_T	Temkin isotherm constant, related to the heat of adsorption, J mol^{-1}
I	Weber-Morris constant that gives idea about the thickness of boundary layer, $\mu\text{g g}^{-1}$
k_A	Adsorption rate constant
k_D	Desorption rate constant
R	Universal gas constant, $8.314 \text{ J K}^{-1} \text{ mol}^{-1}$

GREEK LETTERS

α	Constant used in Bangham equation
β	Constant used in Redlich-Peterson equation

INTRODUCTION

1.1 GENERAL

Water is a common chemical substance that is essential for the survival of all known forms of life. Water fit for human consumption is called drinking water or potable water. Currently, about 1 billion people around the world routinely drink unhealthy water. Poor water quality and bad sanitation are deadly; some 5 million deaths a year are caused by polluted drinking water. Water, however, is not a finite resource (like petroleum is), but rather re-circulated as potable water in precipitation in quantities many degrees of magnitude higher than human consumption. Therefore, it is the relatively small quantity of water in reserve in the earth (about 1% of our drinking water supply, which is replenished in aquifers around every 1 to 10 years), that is a non-renewable resource, and it is, rather, the distribution of potable and irrigation water which is scarce, rather than the actual amount of it that exists on the earth. Organizations concerned in water protection include International Water Association (IWA), Water Aid, Water 1st, American Water Resources Association. Water related conventions are United Nations Convention to Combat Desertification (UNCCD), International Convention for the Prevention of Pollution from Ships, United Nations Convention on the Law of the Sea and Ramsar Convention.

Parameters for drinking water quality typically fall under two categories: chemical/physical and microbiological. Chemical/physical parameters include heavy metals, trace organics, total suspended solids (TSS), and turbidity. Microbiological parameters include Coliform bacteria, E. coli, and specific pathogenic species of bacteria (such as cholera-causing *Vibrio cholerae*), viruses, and protozoan parasites. (http://en.wikipedia.org/wiki/Drinking_water)

Chemical parameters tend to pose more of a chronic health risk through buildup of heavy metals although some components like nitrates/nitrites and arsenic may have a more immediate impact. Physical parameters affect the aesthetics and taste of the drinking water and may complicate the removal of microbial pathogens.

In 1990, the challenge of ensuring universal access to safe drinking water by 2000 meant reaching 1.2 billion people, or 23 per cent of the world's population, with clean, sustainable water supplies. This challenge remained despite the gains made during the International Drinking Water Supply and Sanitation Decade (1981-1990).

According to UNICEF census in the year 2000, 1.1 billion people are still without access to safe drinking water and percentage contribution of the various parts of the world is given in Table 1.1.1 (Source: www.unicef.org/specialsession/about/sgreport.pdf /03_SafeDrinkingWater.)

Table 1.1.1 Percent of population without access to drinking water in various parts of the world (Total = 1.1 billion)

Region	Percent of population with out access to safe drinking water
Middle East/ North Africa	4%
CEE/CIS	4%
Latin America/Caribbean	6%
South Asia	19%
Sub-Saharan Africa	25%
East Asia/Pacific	42%

Table 1.1.2 illustrates the comparison of the percentage of population without access to safe drinking water in the Asian continent. (Source: http://en.wikipedia.org/wiki/Drinking_water)

Table 1.1.2 Percent of population without access to safe drinking water in Asian continent

Country	Percent of population with out access to safe drinking water	
	1990	2000
Bangladesh	6	3
Pakistan	17	10
Nepal	33	12
India	32	16
Sri Lanka	32	23
Bhutan	-	38
Afghanistan	Not Specified	87

1.2 CHARACTERISTICS OF ARSENIC

Arsenic is a naturally occurring chemical found in the earth's crust, but can be dangerous to humans when released into drinking water supplies when rocks, minerals, and soil erode. Arsenic (atomic number 33) is ubiquitous and ranks 20th in natural abundance, comprising about 0.00005% of the earth's crust, 14th in the seawater, and 12th in the human body. It's concentration in most rocks ranges from 0.5 to 2.5 mg kg⁻¹, though higher concentrations are found in finer grained argillaceous sediments and phosphorites. It is a silver-grey brittle crystalline solid with atomic weight 74.9; specific gravity 5.73, melting point 817°C (at 28 atm), boiling point 613°C and vapor pressure 1mm Hg at 372°C, (Mohan and Pittman Jr., 2007).

Since its isolation in 1250 A.D. by Albertus Magnus, this element has been a continuous center of controversy. Studies have linked long-term exposure to arsenic contamination with cancer and cardiovascular, pulmonary, immunological, neurological and endocrine effects. (http://en.wikipedia.org/wiki/Arsenic_poisoning) Arsenic (As)

contamination of drinking water is a major health concern, because drinking arsenic contaminated water is linked to several types of cancers. Long-term uptake of arsenic contaminated water causes liver, lung, kidney, bladder, skin and nerve tissue injuries. The characteristics of arsenic are presented in Table 1.2.1.

This is a notoriously poisonous metalloid that has many allotropic forms: yellow (molecular non-metallic) and several black and gray forms (metalloids) are a few that are seen. Three metalloidal forms of arsenic with different crystal structures are found free in nature. But, it is more commonly found as arsenide and arsenate compounds. Several hundred such mineral species are known. Arsenic and its compounds are used as pesticides, herbicides, insecticides and various alloys. A brief outline of arsenic and its properties are given in Table 1.2.2.

1.2.1 Notable characteristics

The most common oxidation states for arsenic are -3 (arsenides: usually alloy-like intermetallic compounds), +3 (arsenates(III) or arsenites, and most organoarsenic compounds), and +5 (arsenates(V): the most stable inorganic arsenic oxycompounds). Arsenic also bonds readily to itself, forming, for instance, As-As pairs in the red sulfide realgar and square As_4^{3-} ions in the arsenide skutterudite. In the +3 oxidation state, the stereochemistry of arsenic is affected by possession of a lone pair of electrons. (<http://en.wikipedia.org/wiki/Arsenic>).

Arsenic is very similar chemically to its predecessor, phosphorus. Like phosphorus, it forms colourless, odourless, crystalline oxides As_2O_3 and As_2O_5 which are hygroscopic and readily soluble in water to form acidic solutions. Arsenic (V) acid, like phosphoric acid, is a weak acid. Like phosphorus, arsenic forms an unstable, gaseous hydride: arsine (AsH_3). The similarity is so great that arsenic will partly substitute for phosphorus in biochemical reactions and is thus poisonous. However, in subtoxic doses, soluble arsenic compounds act as stimulants, and were once popular in small doses as medicinals by people in the mid 18th century.

Table 1.2.1 Characteristics of Arsenic

Atomic Number	33
Symbol	As
Atomic Weight	74.9216 g mol ⁻¹
Physical state (at 20°C and 1 atm)	Solid
Density	5.727 g cm ⁻³ at 14°C
Melting point	817°C (28 atm)
Boiling point	614°C (sublimation)
Critical temperature	1400°C
Vanderwaals radius	0.185 nm
Ionic radius	0.222 nm (-2) 0,047 nm (+5) 0,058 (+3)
Isotopes	8
Electronic shell	[Ar] 3d ¹⁰ 4s ² 4p ³
Energy of first ionisation	947 kJ mol ⁻¹
Energy of second ionisation	1798 kJ mol ⁻¹
Energy of third ionisation	2735 kJ mol ⁻¹
Enthalpy of Atomization	301.3 kJ mol ⁻¹ @ 25°C
Enthalpy of Fusion:	24.44 kJ mol ⁻¹
Enthalpy of Vaporization	34.76 kJ mol ⁻¹

1.2.2 Occurrence

In 2005, China was the top producer of white arsenic with almost 50% world share followed by Chile and Peru, reports the British Geological Survey. Arsenopyrite also unofficially called mispickel (FeAsS) is the most common arsenic-bearing mineral. On roasting in air, the arsenic sublimes as arsenic (III) oxide leaving iron oxides.

Table 1.2.2 Properties of Arsenic

Discovery	Albertus Magnus 1250 and Schroeder published two methods of preparing elemental arsenic in 1649.
Properties	Arsenic has a valence of -3, 0, +3, or +5. The elemental solid primarily occurs in two modifications, though other allotropes are reported. Yellow arsenic has a specific gravity of 1.97, while gray or metallic arsenic has a specific gravity of 5.73. Gray arsenic is the usual stable form, with a melting point of 817°C (28 atm) and sublimation point at 613°C. Gray arsenic is a very brittle semi-metallic solid. It is steel-gray in color, crystalline, tarnishes readily in air, and is rapidly oxidized to arsenous oxide (As_2O_3) upon heating (arsenous oxide exudes the odor of garlic). Arsenic and its compounds are poisonous.
Uses	Arsenic is used as a doping agent in solid-state devices. Gallium arsenide is used in lasers which convert electricity into coherent light. Arsenic is used pyrotechny, hardening and improving the sphericity of shot, and in bronzing. Arsenic compounds are used as insecticides and in other poisons.
Sources	Arsenic is found in its native state, in realgar and orpiment as its sulfides, as arsenides and sulfarsenides of heavy metals, as arsenates, and as its oxide. The most common mineral is <i>Mispickel</i> or arsenopyrite (FeSAs), which can be heated to sublime arsenic, leaving ferrous sulfide.

The most important compounds of arsenic are arsenic (III) oxide, As_2O_3 , (white arsenic), the yellow sulfide orpiment (As_2S_3) and red realgar (As_4S_4), Paris Green, calcium arsenate, and lead hydrogen arsenate. The latter three have been used as agricultural insecticides and poisons. Orpiment and realgar were formerly used as painting pigments, though they have fallen out of use due to their toxicity and reactivity. Although arsenic is sometimes found native in nature, its main economic source is the mineral arsenopyrite mentioned above; it is also found in arsenides of metals such as

silver, cobalt (cobaltite, CoAsS and skutterudite, CoAs_3) and nickel, as sulfides, and when oxidised as arsenate minerals such as mimetite, $\text{Pb}_5(\text{AsO}_4)_3\text{Cl}$ and erythrite, $\text{Co}_3(\text{AsO}_4)_2 \cdot 8\text{H}_2\text{O}$, and more rarely arsenites, AsO_3^{3-} as opposed to arsenate (V), AsO_4^{3-}). In addition to the inorganic forms mentioned above, arsenic also occurs in various organic forms in the environment.

Inorganic arsenic and its compounds, upon entering the food chain, are progressively metabolised to a less toxic form of arsenic through a process of methylation. For example certain molds produce significant amounts of trimethylarsine if inorganic arsenic is present. The organic compound arsenobetaine is found in some marine foods such as fish and algae, and also in mushrooms in larger concentrations. The average person's intake is about 10-50 $\mu\text{g day}^{-1}$. (Source: <http://en.wikipedia.org/wiki/Arsenic>)

1.2.3 Toxicity

Arsenic and many of its compounds are especially potent poisons. Arsenic disrupts ATP production through several mechanisms. At the level of the citric acid cycle, arsenic inhibits pyruvate dehydrogenase and by competing with phosphate it uncouples oxidative phosphorylation, thus inhibiting energy-linked reduction of NAD^+ , mitochondrial respiration, and ATP synthesis. Hydrogen peroxide production is also increased, which might form reactive oxygen species and oxidative stress. These metabolic interferences lead to death from multi-system organ failure probably from necrotic cell death, not apoptosis. A post mortem reveals brick red colored mucosa, due to severe hemorrhage. Although arsenic causes toxicity, it can also play a protective role. Elemental arsenic and arsenic compounds are classified as "toxic" and "dangerous for the environment" in the European Union under directive 67/548/EEC. Council Directive 67/548/EEC of 27th June 1967 on the approximation of laws, regulations and administrative provisions relating to the classification, packaging and labelling of dangerous substances (as amended) is the main European Union law concerning chemical safety.

The IARC recognizes arsenic and arsenic compounds as group 1 carcinogens, and the EU lists arsenic trioxide, arsenic pentoxide and arsenate salts as category 1 carcinogens.

Arsenic is known to cause arsenicosis due to its manifestation in drinking water, “the most common species being arsenate [$HAsO_4^{2-}$, As(V)] and arsenite [H_3AsO_3 , As(III)]”. The ability of arsenic to undergo redox conversion between As(III) and As(V) makes its availability in the environment possible.

1.2.4 Arsenic in drinking water

Arsenic poisoning kills by allosteric inhibition of essential metabolic enzymes, leading to death from multi-system organ failure. It primarily inhibits enzymes that require lipoic acid as a cofactor, such as pyruvate and alpha-ketoglutarate dehydrogenase. Because of this, substrates before the dehydrogenase steps accumulate, such as pyruvate (and lactate). It particularly affects the brain, causing neurological disturbances and death.

Arsenic contamination of groundwater has led to a massive epidemic of arsenic poisoning in Bangladesh and neighbouring countries. It is estimated that approximately 57 million people are drinking groundwater with arsenic concentrations elevated above the World Health Organization's standard of 10 parts per billion. The arsenic in the groundwater is of natural origin, and is released from the sediment into the groundwater due to the anoxic conditions of the subsurface. This groundwater began to be used after western NGOs instigated a massive tube well drinking-water program in the late twentieth century. This program was designed to prevent drinking of bacterially contaminated surface waters, but failed to test for arsenic in the groundwater. Many other countries in South East Asia, such as Vietnam, Cambodia, and Tibet, China, are thought to have geological environments similarly conducive to generation of high-arsenic groundwaters. Arsenicosis was reported in Nakhon Si Thammarat, Thailand in 1987, and the dissolved arsenic in the Chao Phraya River is suspected of containing high levels of naturally occurring arsenic, but has not been a public health problem due to the use of bottled water. (http://en.wikipedia.org/wiki/Arsenic#Arsenic_in_drinking_water)

Analyzing multiple epidemiological studies on inorganic arsenic exposure suggests a small but measurable risk increase for bladder cancer at 10 parts per billion. According to Peter Ravenscroft, of the Department of Geography at the University of Cambridge roughly 80 million people worldwide consume between 10 and 50 parts per

billion arsenic in their drinking water. Countries affected by arsenic contamination and maximum with permissible limits for drinking water are given in Table 1.2.3.

Table 1.2.3 Countries affected by arsenic contamination and maximum with permissible limits for drinking water, (Mohan and Pittman Jr., 2007)

Country	Maximum permissible limits ($\mu\text{g dm}^{-3}$)	Country	Maximum permissible limits ($\mu\text{g dm}^{-3}$)
Argentina	50	Mexico	50
Bangladesh	50	Nepal	50
Cambodia	-	New Zealand	10
China	50	Taiwan	10
Chile	50	USA	10
India	10	Vietnam	10
Japan	-		

If they all consumed exactly 10 parts per billion arsenic in their drinking water, the previously cited multiple epidemiological study analysis would predict an additional 2,000 cases of bladder cancer alone. This represents a clear underestimate of the overall impact, since it does not include lung or skin cancer, and explicitly underestimates the exposure. Those exposed to levels of arsenic above the current WHO standard should weigh the costs and benefits of arsenic remediation.

Arsenic can be removed from drinking water through coprecipitation of iron minerals by oxidation and filtering. When this treatment fails to produce acceptable results, adsorptive arsenic removal media may be utilized. Several adsorptive media systems have been approved for point of service use in a study funded by the United States Environmental Protection Agency (U.S.EPA) and the National Science Foundation (NSF).

Magnetic separations of arsenic at very low magnetic field gradients have been demonstrated in point-of-use water purification with high-surface area and monodisperse magnetite (Fe_3O_4) nanocrystals. Using the high specific surface area of Fe_3O_4 nanocrystals the mass of waste associated with arsenic removal from water has been dramatically reduced.

1.2.5 Applications

Lead hydrogen arsenate was used well into the 20th century as an insecticide on fruit trees. Its use sometimes resulted in brain damage to those working the sprayers. In

the last half century, monosodium methyl arsenate (MSMA), a less toxic organic form of arsenic, has replaced lead arsenate's role in agriculture.

The application of most concern to the general public is probably that of wood treated with chromated copper arsenate, also known as CCA or Tanalith. The vast majority of older pressure-treated wood was treated with CCA. CCA lumber is still in widespread use in many countries, and was heavily used during the latter half of the 20th century as a structural and outdoor building material. It was commonly used in situations where rot or insect infestation was a possibility. Although the use of CCA lumber was banned in many areas after studies showed that arsenic could leach out of the wood into the surrounding soil (from playground equipment, for instance), a risk is also presented by the burning of older CCA timber. The direct or indirect ingestion of wood ash from burnt CCA lumber has caused fatalities in animals and serious poisonings in humans; the lethal human dose is approximately 20 gram of ash. Scrap CCA lumber from construction and demolition sites may be inadvertently used in commercial and domestic fires. Protocols for safe disposal of CCA lumber do not exist evenly throughout the world; there is also concern in some quarters about the widespread landfill disposal of such timber. (<http://en.wikipedia.org/wiki/Arsenic#Applications>)

During the 18th, 19th, and 20th centuries, a number of arsenic compounds have been used as medicines, including arsphenamine (by Paul Ehrlich) and arsenic trioxide (by Thomas Fowler). Arsphenamine as well as Neosalvarsan was indicated for syphilis and trypanosomiasis, but has been superseded by modern antibiotics. Arsenic trioxide has been used in a variety of ways over the past 200 years, but most commonly in the treatment of cancer. The US Food and Drug Administration in 2000 approved this compound for the treatment of patients with acute promyelocytic leukemia that is resistant to ATRA. It was also used as Fowler's solution in psoriasis.

Copper acetoarsenite was used as a green pigment known under many different names, including 'Paris Green' and 'Emerald Green'. It caused numerous arsenic poisonings.

Other uses;

- Various agricultural insecticides, termination and poisons.

- Used in animal feed, particularly in the US as a method of disease prevention and growth stimulation.
- Gallium arsenide is an important semiconductor material, used in integrated circuits. Circuits made using the compound are much faster (but also much more expensive) than those made in silicon. Unlike silicon it is direct band gap, and so can be used in laser diodes and LEDs to directly convert electricity into light.
- Also used in bronzing and pyrotechny.

1.3 ARSENIC REMOVAL TECHNOLOGIES

Several investigators have investigated the removal of arsenic using different methodologies for the removal of arsenic from aqueous solutions. The most commonly used technologies include oxidation, co-precipitation and adsorption onto coagulated flocs, lime treatment, adsorption onto sorptive media, ion exchange resin and membrane techniques. The major arsenic removal technologies are compared in Table 1.3.1. The major disadvantage of most of the techniques presented in Table 1.3.1 is that they are unable to remove As(III) efficiently.

1.4 BAGGASE FLY ASH AND RICE HUSK ASH AS ADSORBENTS

1.4.1 Baggase Fly Ash

Coal and baggase combustion produces a huge amount of by-product fly ash and bottom ash, whose disposal requires large quantities of land and water. Currently, fly ash applications are limited to civil engineering uses including cement and brick production and roadbeds. Bottom ash can also serve as an adsorbent. Resource recovery from coal fly ash is one of the most important issues in waste management worldwide. Since the major chemical compounds contained in fly ash are aluminosilicate, intensive efforts have been recently made to utilize this material as an adsorbent. Fly ash obtained from coal power stations was examined for As(V) removal from water and to restrict As(V) migration in the solid wastes or the soil (Wang et al., 2008). BFA has been used for the removal of various materials like pyridine and its derivatives (Lataye et al., 2008), phenol, malachite green dye (Srivastava et al., 2006a, Mall et al., 2005) etc.

Table 1.3.1 Comparison of Major Arsenic Removal Technologies (USEPA, 2000; Mohan and Pittman Jr., 2007; Parga et al., 2005, Jalil et al., 2000).

Major oxidation/precipitation technologies	Advantages	Disadvantages	% Removal
Oxidation/precipitation:			
Air oxidation (Dutta et al., 2005)	Relatively simple, low-cost but slow process; in situ arsenic removal; also oxidizes other inorganic and organic constituents in water.	Mainly removes arsenic(V) and accelerate the oxidation process.	80
Chemical oxidation, (Borho and Wilderer, 1996).	Oxidizes other impurities and kills microbes; relatively simple and rapid process; minimum residual mass.	Efficient control of the pH and oxidation step is needed.	90
Major coagulation/coprecipitation technologies	Advantages	Disadvantages	
Coagulation/electrocoagulation/coprecipitation:			
Alum coagulation	Durable powder chemicals are available; relatively low capital cost and simple in operation effective over a wider range of pH.	Produces toxic sludges; low removal of arsenic; pre-oxidation may be required.	90
Iron coagulation, (Ratna Kumar et al., 2004).	Common chemicals are available; more efficient than alum coagulation on weight basis	Medium removal of As(III); sedimentation and filtration needed.	94.5
Lime softening	Chemicals are available commercially	Readjustment of pH is required	91

Major sorption and ion-exchange technologies	Advantages	Disadvantages	% Removal
Sorption and ion-exchange techniques			
Activated alumina (Singh and Pan, 2003).	Relatively well known and commercially available	Needs replacement after four to five regeneration	88
Iron coated sand, (Gupta et al., 2005, Chang et al., 2008).	Cheap; no regeneration is required; remove both As(III) and As(V).	Not standardized; produces toxic solid waste.	93
Ion-exchange resin	Well-defined medium and capacity; pH independent; exclusive ion specific resin to remove arsenic	High cost medium; high-tech operation and maintenance; regeneration creates a sludge disposal problem; As(III) is difficult to remove; life of resins.	87
Major membrane technologies	Advantages	Disadvantages	
Membrane techniques:			
Nanofiltration, (Ballinas et al., 2004, Han et al., 2002).	Well-defined and high-removal efficiency.	Very high-capital and running cost, pre-conditioning; high water rejection.	95
Reverse osmosis, (Gholami et al., 2006).	No toxic solid waste is produced.	High tech operation and maintenance.	96
Electrodialysis, (Basha et al., 2008)	Capable of removal of other contaminants	Toxic wastewater produced	95

1.4.2 Rice Husk Ash

Rice husk is generally used for burning. Rice mills and other rural area based industries use it as a fuel in their boilers/furnaces. Some rice mills also use it as a fuel to produce producer gas. It is a low cost adsorbent which has been used for the removal of various materials like, metals like cadmium and zinc, etc. (Srivastava et al., 2008), pyridine and its derivatives (Lataye et al., 2008), dyes like Indigo Carmine, (Lakshmi et al., 2008) etc.

1.5 OBJECTIVES OF THE PRESENT STUDY

Open literature on the removal of arsenic by low-cost adsorbents such as bagasse fly ash and rice husk ash is scarce. In view of the literature survey and the necessity of developing a treatment process for removing arsenic from arsenic bearing drinking water, the following aims and objectives have been set for the present work.

1. To characterize the agri-based waste materials like bagasse fly ash (BFA), and rice husk ash (RHA) for their physico-chemical and adsorption properties. These characteristics include the analysis of particle size, proximate analysis and the surface and functional characteristics by FTIR and SEM analyses.
2. To use BFA and RHA as adsorbents for the treatment of the As bearing synthetic drinking waters.
3. To study the effect of various parameters like initial pH (pH_0), adsorbent dose (m), contact time (t), initial concentration (C_0), and temperature (T) on the removal of Arsenic from the aqueous solution in batch study.
4. To carry out kinetic and equilibrium adsorption and studies for the adsorption of arsenic onto both the adsorbents and to analyze the experimental data using various kinetic and isotherm models.
5. To carry out the error analysis for the various isotherms data obtained.
6. To understand the thermodynamics of adsorption for arsenic using BFA and RHA as adsorbents.
7. To carry out the thermal degradation of adsorbents before and after adsorption using TGA technique.

LITERATURE REVIEW

Adsorption is a simple and cost effective method for the removal of As. The critical review on the removal of As(III) and As(V) from drinking water by various adsorbents has been discussed in this chapter. The contents of this chapter include:

1. Adsorption of As(III) from drinking waters.
2. Adsorption of As(V) from drinking waters.
3. Adsorption of As(III), As(V) and its Compounds from drinking waters.
4. Sorption of As by metal impregnated adsorbents.

2.1 ADSORPTION OF AS(III) FROM DRINKING WATER

Ayoob et al. (2007) have evaluated the effectiveness of the adsorbent, modified calcined bauxite (MCB), in removing As(III) from aqueous environment by completely mixed batch reactor (CMBR) and continuous flow fixed bed studies. It was observed that an adsorbent dose of 5 g dm^{-3} could effectively remove 99.2% and 93.4% of As(III), from initial concentrations of 1 and 2 mg dm^{-3} , respectively. The sorption kinetics was found to follow pseudo-second-order model. Freundlich isotherm model was well fitted to the experimental equilibrium data rendering a maximum adsorption capacity of 1.362 mg g^{-1} . The sorption process was found unaffected by temperature variations. The removal of As(III) was observed almost consistent over a pH range of 2–8, producing effluent within pH range of 6–7.5. It appears that the mechanism of arsenic removal is dependent on pH, surface charge of the adsorbent and nature of the As(III) speciation.

Gupta et al. (2005) have elucidated the sorption kinetics of the removal of As(III) on iron oxide-coated and uncoated sand in batch and column experiments. They have compared the results of uncoated sand and coated sand and found that coated sand is efficient for the removal. They found the maximum adsorption of As(III) for coated sand is much higher ($28.57 \text{ } \mu\text{g g}^{-1}$) than that for uncoated sand ($5.63 \text{ } \mu\text{g g}^{-1}$) at pH 7.5 in 2 h. They have also done the column studies by varying the contact time, filtration rate, and bed depth on a 160 cm height and 2.54 cm ID column.

Singh and Pan (2003) have studied the Equilibrium, kinetics and thermodynamic studies for adsorption of As(III) on activated alumina. They studied the effect of adsorbent dose, solution pH, and contact time has been investigated. Their kinetics reveal that uptake of As(III) ion is very rapid in the first 6h and equilibrium time is independent of initial As(III) concentration. The arsenite removal was strongly dependent on pH and temperature. Both Freundlich and Langmuir adsorption isotherms were well fit to the experimental data. Thermodynamic parameters depict the exothermic nature of adsorption and the process is spontaneous and favourable.

Table 2.1.1 Literature review on adsorption of As-III by various adsorbents

Authors	Adsorbent	Batch/ Column	Parameters Studied
Ayoob et al. 2007	Modified calcined bauxite	Batch and Column	Removal efficiency, sorption kinetics, Equilibrium isotherms (Freundlich). Filtration rate, bed depth, contact time have also studied
Gupta et al. 2005	Iron coated sand	Batch and Column	Removal efficiency, sorption kinetics, Equilibrium isotherms (Langmuir).
Singh and Pan 2003	Activated alumina	Batch	Removal efficiency, sorption kinetics, Equilibrium isotherms (Langmuir and Freundlich).

2.2 ADSORPTION OF AS(V) FROM DRINKING WATERS

Wang et al. (2008) have studied the effect of arsenic leaching into the atmosphere by the coal fly ash, and tried for the removal of the arsenate using the washed fly ash. They found that the adsorption mechanism is a strict function of pH. When pH was less than 3 or greater than 7, it was observed that increasing amounts of arsenic were leached or desorbed from fly ash. Batch adsorption experiments were conducted to examine the adsorption behavior of As(V) onto NaOH washed ash. They have studied the effect of initial concentration, S/L ratio, where S: amount of dried raw ash, g; L: amount of deionized water.

Chutia et al. (2008) have elucidated the sorption studies of arsenate using Natural mordenite (NM), natural clinoptilolite (NC), HDTMA-modified natural mordenite (SMNM) and HDTMA-modified natural clinoptilolite (SMNC) from aqueous solution. They have studied the effect of contact time, initial pH, initial concentration. They have fit the kinetic data with the pseudo-first-order kinetic model for the initial stage of their sorption process. They have fit the Freundlich and Dubinin–Kaganer–Radushkevich (DKR) isotherm models for their isotherm data. They have also done the desorption studies using 0.1 M NaOH.

Investigations on arsenic(V) removal by modified calcined bauxite have been elucidated by (Bhakat et al., 2006). The adsorbent (modified calcined bauxite, MCB) exhibited excellent As(V) removal (99–100%) over a wide range of pH-2–8 in batch studies. The sorption kinetics were found to be the pseudo-second order model. The Langmuir, Freundlich and Dubinin–Radushkevich models were tried to represent the equilibrium data of As(V) adsorption. The sorption process was almost unaffected by temperature variations. During sorption, no appreciable ionic effects except from SO_4^{2-} and EDTA complex were observed from the background ions Ca^{2+} , Fe^{3+} , Cl^- , NO_3^- , PO_4^{3-} and F^- . They have conducted the column studies for different bed depths, flow rates.

Diamadopoulos et al. (1993) have examined the possible use of fly ash for the removal of As(V) from water. Kinetic and equilibrium experiments were performed in order to evaluate the removal efficiency of lignite-based fly ash. They have studied the effect of pH on the adsorption and desorption of As(V) onto fly ash.

2.3 ADSORPTION OF AS(III), AS(V) AND ITS COMPOUNDS FROM DRINKING WATER

Guo et al. (2007) have studied the adsorption behaviour of As(III and V) onto the natural siderite in batch and column tests. They have estimated the adsorption capacities for As(V) and As(III) to be 520 and 1040 $\mu\text{g g}^{-1}$, respectively. They have also conducted the experiments on the arsenic spiked tap water and found that the uptake of As was low from the tap water. They have the TCLP (toxicity characteristic leaching procedure) for the spent adsorbents and found that the adsorbents were inert and can be land filled.

Table 2.2.1 Literature review on adsorption of As-V by various adsorbents

Authors	Adsorbent	Batch/ Column	Parameters Studied
Wang et al. (2008)	coal fly ash	Batch	Effect of pH, initial concentration, S/L ratio.
Chutia et al. (2008)	Natural Zeolites	Batch	Effect of contact time, initial pH, initial concentration, kinetic and isotherm studies and desorption studies using 0.1 M NaOH.
Bhakat et al. 2006	Modified calcined bauxite	Batch and Column	Effect of other ions, Removal efficiency, Equilibrium isotherms (Langmuir and Freundlich).
Diamadopoulos et al. 1993	Fly ash	Batch	Removal efficiency, kinetics, equilibrium studies, effect of pH, desorption studies.

Mohan and Pittman Jr. (2007) have recently reviewed the removal of arsenic from a wide range of adsorbents, such as commercial ACs, agricultural by-products, clay minerals and zeolites. They have compared the various methods available for the removal of arsenic from aqueous solutions. They showed that ACs produced from agricultural wastes offered a low-cost, efficient alternative to commonly used arsenic adsorbents. They have compared the sorption capacities of different available and developed adsorbents. They have also discussed the desorption of arsenic followed by regeneration of sorbents.

Maity et al. (2005) have elucidated the adsorption of As(III) and As(V) on to poly-metallic sea nodule in a Batch process. They have studied the effect of pH, initial concentration. They have also studied the Adsorption Kinetics, Adsorption isotherms and the effect of presence of anions and cations on adsorption kinetics.

Natural iron ores were tested as adsorbents for the removal of arsenic from contaminated water by (Zhang et al., 2004). Investigated parameters included pH, adsorbent dose, contact time, arsenic concentration and presence of interfering species. Iron ore containing mostly hematite was found to be very effective for arsenic adsorption. As(V) was lowered from 1 mg dm^{-3} to below 0.01 mg dm^{-3} (US standard limit for drinking water) in the optimum pH range 4.5–6.5 by using a 5 g dm^{-3} adsorbent dose. The experimental data fitted the first order rate expression and Langmuir isotherm model. The adsorption capacity was estimated to be $0.4 \text{ mg As(V) g}^{-1}$ adsorbent. The presence of silicate and phosphate had significant negative effects on arsenic adsorption, while sulphate and chloride slightly enhanced. The negative effect of silicate could be minimised by operating at a pH around 5. The interference of phosphate would necessitate the use of a relatively high dose of the adsorbent to achieve arsenic levels conforming to drinking water standards.

González et al. (2001) have conducted Steady state experiments on arsenic sorption from aqueous solutions by natural solids to test the feasibility of these materials to act as concentrator for arsenic removal from groundwater and drinking water. The solids considered were natural zeolites, volcanic stone, and the cactaceous powder CACMM. The arsenic species studied were As(III), As(V), dimethylarsinic acid (DMA) and phenylarsonic acid (PHA). The arsenic removed was determined from the data obtained by measuring the concentration diminution of the arsenic species in the liquid phase at equilibrium before and after the adsorption experiment by means of ICP-AES for the total concentration of arsenic and IC-ICP-MS to determine the arsenic species. The sorption of the arsenic species onto zeolites was studied on both non-activated and activated zeolites, as well as on zeolites hydrogenated or modified with iron, and with respect to varying pH.

Equilibrium and kinetic adsorption of trivalent (arsenite) and pentavalent (arsenate) arsenic to activated alumina has been elucidated by (Lin and Wu, 2000). The properties of activated alumina, including porosity, specific surface area, and skeleton

density were first measured. A batch reactor with temperature control was employed to determine both adsorption capacity and adsorption kinetics for arsenite and arsenate to activated-alumina grains. The Freundlich and Langmuir isotherm equations were then used to describe the partitioning behaviour for the system at different pH. A pore diffusion model, coupled with the observed Freundlich or Langmuir isotherm equations, was used to interpret an observed experimental adsorption kinetic curve for arsenite at one specific condition. The model was found to fit with the experimental data fairly well, and pore diffusion coefficients can be extracted. The model, incorporated with the interpreted pore diffusion coefficient, was then employed to predict the experimental data for arsenite and arsenate at various conditions, including different initial arsenic concentrations, grain sizes of activated alumina, and system pH.

Maji et al. (2008) have investigated the sorption characteristics of arsenic on laterite soil, a low-cost natural adsorbent. They have conducted both batch and continuous experiments to investigate the sorption characteristics. They have taken the real life sample water which is containing As of concentration 0.33 ppm. Under optimized conditions the laterite soil could remove up to 98% of total arsenic. The optimum adsorbent dose was 20 g dm^{-3} and the equilibrium time was 30 min. Isotherm studies showed that the process is favorable and spontaneous. The kinetics showed that the removal of arsenic by laterite soil is a pseudo-second-order reaction. They have used a column with inner diameter 2 cm and length 55 cm. In the column study the flow rate was maintained at $1.49 \text{ m}^3 (\text{m}^2 \text{ h})^{-1}$. Using 10 cm column depth, the breakthrough and exhaust time found were 6.75 h and 19.0 h, respectively. Height of adsorption zone was 9.85 cm, and the percentage of the total column saturated at breakthrough was 47.12%. The value of adsorption rate coefficient (K) and the adsorption capacity coefficient (N) were $1.21 \text{ dm}^3 (\text{mg h})^{-1}$ and 69.22 mg dm^{-3} , respectively. They have carried out desorption studies with aqueous NaOH (1 M), and claimed that the regenerated adsorbent showed higher efficiency.

Table 2.3.1 Literature review on adsorption of As-III and As-V by various adsorbents

Authors	Adsorbent	Batch/ Column	Parameters Studied
Maji et al. 2008	laterite soil	Batch and Column	Characterization of adsorbent, effect of contact time, effect of flow rate, desorption study.
Guo et al. 2007	natural siderite	Batch and Column	Effect of initial concentration, kinetics and equilibrium studies, effect of contact time, effect of flow rate, particle size.
Maity et al. 2005	Poly-metallic sea nodule	Batch	Effect of pH, initial concentration, Adsorption kinetics, Adsorption isotherms, Effect of presence of ions
Zhang et al. 2004	Natural iron ores	Batch	Effect of pH, initial concentration, Effect of interfering ions.
González et al. 2001	Natural zeolites, volcanic stone, and cactaceous powder.	Column	The kinetics and the ability to desorb and readsorb the arsenic species were investigated for selected zeolites. effect of pH
Lin and Wu 2000	Activated carbon	Batch	Characterization of adsorbent, kinetics, isotherms, pore diffusion model.

2.4 SORPTION OF AS BY METAL IMPREGNATED ADSORBENTS

Tripathy and Raichur (2008) have investigated the sorption characteristics of Alum-impregnated activated alumina (AIAA) for removal of As(V) from water in batch mode. Adsorption studies at different pH values has been conducted and showed that the efficiency of AIAA is much higher than activated alumina. The effect of adsorbent dose on the removal of As(V) has been studied by taking adsorbent dose ($0.5\text{--}16\text{ g dm}^{-3}$) at pH 7, 3 h equilibration time and 10 mg dm^{-3} As(V) concentration and found that adsorption of As(V) increased with increasing adsorbent dose. The adsorption isotherm experiments indicated that the uptake of As(V) increased with increasing As(V) concentration from 1 to 25 mg dm^{-3} and followed Langmuir isotherm. The equilibrium contact time was found to be 3 h. Intraparticle diffusion and kinetic studies has been done and claimed that adsorption of As(V) was due to physical adsorption as well as through intraparticle diffusion. The effect of interfering ions has been investigated and found that As(V) sorption is strongly influenced by the presence of phosphate ion. Alum-impregnated activated alumina successfully removed As(V) to below 40 ppb from water, when the initial concentration of As(V) is 10 mg dm^{-3} . To regenerate the adsorbent, desorption study was carried out at various pH values by appropriate addition of 0.1N HCl and NaOH solution onto As(V) adsorbed AIAA.

Huang et al. (2008) have elucidated the adsorptive removal of As-III with Zr(IV)-loaded collagen fiber (ZrCF). Collagen fiber is an abundant natural biomass easily obtained from the skin of domestic animals. The fiber has many functional groups and capable of reacting with many kinds of metal ions, such as Cr(III), Al(III), Zr(IV), Ti(IV), etc. They have studied the effect of initial pH on the uptake of the As(III) with 100 mg of ZrCF adsorbent, suspended in a series of 0.1 dm^{-3} As(III) solutions in which the concentration of As(III) was 0.5 mmol dm^{-3} . The initial pH was adjusted between 2.0 – 12.0 by using dilute HNO₃ and NaOH solutions. The optimum pH was found to be 11.0. The equilibrium contact time was found to be 24 h. For carrying out the isotherm experiments they have maintained the initial concentrations in the range of 0.25 - 1.25 mmol dm^{-3} , the pH of 11.0 by using HNO₃ and NaOH solutions, and the adsorption temperatures were 303 and 313 K, respectively and found that the isotherm data was well fit by the Langmuir-Freundlich equation. For carrying out the kinetic experiments, they have taken 100 mg of ZrCF adsorbent and suspended it in As(III) solutions with initial concentrations of 0.25, 0.5, and

0.75 mmol dm⁻³, pH of 11.0, at a temperature of 303 K and found that the kinetic data fits the pseudo-second-order rate equation. The maximum adsorption capacity of As(III) by ZrCF was found to be 54.02 mg As g⁻¹ when the initial concentration of As(III) was 73.00 mg dm⁻³ at 303 K and pH 11.0 They have also studied the effect of coexisting anions such as Cl^- , HCO_3^- , NO_3^- , SO_4^{2-} and HPO_4^{2-} on the adsorption and found that the effects of Cl^- , NO_3^- , SO_4^{2-} and HPO_4^{2-} on the adsorption of As(III) are remarkable.

Shao et al. (2008) have studied the feasibility of using La(III)-, Ce(III)-, Y(III)-, Fe(III)- and Al(III)-loaded Amberlite 200CTNa resin as adsorbents for the removal of As(III and V) from aqueous solution. They have studied the effects of the contact time, pH of solution and initial concentration of solution on the removal of As(III and V) in a batch system. They found that the removal of As(III and V) by using metal(III)-loaded 200CT resins are strictly pH-dependent. They have also fit the experimental batch study data with the pseudo-first-order and pseudo-second-order kinetics and found that, kinetics of As(III) adsorption with Y(III)-200CT and As(V) adsorption with Fe(III)-200CT can be described well by the pseudo-first-order and second-order models. The equilibrium adsorption data were fitted by four isotherm models, viz. Langmuir, Freundlich, Langmuir–Freundlich and Redlich–Peterson isotherms. The fitting results suggested that the Y(III)- and Ce(III)-200CT resins are better adsorbents for the As(III) adsorption and the maximum uptakes are 0.4835 and 0.4592 mol kg⁻¹, respectively. And Fe(III)-200CT resin is the best adsorbent for the removal of As(V) with the maximum capacity of 1.450 mol kg⁻¹. The coexisting ion influence of PO_4^{3-} was bigger than SO_4^{2-} on the removal of As(III and V).

Kalderis et al. (2008) have studied the sorption studies of different polluting substances like arsenic, humic acid, phenol and a municipal solid waste landfill leachate on ZnCl₂ impregnated activated carbon, AC prepared from rice husk and sugarcane bagasse. They produced the AC and characterized it. They have studied the effect of the ZnCl₂ – AC ratio and found that the optimum ratio for rice husk is 1:1, and for bagasse this ratio was 0.75:1. They have conducted the batch experiments on a stock solution of 10 mg dm⁻³ As(V) to know the adsorptive capacities of the adsorbents. They used nine separate Erlenmeyer flasks, each one of them containing 0.2, 0.4, 0.6, 0.8, 1.1, 1.4, 1.8, 2, and 2.2 g of rice husk AC, respectively, and 0.2 dm⁻³ of the stock solution of As. The flasks were then mechanically shaken for 96 h at 180 rpm to achieve equilibrium between As and the carbon surface. They

have fit the experimental data using Langmuir and Freundlich isotherms. The adsorptive capacity of As(V) was found to be $1.22 \text{ mg As (g AC)}^{-1}$.

Biswas et al. (2008) have examined the adsorption behavior for As(V) and As(III) from an aquatic environment using the Zr(IV)-loaded orange waste gel (Zr(IV)-SOW). They have prepared the adsorbent by taking 3 g of the SOW gel with 0.5 dm^{-3} of 0.1M zirconium solution at pH 2.11 for 24 h. The gel was then filtered and washed with deionized water until neutral pH, followed by drying in vacuum until constant weight. The specific surface area of this gel was measured as $7.25 \text{ m}^2 \text{ g}^{-1}$. They have conducted the batch adsorption tests individually for arsenate and arsenite in the concentration range $5\text{--}900 \text{ mg dm}^{-3}$. They have conducted all the batch studies in 50 ml conical flasks by taking 25 mg (dry weight) of the gel together with 15 ml of the arsenic solution. For kinetic studies they have measured the concentration at 9 different contact times (0 min, 15 min, 30 min, 60 min, 120 min, 360 min, 600 min, 900 min, and 1440 min). They have described the adsorption kinetics of arsenate with pseudo-second-order rate equation. The maximum adsorption capacity of the Zr(IV)-loaded SOW gel was found to be 88 mg g^{-1} and 130 mg g^{-1} for As(V) and As(III). They have carried out the effect of presence of other ions like chloride, sulfate and carbonate and found that the anions hardly interfere the adsorption of arsenic. They have conducted the column studies in 0.8 cm inner diameter and 20 cm high fitted with a glass filter at the bottom column.

Ghimire et al. (2008) have investigated the separation of arsenate and arsenite anions from aqueous medium by using orange waste. Cellulose and orange waste were first chemically modified by means of phosphorylation. The chemically modified gels were further loaded with iron(III) for creating a chelating environment for arsenate and arsenite removal. Adsorption tests were carried out both batchwise and by using a column for breakthrough and elution tests. In the batchwise tests, 25 mg of dried gel was placed in a conical flask together with 15 ml aqueous solutions of metal ions. The pH of the aqueous solutions was adjusted by adding small amounts of HCl or NaOH solutions. The flask was shaken vigorously in a thermostatic shaker at 30°C for 24 h. They have studied the effect of contact time and found that the equilibrium contact time was 24 h. They have also conducted the experiments to find the effect of initial pH of arsenite and arsenate. In the tests using a column, they have carried out the arsenic removal in a glass column of 8mm inner diameter

packed with 0.1 g of iron-loaded POW gel. The sample solution, containing 15 mg dm^{-3} of arsenate, whose pH was maintained at 4, was percolated through the column at a constant flow rate of 0.098 ml min^{-1} using a peristaltic pump. Effluent samples were collected at 1 h time intervals by using a fraction collector.

Selvakumar et al. (2008) have carried out the Sorption of arsenic from aqueous solution out using polyvinyl pyrrolidone K25 coated cassava peel carbon (PVPCC). The molecular formula of PVPCC is Molecular formula $(C_6H_9NO)_n$. They have conducted batch experiments to determine the effect of contact time, initial concentration, pH and desorption. The equilibrium time was found to be 45, 60, 105, 120 and 150 min for 0.5, 1.0, 1.5, 2.0 and 2.5 mg dm^{-3} of As(V) concentration, respectively. Batch sorption data were fitted to Lagergren kinetic studies. They have conducted the column studies to determine the effect of flow rate, bed height for an initial concentration of 0.5 - 2.5 mg dm^{-3} As(V) solution. The optimized flow rate was found to be 2.5 mL min^{-1} and bed height 10 cm. Bed depth-service-time model (BDST) was applied to calculate the adsorption capacity (N_0) of column. The N_0 value of 2.59×10^{-5} , 4.21×10^{-5} , 4.05×10^{-5} , 4.26×10^{-5} and $3.2 \times 10^{-5}\text{ mg g}^{-1}$ were obtained for 0.5, 1.0, 1.5, 2.0 and 2.5 mg dm^{-3} of As(V), respectively. Desorption studies were also carried out using 0.1N HCl and NaOH solutions

Vaughan Jr. and Reed (2005) have worked on As(V) removal by iron oxide impregnated activated carbon using the surface complexation approach. They found that As(V) removal by FeAC was due to the impregnated Fe oxide, not the base carbon material and was a strong function of pH.

Singh and Pan (2005) have investigated the removal of As(III) ions from drinking water by activated alumina and iron oxide impregnated activated alumina (IOIAA). The effect of inlet flow rate, sorbent bed height and initial As(III) concentration on the adsorption of As(III) from aqueous solution have been studied. Compared to activated alumina, iron oxide impregnated activated alumina was found more effective in removing As(III) ions. They have modeled the dynamics of adsorption process by bed depth service time (BDST) and pore diffusion model. They found that adsorption rate constant (k_a) was increased with increase in flow rate and claimed that the overall system kinetics was dominated by external mass transfer in the initial part of the adsorption in the column. Relatively lower critical bed height was observed for As(III) removal onto IOIAA (0.56 cm) compared to AA (1.12 cm) at

identical flow rate ($0.083 \text{ cm}^3 \text{ s}^{-1}$). They found that pore diffusion model explained the breakthrough behaviour for As(III) removal with a high degree of correlation.

Zeng (2003) has explored on the method for preparing iron(III)-based binary oxide adsorbents in a granulated form for arsenic removal. The key step in his method was the simultaneous generation of hydrous ferric oxide (FeOOH) sol and silica sol in situ in one reactor. This eventually led to the formation of Fe–Si complexes. An optimum Si/Fe molar ratio in the balance of adsorbent strength and arsenic adsorption capacity was found to be approximately 0.33. The effects of aging time, drying temperature and process pH on adsorbents were also evaluated in the study. X-ray diffraction analysis confirmed that the iron(III) oxide in the Fe–Si binary oxide adsorbents was amorphous, largely due to the retardation of the iron oxide crystallization by the presence of silicate species. The surface area of the Fe–Si adsorbents and the particle size of Fe–Si complexed suspensions were also determined as well.

Balarama Krishna et al. (2001) has worked with Fenton's reagent (H_2O_2 and Fe II) and zero valent iron as adsorbent for the removal of As(III) and As(V) in a column. They have conducted experiments on Potable municipal water and ground water samples spiked with As(III) and As(V). The arsenic content was determined by ICP–QMS. A HPLC–ICPMS procedure was used for the speciation and determination of both As(III) and (V) in the processed samples, to study the effectiveness of the oxidation step and the subsequent removal of the arsenic.

Matsunaga et al. (1996) have studied the adsorption kinetics of As(III) and As(V) by Iron(III)-loaded chelating resin (Fe-LDA) with lysine-N",N"-diacetic acid in a batch process. They have studied the effects of pH, initial concentration, regeneration of catalyst, time for the desired removal etc.

Lorenzen et al. (1995) have studied the factors affecting the mechanism of the adsorption of As on the Activated carbon. It was found that As(V) is more effectively removed from solution by using activated carbon with a high ash content. Pretreatment of the carbon with Cu(II) solutions improves its arsenic removal capacity. The optimum pH for arsenic adsorption by pretreated carbon was approximately 6. There are two mechanisms of arsenic adsorption which occur simultaneously. The arsenic in solution can form insoluble metal arsenates with the copper impregnated in the carbon.

Table 2.4.1 Literature review on adsorption of arsenic by metal impregnated adsorbents

Authors	Adsorbent	Batch/ Column	Parameters Studied
Tripathy and Raichur, 2008	Alum-impregnated alumina (AIAA)	Batch	Effect of pH, isotherm study, kinetic study, effect of interfering ions, adsorbent dosage, desorption studies.
Selvakumar et al., 2008	Polyvinyl pyrrolidone K25 coated cassava peel carbon.	Batch and column	Effect of pH, equilibrium contact time, kinetic study, effect of flow rate, bed height, and initial concentration, break through studies.
Kalderis et al., 2008	ZnCl ₂ impregnated activated carbon	Batch	Effect of ratio of ZnCl ₂ and AC, isotherm data, dosage, effect of RPM.
Huang et al., 2008	Zr(IV)-loaded collagen fiber (ZrCF)	Batch	Effect of pH, isotherm study, kinetic study, effect of interfering ions.
Shao et al., 2008	Metal(III)-loaded amberlite resins	Batch	Effect of pH, effect of metal loaded on removal, isotherm study, kinetic study, effect of interfering ions.
Ghimire et al., 2008	Iron (III) coated cellulose and orange waste.	Batch and column	Effect of pH, equilibrium contact time, break through.

Authors	Adsorbent	Batch/ Column	Parameters Studied
Biswas et al., 2008	Zr(IV)-loaded orange waste gel	Batch and column	Effect of pH, isotherm study, kinetic study, effect of interfering ions, column studies for break through.
Vaughan Jr. and Reed, 2005	Iron oxide impregnated activated carbon	Batch	Effect of pH, kinetics, surface complexation approach
Singh and Pan, 2005	Activated alumina and iron oxide impregnated activated alumina	Column	Effect of flow rate, bed height, initial concentration, break through, pore diffusion and bed depth service time (BDST) models.
Zeng, 2003	Iron(III) coated silica	Batch	Characterization of adsorbents, aging time, drying temperature, pH.
Balarama Krishna et al., 2001	Fenton's reagent (H ₂ O ₂ and Fe II) impregnated valent iron	Batch	Removal of arsenic, effectiveness of oxidation of fenton's reagent.
Matsunaga et al., 1996	Iron(III)-loaded chelating resin with lysine-N ⁺ ,N ⁺ -diacetic acid	Batch	Effects of pH, initial concentration, regeneration of catalyst, time.
Lorenzen et al., 1995	Cu(II) coated Activated carbon	Batch	Effect pH, desorption studies, adsorption mechanism studies.

ADSORPTION FUNDAMENTALS

3.1 GENERAL

Adsorption is a surface phenomenon. The material adsorbed is called the adsorbate or solute and the adsorbing phase is the adsorbent. The adsorption is called physical when relatively weak intermolecular forces cause the attachment and, chemical when chemical bonding like forces causes this attachment. Adsorption fundamentals have been discussed in this chapter. The contents of this chapter include:

1. Physical Adsorption Vs. Chemisorption.
2. Adsorption Kinetics.
3. Controlling steps In Adsorption Process.
4. Adsorption Isotherms.
5. Factors Effecting Adsorption.
6. Error Analysis.

3.2 PHYSICAL ADSORPTION VS. CHEMISORPTION

Adsorption processes can be classified as either physical adsorption (van der Waals adsorption) or chemisorption (activated adsorption) depending on the type of forces between the adsorbate and the adsorbent. In physical adsorption, the individuality of the adsorbate and the adsorbent are preserved. In chemisorption, there is a transfer or sharing of electron, or breakage of the adsorbate into atoms or radicals, which are bound separately.

Physical adsorption from a gas occurs when the inter-molecular attractive forces between molecules of the solid adsorbent and the gas are greater than those between molecules of the gas itself. In effect, the resulting adsorption is like condensation, which is exothermic and thus is accompanied by the release of heat, similar in magnitude to the heat of condensation.

Physical adsorption occurs quickly and may be monomolecular (unimolecular) layer or monolayer, or two, three or more layers thick (multi-molecular). As physical adsorption takes place, it begins as a monolayer. It can then become multi-layer, and

then, if the pores are close to the size of the molecules, more adsorption occurs until the pores are filled with adsorbate. Accordingly, the maximum capacity of a porous adsorbent can be more related to the pore volume than to the surface area.

In contrast, chemisorption is monolayer, involves the formation of chemical bonds between the adsorbate and adsorbent, often with a release of heat much larger than the heat of condensation. Chemisorption may be slow and irreversible. Most commercial adsorbents rely on physical adsorption, while, catalysis relies on chemisorption. A comparison between physical adsorption and chemical adsorption is given in Table 3.1.

Table.3.2.1: Comparison of Physical and Chemical Adsorption

S. No.	Physical Adsorption	Chemical Adsorption
1.	Vander walls adsorption	Activated adsorption
2.	Heat of adsorption = 5 kcal mol ⁻¹	Heat of adsorption = 20-100 kcal mol ⁻¹
3.	Adsorption only at temp less than the boiling point of the adsorbate	Adsorption can occur even at higher temperature
4.	No activated energy involved in the adsorption process	Activation energy may be involved
5.	Mono and multi layer adsorption	Almost mono layer adsorption
6.	Quantity adsorbed per unit mass is high i.e. entire surface is participating	Quantity adsorbed per unit mass is low i.e. only active surface sites are important
7.	Extent of adsorption depends upon the properties of adsorbent	Extent of adsorption depends on both adsorbate and adsorbent
8.	Rate of adsorption controlled by resistance mass transfer	Rate of adsorption controlled by resistance reaction

3.3 ADSORPTION KINETICS

In order to found out the adsorption processes, various kinetic models are used to describe the time-dependency of adsorption of a species onto an adsorbent, viz. pseudo-first-order, pseudo-second-order, intra-particle diffusion model and Bangham model.

3.3.1 Pseudo-First-Order Model, (Lagergren, 1898; Srivasatava et al., 2006)

The sorption of species from a liquid phase to a solid phase can be considered as a reversible process with equilibrium being established between the two phases. Assuming a non-dissociating molecular adsorption of adsorbates onto adsorbent particles, the sorption phenomenon can be described as (Fogler, 1998)



where, A is adsorbate and S is the active site on the adsorbent and AS is the activated complex. k_A and k_D are the adsorption and desorption rate constants, respectively. It can be shown using first order kinetics that with no adsorbate initially present on the adsorbent (i.e. $C_{AS0} = 0$ at $t = 0$), the fractional uptake of the adsorbate by the adsorbent can be expressed as

$$\frac{X_A}{X_{Ae}} = 1 - \exp\left[-k_A C_S + \frac{k_A}{K_S}\right] t \quad (3.3.2)$$

where, X_{Ae} = fraction of the adsorbate adsorbed on the adsorbent under equilibrium condition (i.e. C_{ASe} / C_{A0})

$$K_S = k_A / k_D$$

C_S = adsorbent concentration in the solution

Thus, the plot of $\ln\left(1 - \frac{X_A}{X_{Ae}}\right)$ versus t for various values of C_{A0} at a constant C_S will give a straight line which will be coincident on the ordinate at $t = 0$. Constants k_A and k_D can be obtained using relevant relations and the slope of each curve for a given value of C_S . The above equation can be transformed as

$$\log(q_e - q_t) = \log q_e - \frac{k_f}{2.303} t \quad (3.3.3)$$

where, $k_f = \left(k_A C_S + \frac{k_A}{K_S}\right)$;

$$q = X_A, \text{ and } q_e = X_{Ae}$$

This equation is the so-called Lagergren equation. This equation is, however,

valid only for the initial period of adsorption. Various investigators have erroneously fitted this equation to the adsorbate uptake data for extended periods, ignoring the data of the initial period. A plot of $\log(q_e - q_t)$ versus t for the initial period enables the determination of the kinetic constants.

Experimental results don't follow pseudo-first order model for the whole period because they differ in two important aspects: (i) $k_f(q_e - q_t)$ does not represent the number of available sites, and (ii) $\log q_e$ was not equal to the intercept of the plot of $\log(q_e - q_t)$ against t .

3.3.2 Pseudo-Second-Order Model (Ho and Mckay, 1998, 1999, 2000)

For cellulose based sorbents having fibers, which may have polar functional groups, chemical bonding of polar functional groups may occur with solute ions and these groups may impart cation exchange capacity to the adsorbents. For such sorption systems, the rate of sorption to the surface should be proportional to a driving force times an area, and the sorption rate equation may be given as:

$$\frac{dq}{dt} = k_s(q_e - q_t)^2 \quad (3.3.4)$$

where k_s is the pseudo second order rate constant ($\text{g } \mu\text{g}^{-1} \text{ min}^{-1}$), q_e the amount of solute ions adsorbed at equilibrium ($\mu\text{g g}^{-1}$) and q_t is the amount of solution ions adsorbed on the sorbent at any time, t ($\mu\text{g g}^{-1}$).

This equation (3.3.4) can be integrated with $q_t = 0$ at $t = 0$, to give

$$q_t = \frac{k_s q_e^2 t}{1 + k_s q_e t} \quad (3.3.5)$$

The linearized plot of t/q_t versus t is the so-called ratio correlation in that t is present in both the ordinate and abscissa of the plot of course would yield a perfect correlation coefficient would be 1.0 in most of the cases.

Eq. 3.3.5. seems to be valid at low and high times of sorption. At $t \rightarrow \infty$, $q_t \rightarrow q_e$ and at $t \rightarrow 0$, $q_t \rightarrow 0$.

For very fast adsorption situation, it is too difficult to measure the adsorption rate in the time-scale of the kinetic experiments. In such situations, it is better to provide a qualitative discussion of the kinetic results.

The q_e and the h along with the k_s can be determined experimentally from the slope and intercept of the plot of t/q_t versus t .

3.3.3 Intra-particle Diffusion Study (Weber and Morris, 1963)

A functional relationship common to most of the treatments of intraparticle transport is that uptake varies almost proportionally with the square root of time, ($t^{0.5}$), rather than time, (t), itself, i.e.

$$q_t = k_{id}t^{0.5} + I \quad (3.3.6)$$

where, k_{id} is the intra-particle diffusion rate constant ($\mu\text{g g}^{-1} \text{min}^{-1/2}$) and I ($\mu\text{g g}^{-1}$) is a constant that gives an idea about the thickness of the boundary layer, i.e., the larger the value of I , the greater is the boundary layer effect. The mathematical dependence of fractional uptake of adsorbate on $t^{0.5}$ is obtained if the sorption process is considered to be influenced by diffusion in the cylindrical (or spherical) particle and the convective diffusion in the adsorbate solution. It is assumed that the external resistance to mass transfer surrounding the particles is significant only in the early stages of adsorption.

The slope of the Weber and Morris plots: q versus $t^{0.5}$, are defined as a rate parameter (k_{id}), characteristic of the rate of adsorption in the region where intra-particle diffusion is rate controlling. The higher the value of k_{id} the higher is the intraparticle diffusion rate.

3.3.4 Bangham's Equation (Aharoni et al., 1979)

Bangham's equation can be used to check the whether pore-diffusion is the only rate-controlling step or not in the adsorption system.

$$\log \log \left(\frac{C_0}{C_0 - q_t m} \right) = \log \left(\frac{k_{0B} m}{2.303V} \right) + \alpha \log(t) \quad (3.3.7)$$

where, α (<1) and k_{0B} are constants.

If the experimental data are represented by Eq. (3.3.7), then it is an indication that the adsorption kinetics is limited by the pore diffusion.

3.4 CONTROLLING STEPS IN ADSORPTION PROCESS

Adsorption is thought to occur in four steps, as the adsorbate concentration increases. (Lataye, 2007)

1. Diffusion of solute molecules from bulk of the solution to the external film surrounding the adsorbent particle. (bulk diffusion)
2. Diffusion of the solute particles from the external film to the surface of the adsorbent particle. (Film diffusion)
3. Diffusion of the adsorbate from the poremouth through the pores to the internal adsorbent surface. (pore, surface and molecular diffusion)
4. Adsorption of the adsorbate onto the interior surface of the adsorbent.

3.5 ADSORPTION ISOTHERMS

When a solution is contacted with a solid adsorbent, molecules of adsorbate get transferred from the fluid to the solid until the concentration of adsorbate in solution as well as in the solid phase are in equilibrium. At equilibrium, equal amounts of solute eventually are being adsorbed and desorbed simultaneously. This is called adsorption equilibrium. The equilibrium data at a given temperature are represented by adsorption isotherm and the study of adsorption is important in a number of chemical processes ranging from the design of heterogeneous chemical reactors to purification of compounds by adsorption.

Many theoretical and empirical models have been developed to represent the various types of adsorption isotherms. Langmuir, Freundlich, Temkin, Redlich-Peterson (R-P) etc. are most commonly used adsorption isotherm models for describing the dynamic equilibrium. The isotherm equations used for the study are described follows:

3.5.1 Langmuir Isotherm (Langmuir, 1919)

This equation based on the assumptions that:

1. Only monolayer adsorption is possible.
2. Adsorbent surface is uniform in terms of energy of adsorption.
3. Adsorbed molecules do not interact with each other.
4. Adsorbed molecules do not migrate on the adsorbent surface

The adsorption isotherm derived by Langmuir for the adsorption of a solute from a liquid solution is:

$$Q_e = \frac{Q_m K_A C_e}{1 + K_A C_e} \quad (3.5.1)$$

where,

Q_e = Amount of adsorbate adsorbed per unit amount of adsorbent at equilibrium

Q_m = Amount of adsorbate adsorbed per unit amount of adsorbent required for monolayer adsorption (limiting adsorbing capacity).

K_A = Constant related to enthalpy of adsorption

C_e = Concentration of adsorbate solution at equilibrium

The Langmuir isotherm can be rearranged to the following linear forms:

$$\frac{C_e}{Q_e} = \frac{1}{K_A Q_m} + \frac{C_e}{Q_m} \quad (3.5.2)$$

$$\frac{1}{Q_e} = \left(\frac{1}{K_A Q_m} \right) \left(\frac{1}{C_e} \right) + \left(\frac{1}{Q_m} \right) \quad (3.5.3)$$

3.5.2 Freundlich Isotherm (Freundlich, 1906)

The heat of adsorption in many instances decreases in magnitude with increasing extent of adsorption. This decline in heat of adsorption is logarithmic, implying that adsorption sites are distributed exponentially with respect to adsorption energy. This isotherm does not indicate an adsorption limit when coverage is sufficient to fill a monolayer. The equation that describes such isotherm is the Freundlich Isotherm, given as:

$$Q_e = K_F C_e^{\frac{1}{n}} \quad (3.5.4)$$

where ,

K_F and n are the constants

C_e = the concentration of adsorbate solution at equilibrium

By taking logarithm of both sides, this equation is converted into a linear form:

$$\ln Q_e = \ln K_F + \frac{1}{n} \ln C_e \quad (3.5.5)$$

Thus a plot between $\ln Q_e$ and $\ln C_e$ is a straight line. The Freundlich equation is most useful for dilute solutions over small concentration ranges. It is frequently applied to the adsorption of impurities from a liquid solution on to the activated carbon. A high K_F and high 'n' value is an indication of high adsorption through out the concentration range. A low K_F and high 'n' indicates a low adsorption through out the concentration range. A low 'n' value indicates high adsorption at strong solute concentration

3.5.3 Redlich-Peterson isotherm, (Redlich and Peterson 1959)

They combined elements from both the Langmuir and Freundlich equation and the mechanism of adsorption is a hybrid and does not follow ideal monolayer adsorption. The Redlich-Peterson isotherm has a linear dependence on concentration in the numerator and an exponential function in the denominator. The R-P equation is a combination of the Langmuir and Freundlich models. It approaches the Freundlich model at high concentration and is in accord with the low concentration limit of the Langmuir equation. Furthermore, the R-P equation incorporates three parameters into an empirical isotherm, and therefore, can be applied either in homogenous or heterogeneous systems due to the high versatility of the equation. (Mall et al., 2006)

It can be described as follows:

$$Q_e = \frac{K_R C_e}{1 + a_R C_e^\beta} \quad (3.5.6)$$

Where K_R is R-P isotherm constant ($\text{dm}^3 \text{g}^{-1}$), a_R is R-P isotherm constant ($\text{dm}^3 \mu\text{g}^{-1}$) and β is the exponent which lies between 1 and 0, where $\beta=1$

$$Q_e = \frac{K_R C_e}{1 + a_R C_e} \quad (3.5.7)$$

It becomes a Langmuir equation. Where $\beta=0$

$$Q_e = \frac{K_R C_e}{1 + a_R} \quad (3.5.8)$$

i.e. the Henry's Law equation

the above equation can be converted to a linear form by taking logarithms:

$$\ln\left(K_R \frac{C_e}{Q_e} - 1\right) = \ln a_R + \beta \ln C_e \quad (3.5.9)$$

Plotting the left-hand side of the above equation against $\ln C_e$ to obtain the isotherm constants is not applicable because of the three unknowns, a_R , K_R and β . Therefore, a minimization procedure was adopted to solve the equation by maximizing the correlation coefficient between the theoretical data for Q_e predicted from equation the and experimental data. Therefore, the parameters of the equations were determined by minimizing the distance between the experimental data points and the theoretical model predictions with any suitable computer programme.

3.5.4 The Temkin isotherm (Mall et al., 2005a)

It is given as

$$q_e = \frac{RT}{b} \ln(K_T C_e) \quad (3.5.10)$$

which can be linearized as:

$$q_e = B_1 \ln K_T + B_1 \ln C_e \quad (3.5.11)$$

$$\text{Where } B_1 = \frac{RT}{b}$$

Temkin isotherm contains a factor that explicitly takes into the account adsorbing species-adsorbent interactions. This isotherm assumes that (i) the heat of adsorption of all the molecules in the layer decreases linearly with coverage due to adsorbent-adsorbate interactions, and that (ii) the adsorption is characterized by a uniform distribution of binding energies, up to some maximum binding energy. A plot of q_e versus $\ln C_e$ enables the determination of the isotherm constants B_1 and K_T from the slope and the intercept, respectively. K_T is the equilibrium binding constant ($\text{dm}^3 \text{mol}^{-1}$) corresponding to the maximum binding energy and constant B_1 is related to the heat of adsorption.

3.6 FACTORS EFFECTING ADSORPTION

The amount adsorbed by an adsorbent from the adsorbate solution is influenced by a number of factors are given as: (Srivastava, 2006)

1. Initial concentration
2. Temperature
3. pH
4. Contact time
5. Degree of agitation

3.6.1 Initial Concentration

The initial concentration of pollutant has remarkable effect on its removal by adsorption. The amount of adsorbed material increases with the increasing adsorbate concentration as the resistance to the uptake to the solution from solution of the adsorbate decreases with increasing solute concentration. Percent removal increases with decreasing concentrations.

3.6.2 Temperature

Temperature is one of the most important controlling parameter in adsorption. Adsorption is normally exothermic in nature and the extent and rate of adsorption in most cases decreases with increasing temperature of the system. Some of the adsorption studies show increased adsorption with increasing temperature. This increase in adsorption is mainly due to increase in number of adsorption sites caused by breaking of some of the internal bonds near the edge of the active surface sites of the adsorbents.

3.6.3 pH

Adsorption from solution is strongly influenced by pH of the solution. The adsorption of cations increases while that of the anions decreases with increase in pH. The hydrogen ion and hydroxyl ions are adsorbed quite strongly and therefore the adsorption of other ions is affected by pH of solution. Change in pH affects the adsorptive process through dissociation of functional groups on the adsorbent surface active sites. This subsequently leads to a shift in reaction kinetics and equilibrium characteristics of adsorption process. It is an evident observation that the surface adsorbs anions favorably at lower pH due to presence of H^+ ions, whereas the surface is active for the adsorption of cations at higher pH due to the deposition of OH^- ions.

3.6.4 Contact time

The studies on the effect of contact time between adsorbent and adsorbate have significant importance. In physical adsorption, most of the adsorbate species are adsorbed on the adsorbent surface with in short contact time. The uptake of adsorbate is fast in the initial stages of the contact period and becomes slow near equilibrium. Strong chemical binding of adsorbate with adsorbent requires a longer contact time for the attainment of equilibrium. Available adsorption results reveal that the uptake of heavy metals is fast at the initial stages of the contact period, and there after it becomes slow near equilibrium.

3.6.5 Degree of agitation

Agitation in batch adsorbers is most important to ensure proper contact between the adsorbent and the solution. At lower agitation speed, the stationary fluid film around the particle is thicker and the process is mass transfer controlled. With the increase in agitation this film decreases in thickness and the resistance to mass transfer due to this film reduces and after a certain point the process becomes intra particle diffusion controlled. Whatever is the extent of agitation the solution inside the process remain unaffected and hence for intraparticle mass transfer controlled process agitation has no effect on the rate on the adsorption.

3.7 ERROR ANALYSIS (Mall et al., 2005b, 2006)

Five different error functions are used to check the deviation from the experimental values and that of values got by applying different isotherms. The error may be caused due to the various assumptions made while deriving the isotherms.

3.7.1 The sum of the squares of the errors (SSE)

This error function, SSE, is given as:

$$SSE = \sum_{i=1}^n (q_{e,calc} - q_{e,exp})_i^2 \quad (3.7.1)$$

Here, $q_{e,cal}$ and $q_{e,exp}$ are, respectively, the calculated and the experimental value of the equilibrium adsorbate solid concentration in the solid phase ($\mu\text{g g}^{-1}$) and n is the number of data points. This most commonly used error function, SSE, has one major drawback is that it will result in the calculated isotherm parameters providing a better fit at the higher end of the liquid phase concentration range. This is because of the magnitude of the errors, which increase as the concentration increases, (Mall et al., 2005b).

EXPERIMENTAL PROGRAMME

This chapter deals with the materials and methods of analysis, and the experimental procedures adopted to take the experimental data.

4.1 MATERIALS

4.1.1 Adsorbents

Adsorption of Arsenic was studied using two adsorbents, namely, FeCl₃ coated bagasse fly ash (BFA) and FeCl₃ coated rice husk ash (RHA). BFA was obtained from a nearby sugar mill (Deoband sugar Mills, U.P., India), sieved and a mass fraction between -600 + 180 μm was used for the sorption study. RHA was obtained from Bhawani Paper Mills, Raebareli, U.P. (India). RHA was sieved and a mass fraction between -600 + 180 μm was used for the sorption study of As from the aqueous solutions. BFA and RHA were washed with hot water (70 °C) dried and sieved. The samples were sieved using IS sieves (IS 437, 1979).

4.1.2 Adsorbates

All the chemicals used in the study were of analytical reagent (AR) grade. Sodium Arsenite (As III) and Sodium Arsenate (As-V) were procured from, Loba Chemie Pvt. Ltd., Mumbai (India). The stock aqueous solutions of 1000 mg dm⁻³ concentration were prepared for both the compounds by taking respective amount of chemicals in Millipore water. The concentration range of sorbate test solutions prepared from the stock solutions varied between 20 and 500 μg dm⁻³. These test solutions were prepared by diluting the stock solutions of arsenic with Millipore water.

4.1.3 Other Chemicals

All other chemicals used in the study viz., acids, alkalies, KNO₃, KBr - FTIR grade, etc were supplied by S.D. Fine Chemicals, Mumbai, India.

4.1.4 Preparation of Adsorbents

BFA and RHA were impregnated with 1 M FeCl₃ solution to improve their

adsorptive capacity. The adsorbents were drenched in the FeCl_3 solution for 24h and then dried in the oven for 48h at 80°C till the adsorbents dried completely.

4.2 ADSORBENT CHARACTERISATION

The physical characteristics of the two adsorbents were determined by using standard procedure as detailed below.

4.2.1 Proximate Analysis

Proximate analyses of the adsorbents were carried out using the procedure given in IS 1350:1984.

A small amount of the adsorbent was finely ground and a representative sample was then taken for analysis. Sample was divided into two portions. The first portion of the sample was placed in a silica crucible and its moisture was determined. To determine the moisture content, sample was weighed and kept in oven at 105°C , for 1 h. After 1 h the dry weight of sample was taken and % moisture was determined from the difference of initial weight and final weight (dry weight). After that, the sample was heated to 750°C in a muffle furnace and maintained at this temperature for 2 h or more till a constant weight of the residue was obtained. The weight of the residue represented the ash content of the adsorbent. The second portion of the sample was placed in a crucible, covered with a lid and heated in the furnace at 600°C for six minutes and thereafter at 950°C in the furnace for another six minutes. Thereafter the crucible was kept in a dessicator for cooling and then the crucible was weighed. The difference in weights was due to the loss of volatilities and moisture in the sample. The volatile matter was found by subtracting the corresponding moisture determined previously. Chemical analyses of the adsorbents were carried out as per IS 355: 1984.

4.2.2 Particle Size

Particle size analyses of the adsorbents were carried out as per IS 2720 (part-4), 1985 using standard sieves.

4.2.3 Density

Bulk density of the adsorbents were determined by using MAC bulk density meter.

4.2.4 Scanning Electron Microscopic Analysis

To understand the morphology of the adsorbents before and after the adsorption of arsenic, the scanning electron microscope (SEM) micrographs were taken using LEO, Model 435 VP, England. The adsorption particles were first gold coated to make the sample conductive, using Sputter Coater, Edwards S150, then the SEMs were taken at various magnification.

4.2.5 Fourier Transform Infra Red (FTIR) Spectral Analysis

FTIR spectrometer (Thermo nicolet, Model Magna 760) was employed to determine the presence of functional groups in the adsorbents before and after the adsorption of arsenic at room temperature. Pellet (pressed-disk) technique has been used for this purpose. The sample was mixed with KBr (IR spectroscopy, grade) thoroughly and pellet was made by using a special mold provided to make pellet under the pressure of 15 ton. The spectral range was from 4000 to 400 cm^{-1} .

4.3 BATCH EXPERIMENTAL PROGRAMME

A temperature controlled orbital shaker (Remi Instruments, Mumbai) was used for the batch adsorption study. The temperature range for the studies was from 283 to 323 K. All the batch studies were performed at the shaking rate of 150 revolutions per minute (rpm). For each experimental run, 0.050 dm^3 aqueous solution of the known concentration of As-III and As-V was taken in a 0.25 dm^3 conical flask containing a known mass of the adsorbent. These flasks were agitated at a constant shaking rate of 150 rpm in a temperature controlled orbital shaker maintained at a constant temperature. The pH_0 of the adsorbate solution was adjusted using 1 N H_2SO_4 or 1 N NaOH aqueous solution without any further adjustment during the sorption process. To check whether the equilibrium has been attained, the samples were withdrawn from the flasks at different time intervals, centrifuged using a Research Centrifuge (Remi Instruments, Mumbai) at 5000 rpm for 5 min and then the supernatant liquid was analyzed for residual concentration of respective compound using Perkin Elmer Lambda 35 double beam spectrophotometer.

4.3.1 Effect of Initial pH (pH_0)

The sorption of Arsenic by the adsorbents was studied over a pH_0 range of 2-11 at 303 K and over a contact time of 5 h. C_0 used was $100 \mu\text{g dm}^{-3}$ for As-III and As-V solutions.

4.3.2 Batch Kinetic Study

To study the adsorption kinetics, 0.05 dm^3 of the aqueous solution containing $100 \mu\text{g dm}^{-3}$ of the specific adsorbate was taken in a series of conical flasks. Known amounts of the adsorbents were added to flasks. The flasks were kept in a temperature-controlled shaker and the aqueous solution-adsorbent mixtures were stirred at 150 rpm. At the end of the predetermined time, t , the flasks were withdrawn, their contents were centrifuged, and the filtrate was analyzed for the arsenic concentration. Adsorption kinetics was followed for 5 h and it was observed that after 1 h, there was gradual but very slow removal of the adsorbate from the solution. In order to understand the kinetics of adsorption of the sorbates, various kinetic models, like pseudo-first-order, pseudo-second-order, intra-particle diffusion and Bangham models were studied.

4.3.3 Adsorption Equilibrium Study

Experiments were carried out at the optimum pH_0 by contacting a fixed amount of adsorbent with 0.050 dm^3 of the respective sorbate solutions having C_0 in the range of $20\text{-}500 \mu\text{g dm}^{-3}$. After 3 h contact time the mixture was centrifuged the filtrate was analyzed for finding out the residual sorbates concentration. The sorbet uptake by the adsorbent was determined as:

$$q_e = \frac{(C_0 - C_e)V}{W} \quad (4.3.1)$$

where q_e is equilibrium amount of adsorbate adsorbed ($\mu\text{g g}^{-1}$), C_0 is initial concentration of adsorbate in aqueous solution ($\mu\text{g dm}^{-3}$), C_e equilibrium concentration ($\mu\text{g dm}^{-3}$), V is volume of aqueous solution (dm^3) and W is the weight of adsorbent (g).

Three two-parameter models, viz., Langmuir, Freundlich, and Temkin, and three-parameter model, Redlich-Peterson, were used to correlate the experimental equilibrium adsorption data.

4.3.4 Effect of Temperature and Estimation of Thermodynamic Parameters

The effect of temperature on the sorption characteristics was investigated by determining the adsorption isotherms at 283, 293, 303, 313 and 323 K. Isothermic heats of adsorption at various surface coverages have been determined using classical thermodynamic equations. C_0 was varied from 20 $\mu\text{g dm}^{-3}$ to 500 $\mu\text{g dm}^{-3}$ but the pH_0 of the solutions was maintained at 6.3-6.5.

4.3.5 Analysis of Arsenic

The analysis of the samples of As(III) and As(V) were done by using a Perkin Elmer, ICP-MS from the Institute Instrumentation Centre, Indian Institute of Technology, Roorkee, using Elanta software.

The percentage removal of the respective compound and equilibrium adsorption uptake in solid phase, q_e ($\mu\text{g g}^{-1}$), were calculated using the following relationships:

$$\text{Percentage removal} = 100 \frac{(C_0 - C_e)}{C_0} \quad (4.3.2)$$

Amount of adsorbate adsorbed per g of adsorbent,

$$q_e = \frac{(C_0 - C_e)V}{W}$$

where, C_0 is the initial concentration ($\mu\text{g dm}^{-3}$), C_e is the equilibrium concentration ($\mu\text{g dm}^{-3}$), V is the volume of the solution (dm^3) and W is the mass of the adsorbent (g).

4.4 ANALYSIS AND DISPOSAL OF SPENT ADSORBENTS

The spent adsorbents obtained as a result of adsorption of As-III and As-V were characterized by FTIR, SEM, and Thermogravimetric analyses.

4.4.1 Thermal Analysis

The thermal degradation (gasification) characteristics of the blank and spent adsorbents were studied using the thermo-gravimetric (TGA) and differential Thermal (DTA) analysis techniques. The thermal degradation of the adsorbents was carried out non-isothermally using the TGA analyzer from Perkin Elmer (Pyris Diamond).

In the present study, the operating pressure was kept slightly positive. The samples were prepared carefully after crushing and sieving so as to obtain homogeneous material properties. The sample was uniformly spread over the crucible base in all the experiments and the quantity of sample taken was 5-10 mg in all the runs. Experimental runs were taken under both nitrogen and air (oxidizing) atmospheres at $100^{\circ}\text{C min}^{-1}$ heating rate. The tests were conducted over a temperature range of temperature from the ambient temperature to 1000°C . Flow rate of nitrogen/air was maintained at 200 ml min^{-1} .

The weight loss at the constant heating rate was continuously recorded and downloaded using the software, Muse, Pyris Diamond. The instrument also provided the continuous recording of the results of the differential thermal gravimetry (DTG) and differential thermal analysis (DTA) as a function of sample temperature and time. The TG, DTG and DTA curves obtained in each case were analyzed to understand the behavior of thermal degradation.

RESULTS AND DISCUSSION

5.1 GENERAL

This chapter deals with the various results obtained from the experimental data.

These results include:

1. Characterization of adsorbents,
2. Batch adsorption Studies,
3. Kinetics of adsorption studies,
4. Studies on fit of various available isotherms,
5. Estimation of effective diffusivity, D_e ,
6. Thermal degradation kinetics of the spent adsorbents.

5.2 CHARACTERIZATION OF ADSORBENTS

5.2.1 Physical Characterization of Adsorbents

The fractional sieve analysis of the particles of BFA-Fe showed: -600+425 mesh size: 31.42%; -425+180 mesh size: 58.43%. The average particle diameter was found to be 381.45 mesh sizes. The fractional sieve analysis of the particles of RHA-Fe showed -600+425 mesh size: 35.72%; -425+300 mesh size: 49.58%; -300+180 mesh size: 13.50%. The average particle diameter was found to be 412 mesh sizes. The physical characteristics of the two adsorbents are presented in Table 5.2.1. Photograph of $FeCl_3$ coated BFA and RHA is given in Fig. 5.2.1.

Table 5.2.1 Physical characteristics of adsorbents

CHARACTERISTICS	BFA-Fe	RHA-Fe
Proximate analysis		
Moisture (%)	13.39	10.80
Volatile matter (%)	10.80	14.35
Ash (%)	55.22	70.58
Fixed Carbon (%)	19.59	4.25
Bulk density ($kg\ m^{-3}$)	133.3	175.3
Average particle size (μm)	381.45	412
BET Surface area of pores ($m^2\ g^{-1}$)	244.54	55.35

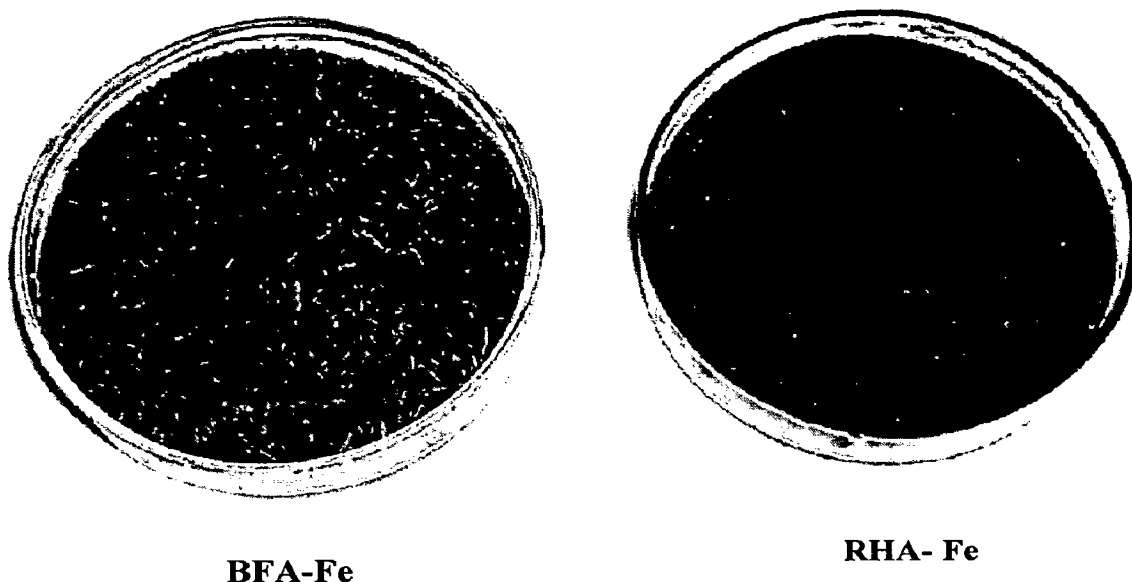


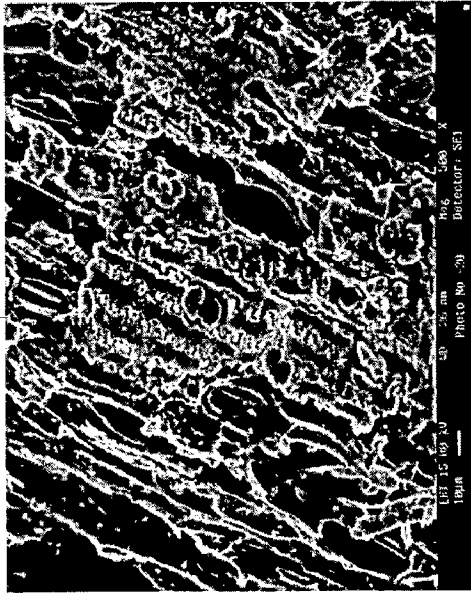
Fig. 5.2.1 Photograph of FeCl_3 coated BFA and RHA

It is observed that BFA-Fe has low bulk density when compared to RHA-Fe. The amount of ash is very high in RHA-Fe as compared to that of in BFA-Fe. High amount of ash indicates inorganic nature of RHA-Fe. The amount of carbon content is high in BFA-Fe when compared to RHA-Fe. Due to low carbon content, RHA-Fe is expected to have low porosity, and thereby low surface area.

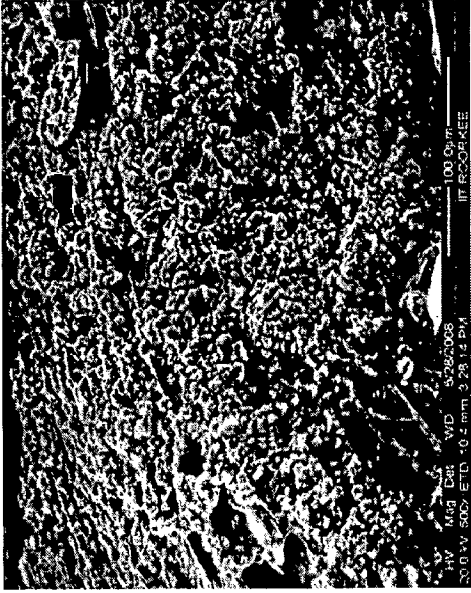
The morphologies of blank and As(III), and As(V)-loaded BFA-Fe, and RHA-Fe were examined by scanning electron microscopy (SEM) at 500x and 1000x magnifications. The SEM photographs of blank and As(III), and As(V)-loaded BFA-Fe and RHA-Fe were shown in Fig. 5.2.2 through 5.2.3. These figures reveal the surface texture and porosity of the blank and loaded adsorbents. SEM micrographs of BFA-Fe at 1000X magnification (Fig. 5.2.2) shows the fibrous structure and strands of the fiber. It can be inferred from these figures that the surface texture of the blank adsorbents changes after the adsorption of As. Similar changes after adsorption can be observed for the adsorption of As onto RHA-Fe (Fig. 5.2.3).

5.2.2 Energy dispersive X-ray analysis

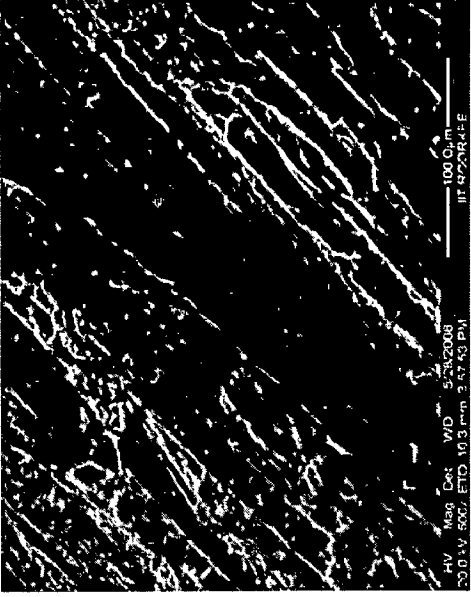
EDAX analysis of the adsorbents before and after adsorption was performed to estimate the composition of various elements present in the adsorbents. One of the SEM EDAX spectra for the blank BFA-Fe and RHA-Fe are shown in the Fig. 5.2.4, respectively. The analysis shows the BFA-Fe has more carbon content when compared to RHA-Fe. BFA-Fe has more affinity to impregnate FeCl_3 than that of RHA-Fe as shown by higher content of iron and chloride in BFA-Fe, (Table 5.2.2).



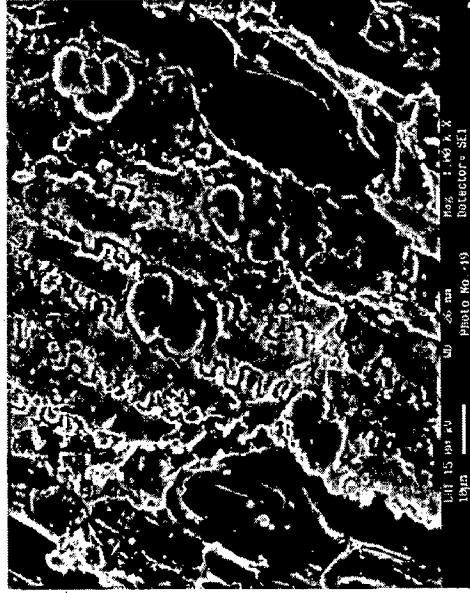
(a) Blank 500X



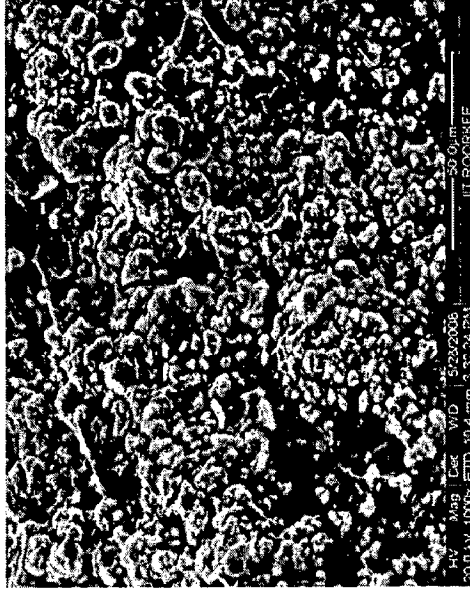
(b) BFA-As(III) 500X



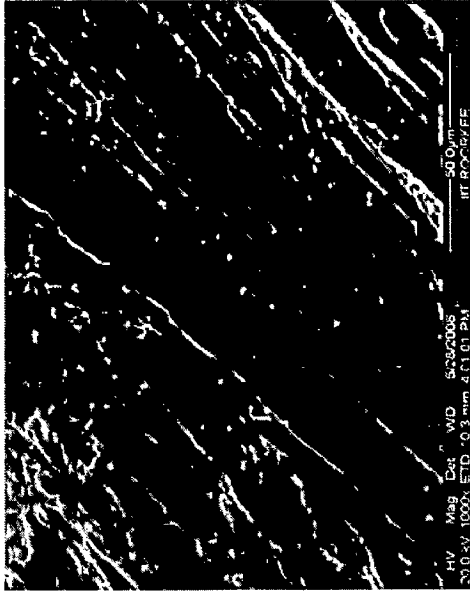
(c) BFA-As(V) 500X



(d) Blank 1000X



(e) BFA-As(III) 1000X

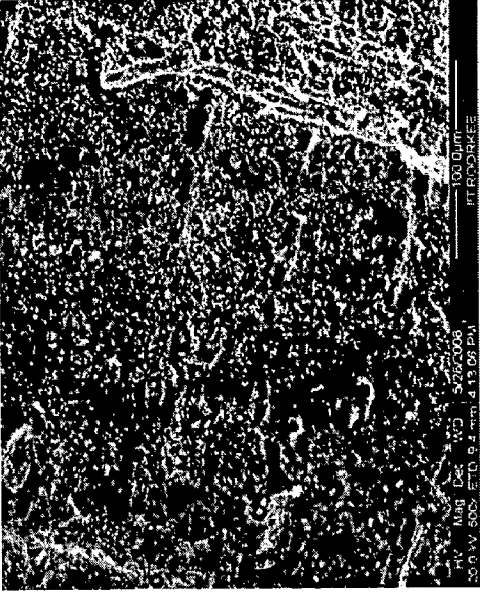


(f) BFA-As(V) 1000X

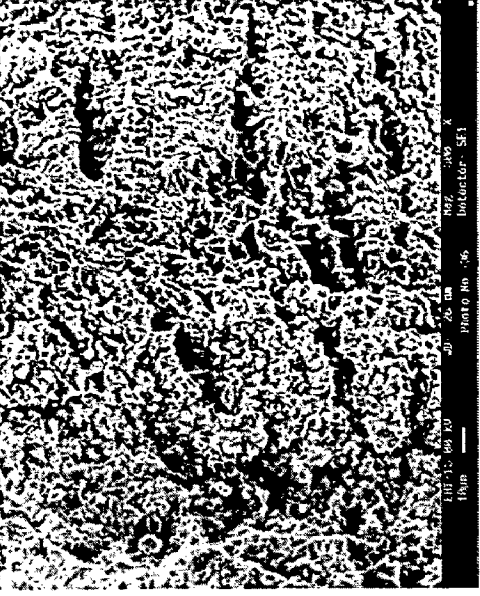
Fig. 5.2.2 SEM of blank, As(III) and As(V) loaded BFA-Fe at 500X and 1000X, respectively



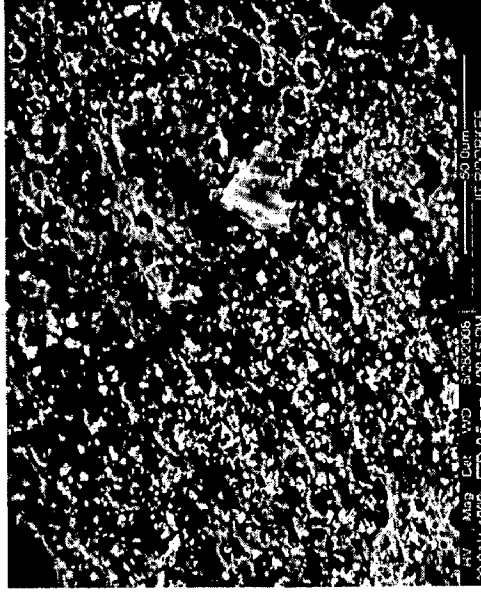
(a) Blank 500X



(b) RHA-As(III) 500X



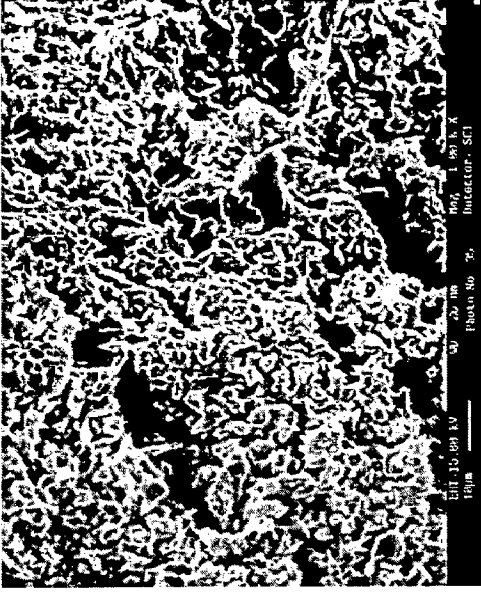
(c) RHA-As(V) 500X



(d) Blank 1000X

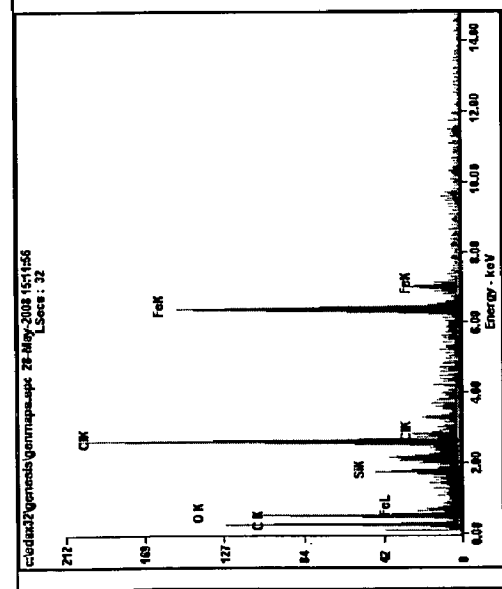


(e) RHA-As(III) 1000X

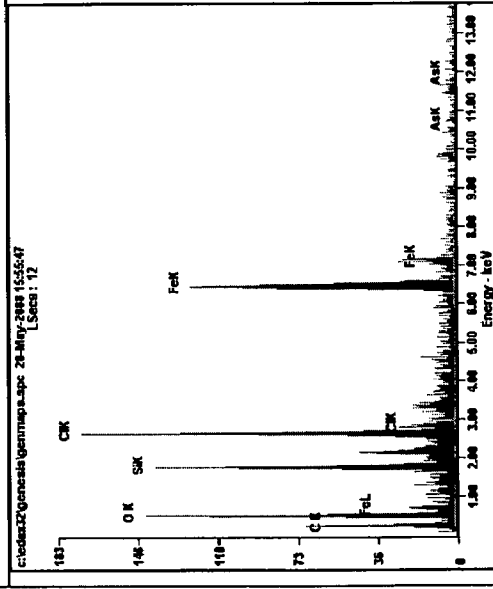


(f) RHA-As(V) 1000X

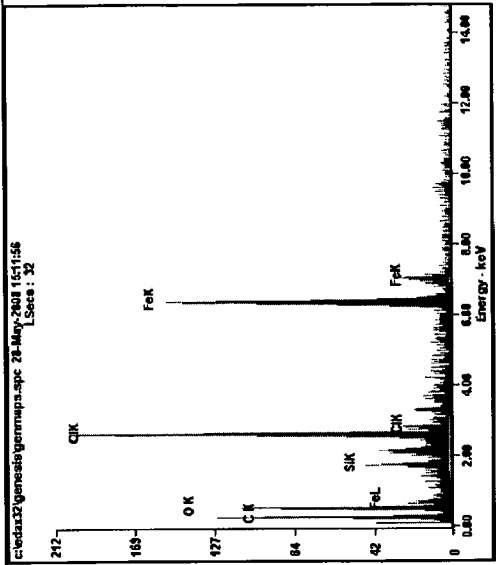
Fig. 5.2.3 SEM of blank As(III), and As(V) loaded RHA-Fe at 500X and 1000X, respectively.



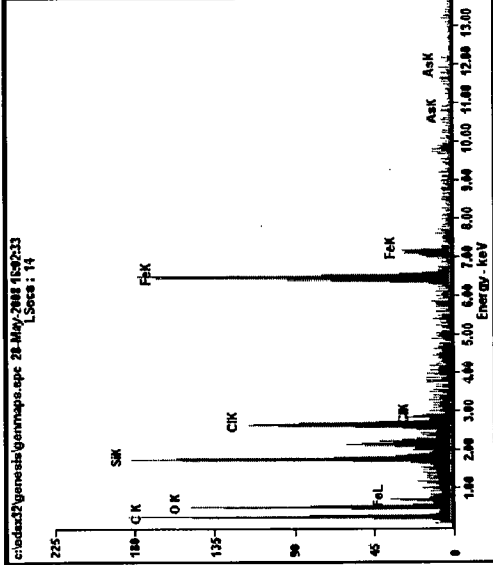
(a) BFA-Fe



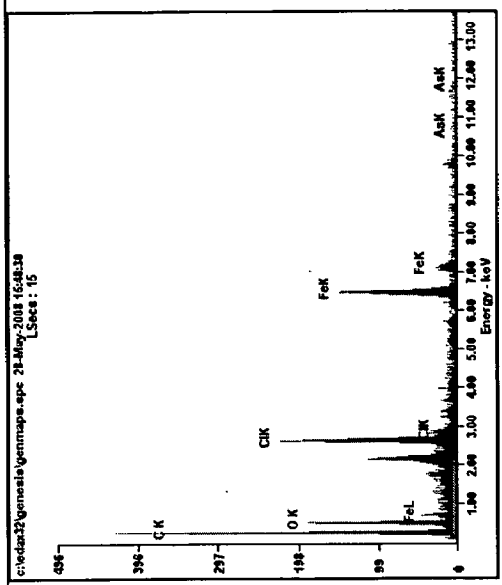
(d) RHA-Fe



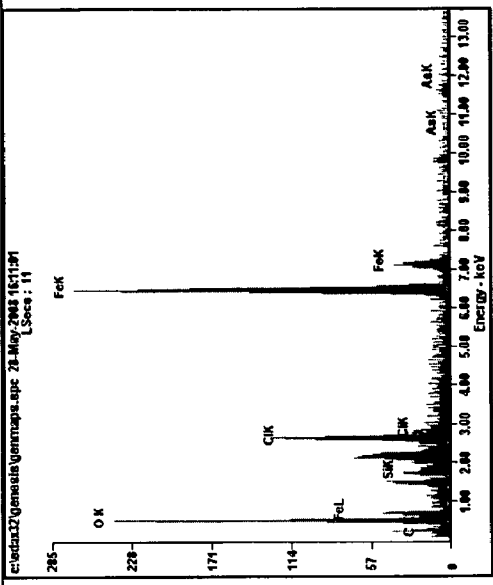
(b) BFA-Fe-As(III)



(e) RHA-Fe-As(III)



(c) BFA-Fe-As(V)



(f) RHA-Fe-As(V)

Fig. 5.2.4 EDAX spectra analysis of adsorbents before and after adsorption

Table 5.2.2 Elemental composition of adsorbents before and after adsorption

Element	Weight %					
	BFA-Fe	BFA-Fe-As(III)	BFA-Fe-As(V)	RHA-Fe	RHA-Fe-As(III)	RHA-Fe-As(V)
C	37.99	24.49	54.70	32.27	39.25	10.70
O	17.32	18.5	19.23	21.92	18.51	25.88
Si	2.00	0.34	0.00	7.48	7.00	1.39
Cl	10.44	4.79	6.61	9.19	5.08	6.97
Fe	32.25	50.48	19.17	29.14	29.08	53.22
As	0.00	1.40	0.30	0.00	1.09	1.83

5.2.3 FTIR Spectroscopy of the Adsorbents

The chemical structure of the adsorbents is very important in understanding the sorption process. The sorption capacity of adsorbents is strongly influenced by the chemical structure of their surface. The carbon-oxygen functional groups are by far the most important structures in influencing the surface characteristics and surface behavior of adsorbents. BFA-Fe and RHA-Fe have similar spectra as shown in Figs. 5.2.5 and 5.2.6. A broad band between 3100 and 3400 cm^{-1} in both the adsorbents is indicative of the presence of both free and hydrogen bonded OH groups on the adsorbent. This stretching is due to both the silanol groups (Si-OH) and adsorbed water (peak at 3400 cm^{-1}) on the surface. C-O group stretching from aldehydes and ketones can also be inferred from peaks at $\sim 1500 \text{ cm}^{-1}$. The band around $\sim 1400 \text{ cm}^{-1}$ in all both the adsorbents may be attributed to the carboxyl-carbonate structures. The functional groups suggested most often are: (i) carboxyl groups, (ii) phenolic hydroxyl groups, (iii) carbonyl groups (e.g. quinone-type), and (iv) lactone groups (e.g. fluorescein-type) Figs. 5.2.5 to Fig. 5.2.6 show the FTIR spectra of the blank various adsorbate and loaded adsorbents. Two clear peaks around 1400 to 1500 cm^{-1} and 1520 to 1550 cm^{-1} can be identified which seemed to be affected due to As-adsorption onto BFA-Fe and RHA-Fe. These peaks are normally attributed to adsorbed bound water onto the sorbent surface. The peak around 1400 cm^{-1} corresponds to bound water coordinated to cations. This may also be attributed to single C-N bond (not to hydrogen). The peak around 1530 cm^{-1} is attributed to hydrogen bending vibrations reflecting the presence of bound water. Upon As adsorption, these peaks get slightly shifted with the increase in transmittance.

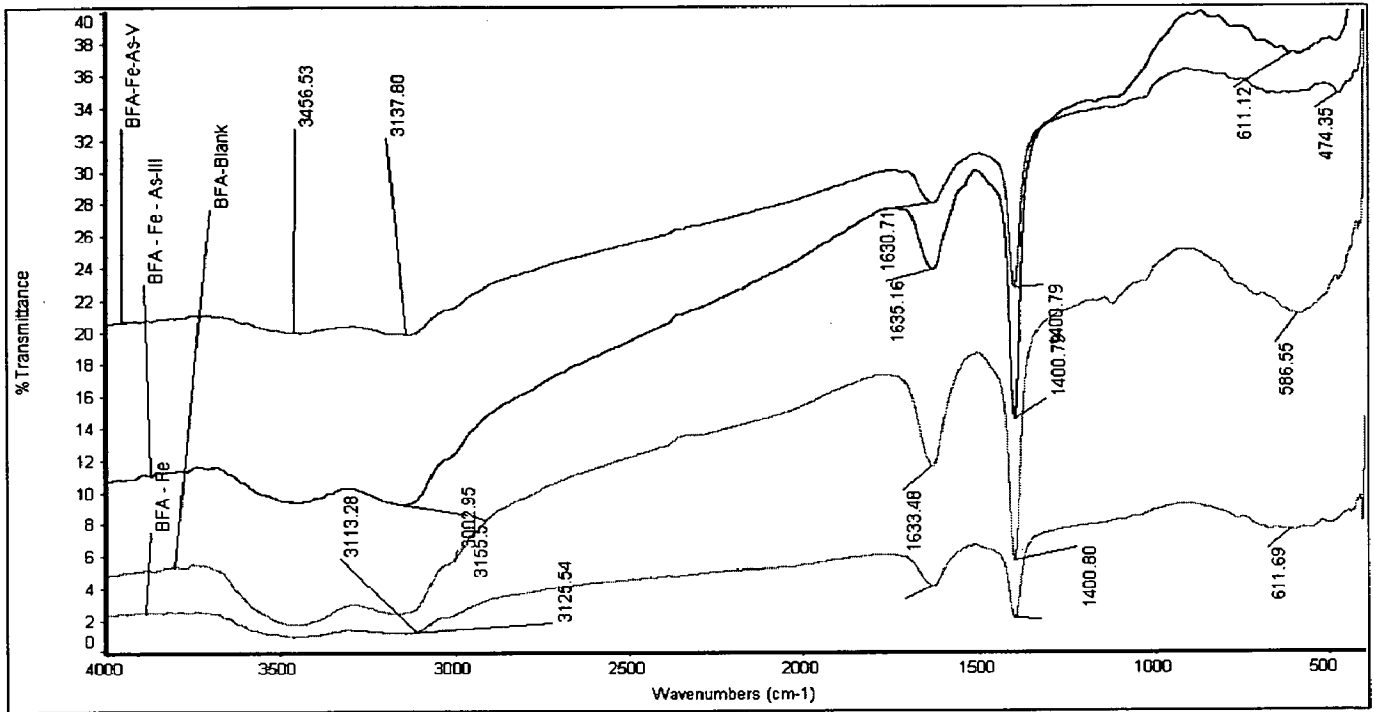


Fig 5.2.5 FTIR spectra of blank, As(III) and As(V) loaded BFA-Fe

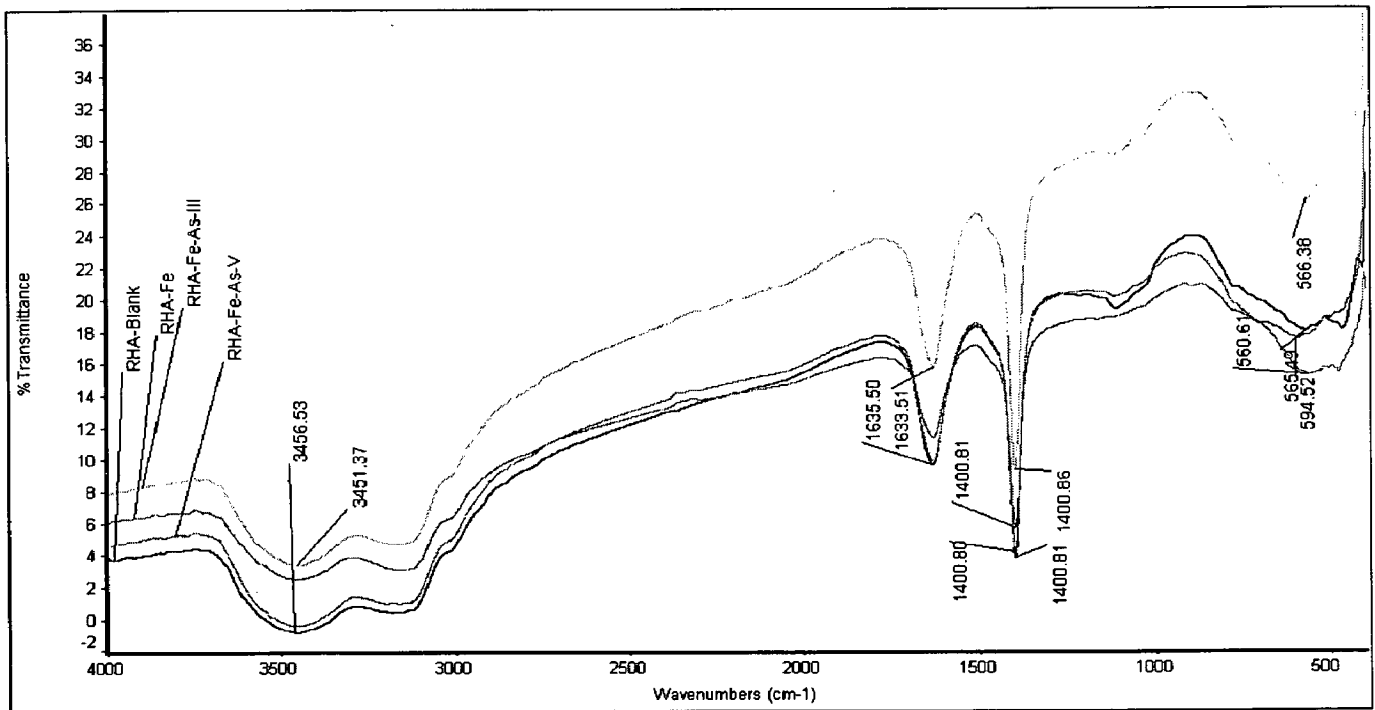


Fig 5.2.6 FTIR spectra of blank, As(III) and As(V) loaded RHA-Fe

5.3 BATCH ADSORPTION OF ARSENIC ONTO BFA-Fe AND RHA-Fe

Batch adsorption studies have been conducted for the removal of Arsenic (As(III) and As(V)), from aqueous solutions by BFA-Fe and RHA-Fe. Effect of various parameters viz. adsorbent dose (m), initial pH (pH_0), contact time (t), initial concentration (C_0), temperature (T) on the adsorption of As onto these adsorbents have been discussed in this section.

5.3.1 Effect of Adsorbent Dosage (m)

The effect of adsorbent dosage (m) on the amount adsorbed ($\mu\text{g g}^{-1}$ of adsorbent (q_e)), and the removal of As(III) and As(V) ($C_0 = 100 \mu\text{g dm}^{-3}$), by BFA-Fe and RHA-Fe are shown in Figs. 5.3.1 - 5.3.2. From the figures, it is found that the removal for a fixed concentration increases with an increase in amount of adsorbent but the capacity of the adsorbent for the sorption of adsorbate, i.e. the amount of adsorbate sorbed per unit weight of adsorbent, decreases with an increase in adsorbent dose. The increase in the removal of adsorbate with an increase in m for a fixed C_0 can be attributed to the greater surface area and increased number of adsorption sites (Lataye et al., 2005). From the Fig. 5.3.1 the optimum dosage of BFA-Fe for the removal of As(III) and As(V) is found to be 3 g dm^{-3} . Similarly, (Fig. 5.3.2) for the RHA-Fe the optimum dosage is 3 g dm^{-3} . Due to saturation in the sorption of the arsenic there is no much increase in the percent removal after that point.

5.3.2 Effect of Initial pH (pH_0)

The effect of pH_0 on the sorption of arsenic at the surface of BFA-Fe and RHA-Fe was studied with an initial arsenic concentration of $100 \mu\text{g dm}^{-3}$ at different pH ranging from 2-10. Effect of pH_0 on the removal of As(III) and As(V) by BFA-Fe, RHA-Fe is shown in Figs. 5.3.3 – 5.3.4, respectively. Percent removal and the final pH of the solution were measured and the results are shown in Table 5.3.1. From the results, it is apparent that maximum adsorption of arsenic on BFA-Fe and RHA-Fe was observed around pH 6.5 (Natural). In general, arsenate removal was slightly better in acidic region compared to basic conditions (Lakshmiathiraj et al., 2005). Fig. 5.3.3 and Fig. 5.3.4 reveals that, the efficiency of removal of As(III) and As(V) increases with an increase in pH from 2 to 6.5 and then slightly decreases on further increase in pH up to 10.5. The maximum As(III) and As(V) removal efficiency at pH 6.3 is $\sim 95\%$ and $\sim 94\%$, respectively.

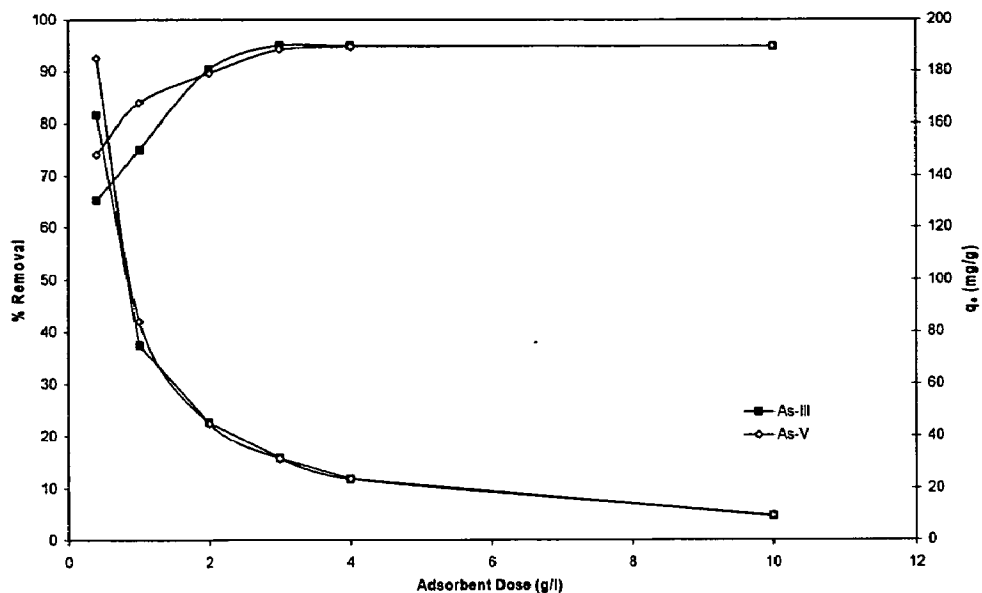


Fig. 5.3.1. Effect of BFA-Fe dose on the removal of As(III) and As(V) ($C_0 = 100 \mu\text{g dm}^{-3}$, $pH_0 = 6.3$ and 6.5 for As(III) and As(V) respectively, $T = 303 \text{ K}$, $t = 5 \text{ h}$).

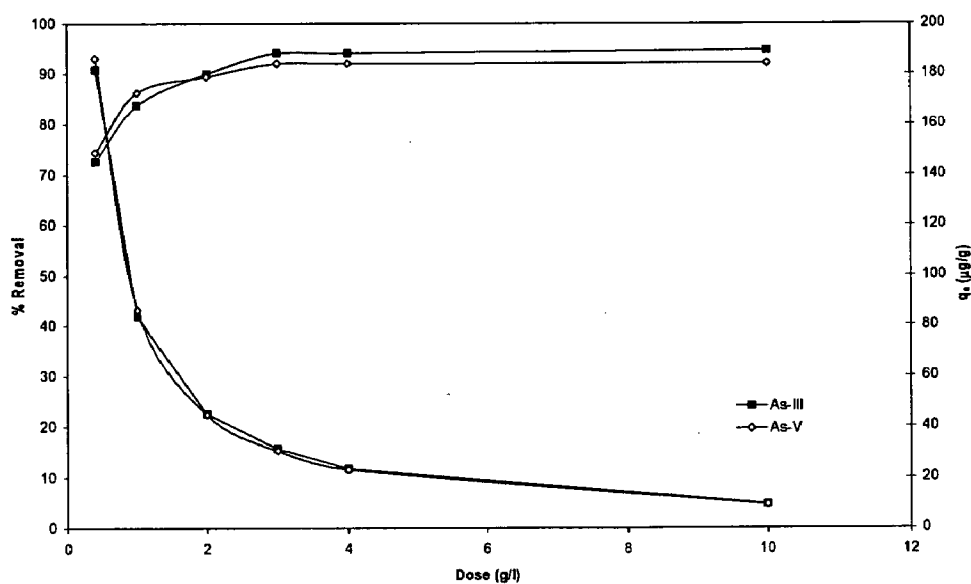


Fig. 5.3.2. Effect of RHA-Fe dose on the removal of As(III) and As(V) ($C_0 = 100 \mu\text{g dm}^{-3}$, $pH_0 = 6.3$ and 6.5 for As(III) and As(V) respectively, $T = 303 \text{ K}$, $t = 5 \text{ h}$).

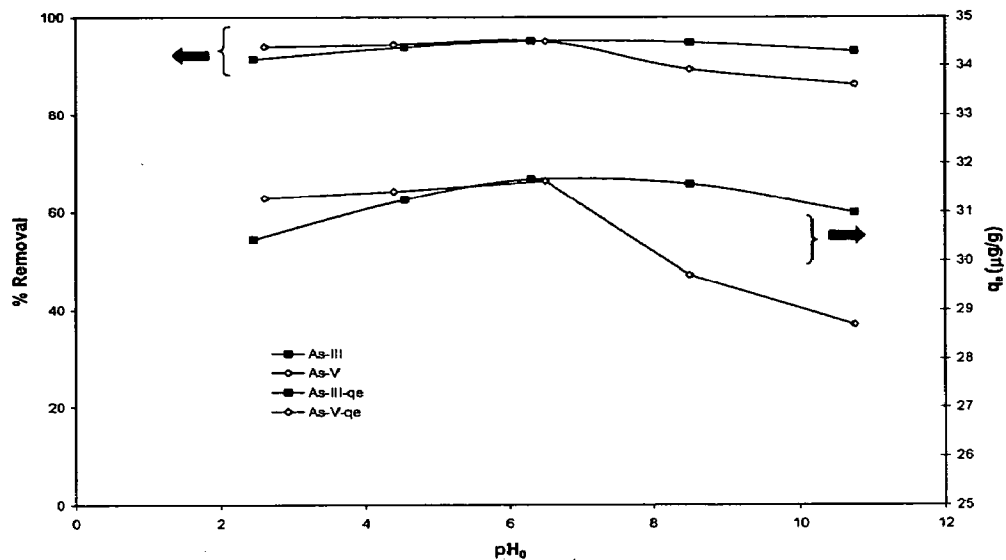


Fig. 5.3.3 Effect of initial pH on the equilibrium uptake and % removal of As(III) and As(V) ($C_0 = 100 \mu\text{g dm}^{-3}$, $m = 3 \text{ g dm}^{-3}$, $T = 303 \text{ K}$, $t = 5 \text{ h}$, $\text{RPM} = 150$) by BFA-Fe.

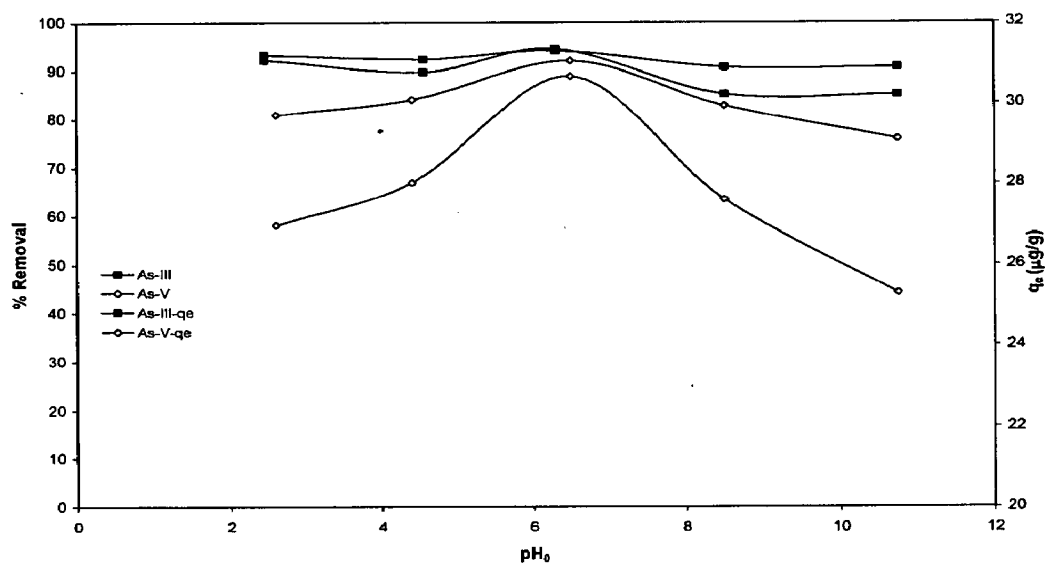


Fig. 5.3.4. Effect of initial pH on the equilibrium uptake and % removal of As(III) and As(V) ($C_0 = 100 \mu\text{g dm}^{-3}$, $m = 3 \text{ g dm}^{-3}$, $T = 303 \text{ K}$, $t = 5 \text{ h}$, $\text{RPM} = 150$) by RHA-Fe.

Table 5.3.1 Effect of initial pH of As on % Removal

BFA-Fe As(III)			BFA-Fe As(V)		
pH ₀	% Removal	pH _f	pH	% Removal	pH _f
2.45	91.30	2.53	2.50	93.85	2.29
4.55	93.77	2.47	4.40	94.11	2.48
6.30	95.02	2.44	6.50	94.25	2.54
8.50	94.74	1.77	8.50	89.15	2.54
10.75	92.97	2.55	10.75	85.08	2.55
RHA-Fe As(III)			RHA-Fe As(V)		
pH ₀	% Removal	pH _f	pH	% Removal	pH _f
2.45	93.19	2.23	2.50	80.9	2.39
4.55	92.29	2.53	4.40	84.04	2.52
6.30	93.99	2.5	6.50	91.97	2.52
8.50	90.55	2.55	8.50	82.77	2.55
10.75	90.54	2.84	10.75	75.85	2.79

5.3.3 Effect of Initial Concentration (C_0)

The effect of C_0 on the adsorption of As(III) and As(V) is shown in Figs. 5.3.5–5.3.6. The removal of As(III) and As(V) decreased with an increase in C_0 , although the total amount of adsorbate adsorbed per unit mass of adsorbent, i.e. q increased with an increase in C_0 . The increase in adsorption uptake with an increase in C_0 can be attributed to an increase in the driving force for adsorption.

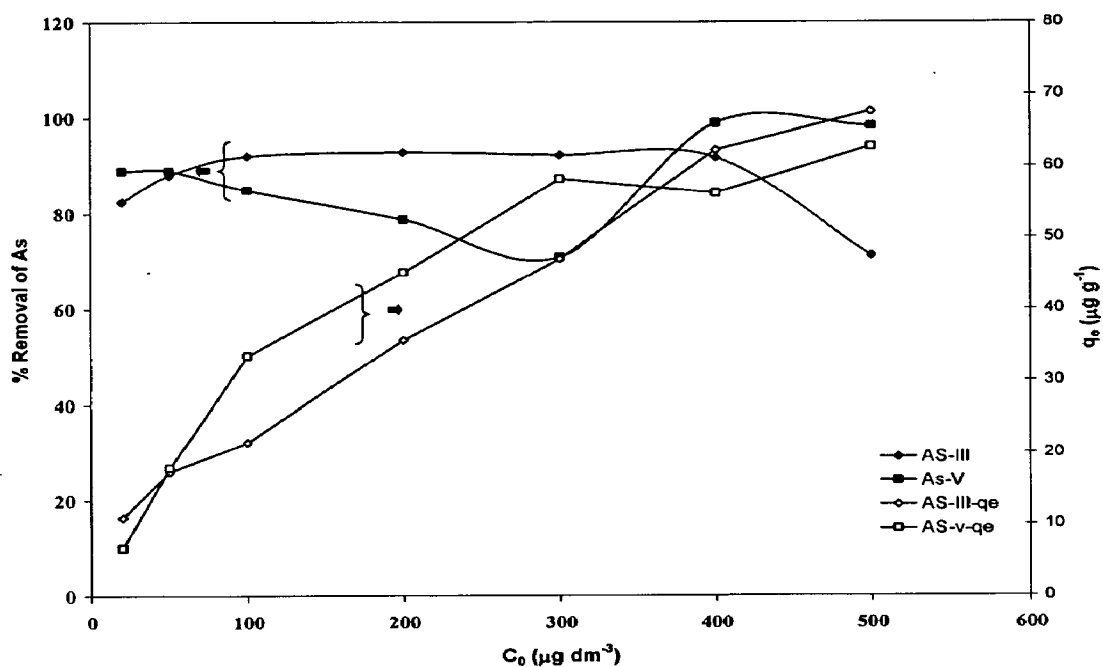


Fig. 5.3.5. Effect of initial concentration on the removal of As(III) and As(V) ($m = 3 \text{ g dm}^{-3}$, $T = 303 \text{ K}$, $\text{pH}_0 = \text{Natural (6.3)}$, $\text{RPM} = 150$, $\text{Time} = 5\text{h}$) by BFA-Fe.

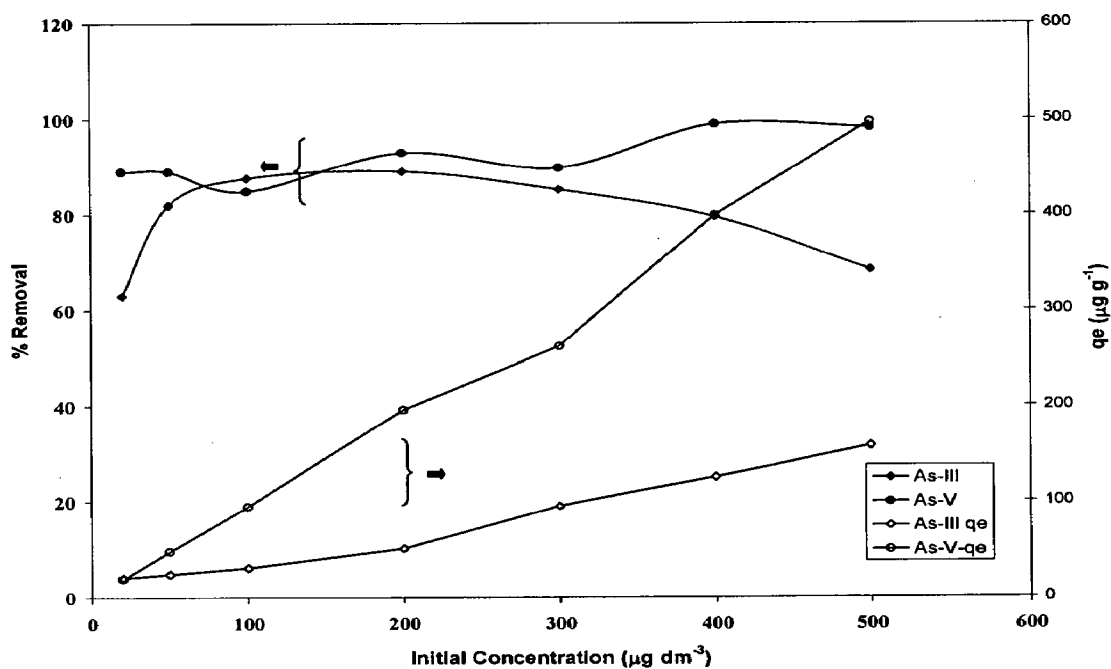


Fig. 5.3.6. Effect of initial concentration on the removal of As(III) and As(V) ($m = 3 \text{ g dm}^{-3}$, $T = 303 \text{ K}$, $\text{pH}_0 = \text{Natural (6.5)}$, $\text{RPM} = 150$, $\text{Time} = 5\text{h}$) by RHA-Fe.

5.3.4 Effect of Contact Time

The contact time, t between adsorbate and adsorbents is an important factor in the adsorption process. A rapid uptake of the adsorbate and the establishment of equilibrium in a short period signifies the efficacy of the adsorbent for its use in the removal processes. In physical adsorption, most of the adsorbate species are adsorbed within a short interval of contact time. The effect of t on the removal of As(III) and As(V) ($C_0 = 100 \mu\text{g dm}^{-3}$, $m = 3 \text{ g dm}^{-3}$) by BFA-Fe and RHA-Fe at $T = 303 \text{ K}$, and $pH_0 = 6.3-6.5$ is shown in Fig. 5.3.7- Fig. 5.3.11.

The figures show adsorption of arsenic is gradual over a period of 180 min and the residual As concentration after 180 min is $\sim 7 \mu\text{g dm}^{-3}$. For BFA-Fe-As system, about 85-87% of As from an aqueous solution of $C_0 = 100 \mu\text{g dm}^{-3}$ is adsorbed in ~ 50 min of contact time, thereafter, the As removal is low. The residual As concentration is $4-7 \mu\text{g dm}^{-3}$ after 3 h contact time. Since the difference in As removal at 3 h and 5 h is less than 1% of the 72 h removal, a steady-state approximation was assumed and a quasi-equilibrium situation was accepted at $t = 3 \text{ h}$ and further experiments were conducted under vigorous shaking conditions, at $t = 3 \text{ h}$ only.

Similar trends were observed for RHA-Fe-As adsorbate-adsorbent systems also. This is obvious from the fact that a large number of vacant surface sites are available for adsorption during the initial stage, and after a lapse of time, the remaining vacant surface sites are difficult to be occupied due to repulsive forces between the solute molecules on the solid surface and in the bulk solution phase. This results in the slowing down of the adsorption during the later period of adsorption. The residual concentrations at 3 h contact time were found to be higher by a maximum of $\sim 1\%$ than those obtained after 5 h contact time. Therefore, after 5 h contact time, a steady state approximation was assumed and a quasi-equilibrium situation was accepted for As with, RHA-Fe. Accordingly all the batch experiments were conducted with a contact time of 3 h under vigorous shaking conditions for RHA-Fe and BFA-Fe. Fig. 5.3.7 presents the plot of the time-course of As onto BFA-Fe and RHA-Fe.

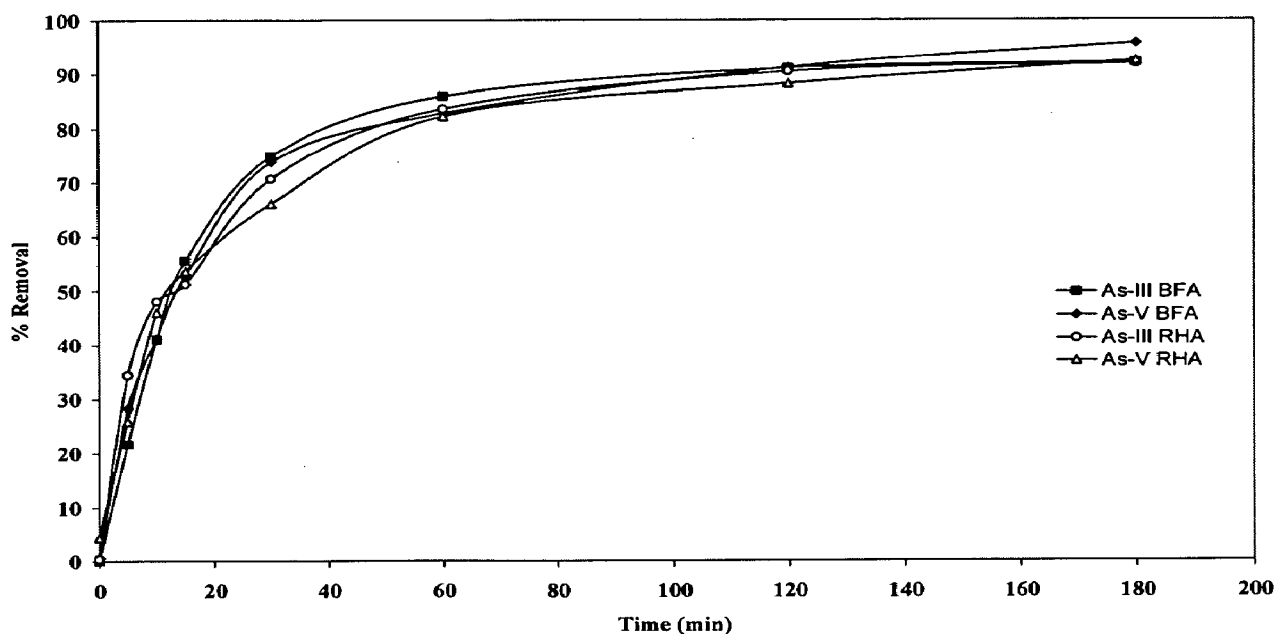


Fig. 5.3.7 Effect of contact time on the removal of As(III) and As(V) ($C_0 = 100 \mu\text{g dm}^{-3}$, $m = 3 \text{ g dm}^{-3}$, $T = 303 \text{ K}$, $\text{pH} = 6.3-6.5$, $\text{RPM} = 150$) by BFA-Fe and RHA-Fe.

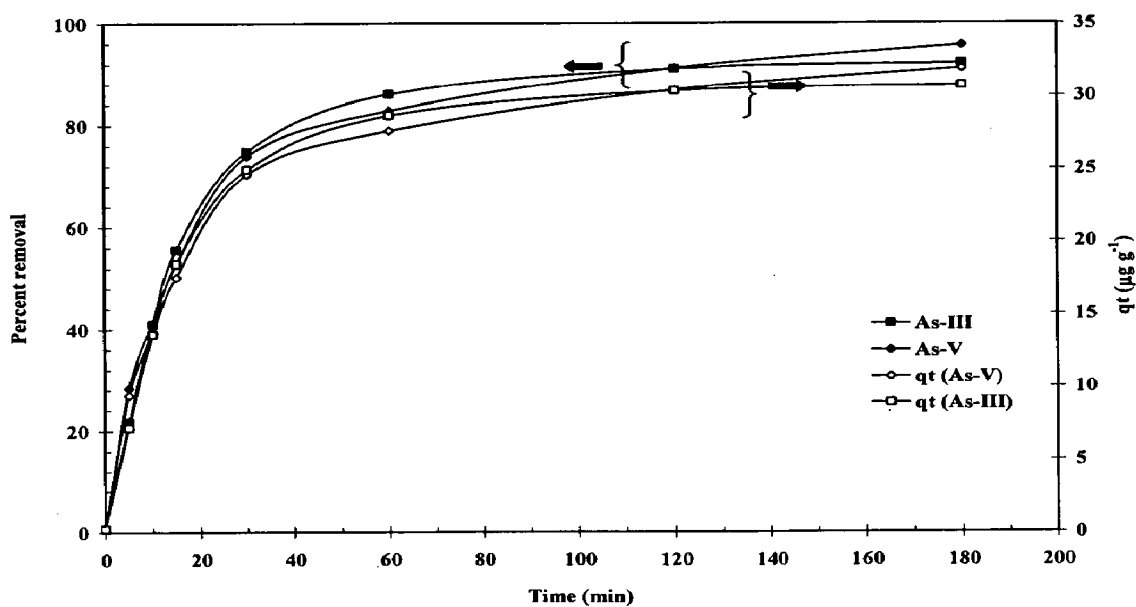


Fig. 5.3.8. Time versus Percent Removal plot for the removal of As(III) and As(V) by BFA-Fe. $T = 303 \text{ K}$, $C_0 = 100 \mu\text{g dm}^{-3}$, $m = 3 \text{ g dm}^{-3}$, $\text{RPM} = 150$.

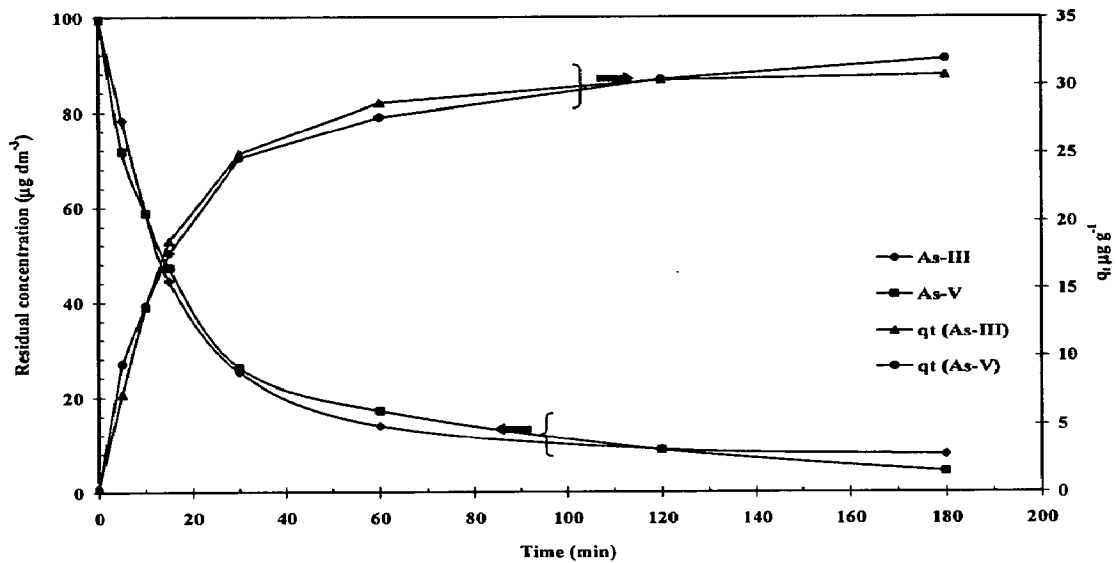


Fig. 5.3.9. Time versus Residual Concentration plot for the removal of As(III) and As(V) by BFA-Fe. $T = 303 \text{ K}$, $C_0 = 100 \mu\text{g dm}^{-3}$, $m = 3 \text{ g dm}^{-3}$, RPM = 150.

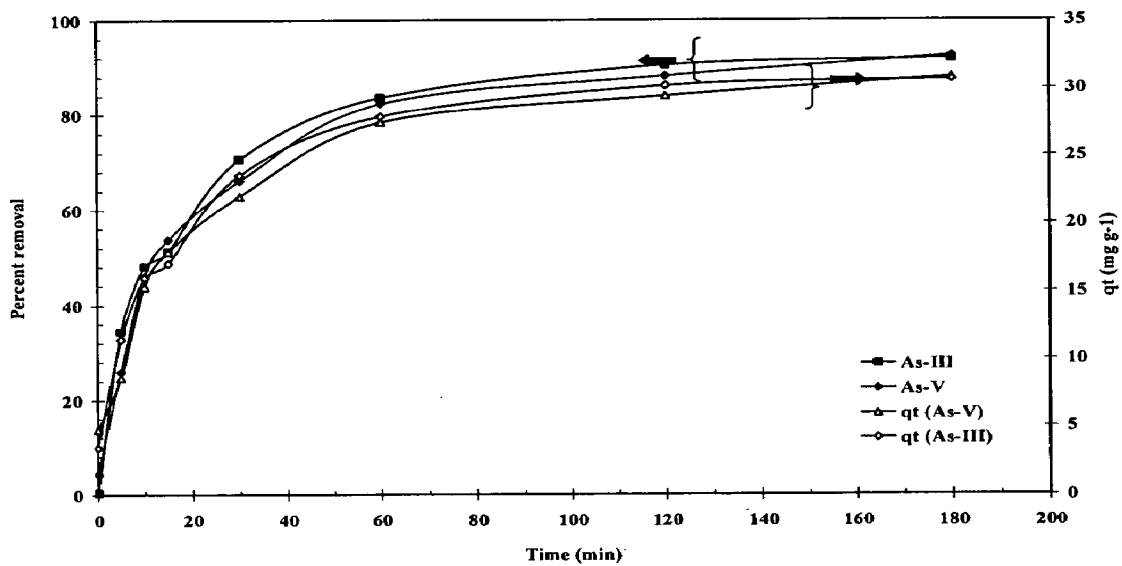


Fig. 5.3.10. Time versus Percent Removal plot for the removal of As(III) and As(V) by RHA-Fe. $T = 303 \text{ K}$, $C_0 = 100 \mu\text{g dm}^{-3}$, $m = 3 \text{ g dm}^{-3}$, RPM = 150.

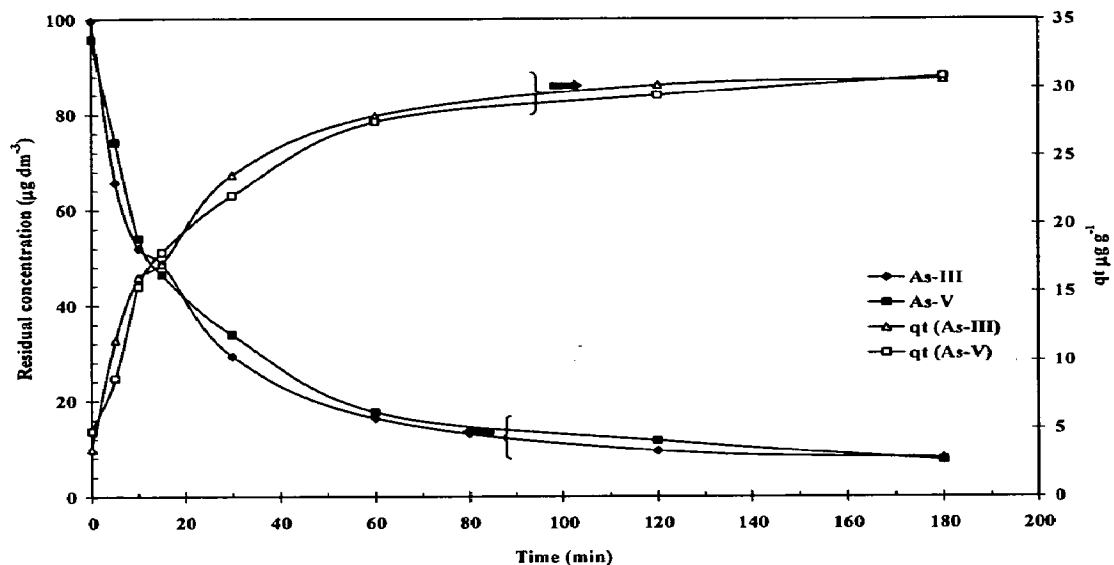


Fig. 5.3.11. Time versus Residual Concentration plot for the removal of As(III) and As(V) by RHA-Fe. $T = 303$ K, $C_0 = 100 \mu\text{g dm}^{-3}$, $m = 3 \text{ g dm}^{-3}$, RPM = 150.

5.3.5 Effect of Temperature

Temperature has a significant effect on the adsorptive capacity of the adsorbents. The effect of temperature on the removal of arsenic on BFA-Fe and RHA-Fe from drinking water was studied by varying the temperature from 283K to 323K. Figs. 5.3.12 - 5.3.15 shows the experimental adsorption isotherms, q_e versus C_e plots for the adsorption of As onto BFA-Fe and RHA-Fe. It is found that the sorption of As increases with an increase in temperature. Generally, sorption is an exothermic process and the sorption of As onto BFA-Fe and RHA-Fe shows the same behavior.

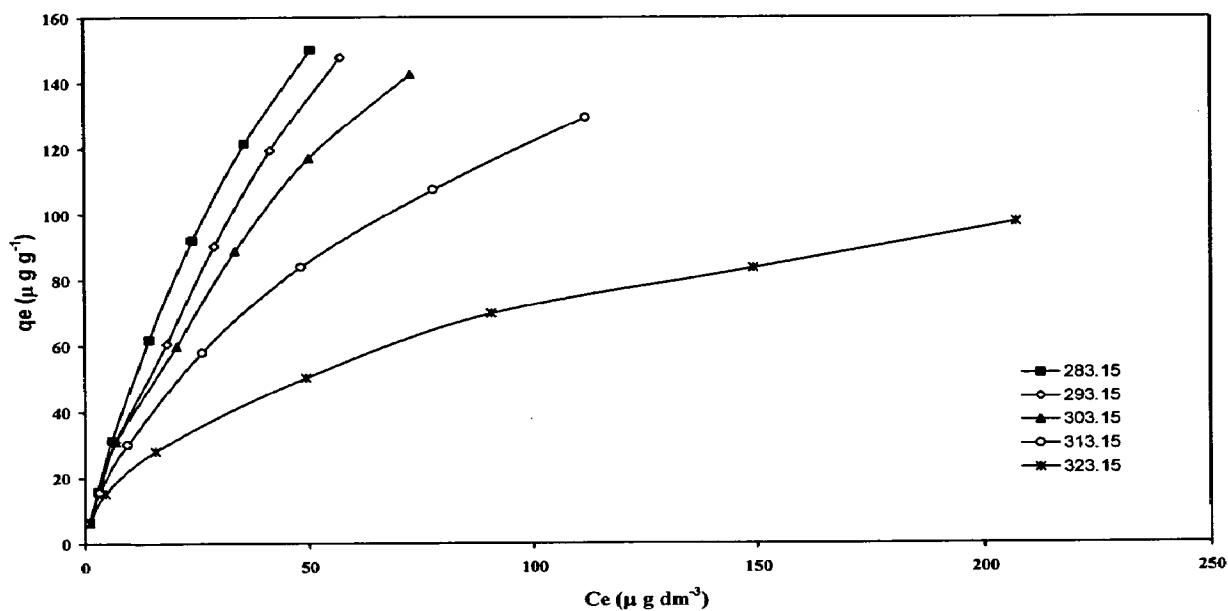


Fig. 5.3.12. Equilibrium adsorption isotherms at different temperatures for adsorption of As(III) onto BFA-Fe. ($pH_0=6.3$, $C_0 = 20-500 \mu\text{g dm}^{-3}$, $m = 3 \text{ g dm}^{-3}$).

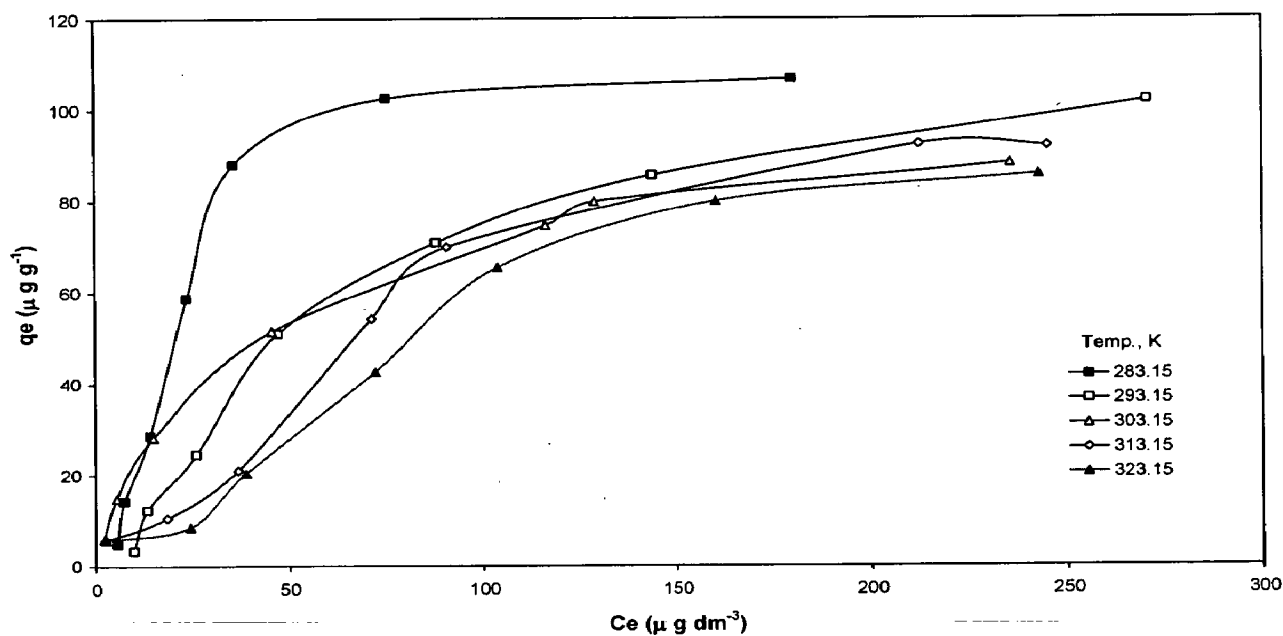


Fig. 5.3.13. Equilibrium adsorption isotherms at different temperatures for adsorption of As(V) onto BFA-Fe. ($pH_0= 6.5$, $C_0 = 20-500 \mu\text{g dm}^{-3}$, $m = 3 \text{ g dm}^{-3}$).

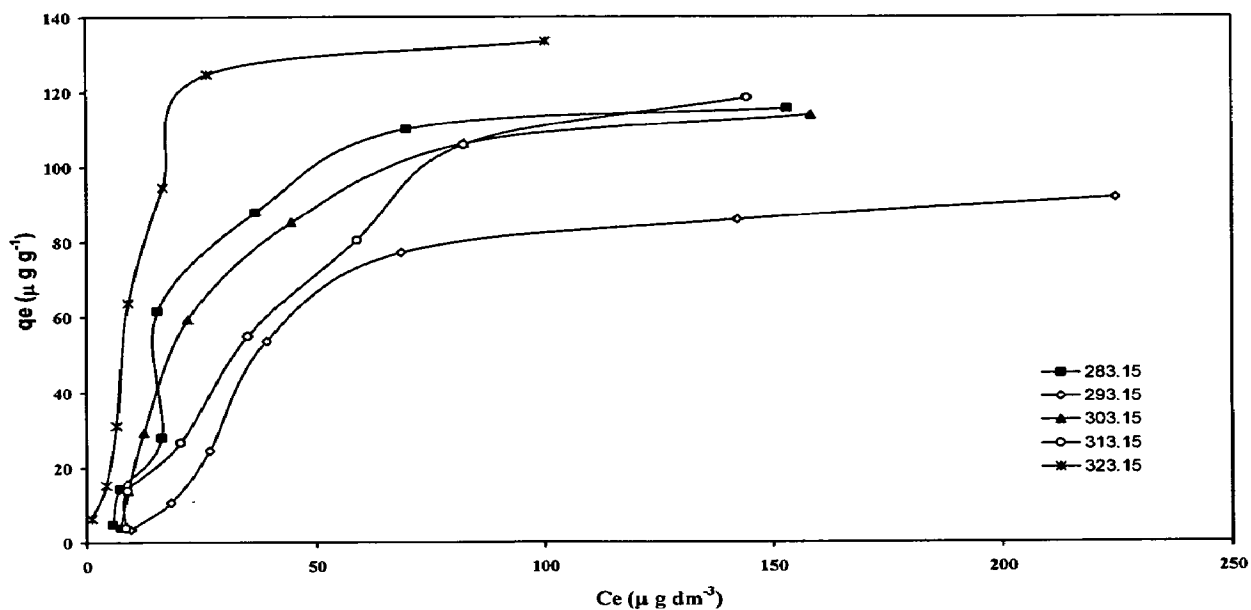


Fig. 5.3.14. Equilibrium adsorption isotherms at different temperatures for adsorption of As(III) onto RHA-Fe. ($pH_0 = 6.3$, $C_0 = 20-500 \mu\text{g dm}^{-3}$, $m = 3 \text{ g dm}^{-3}$).

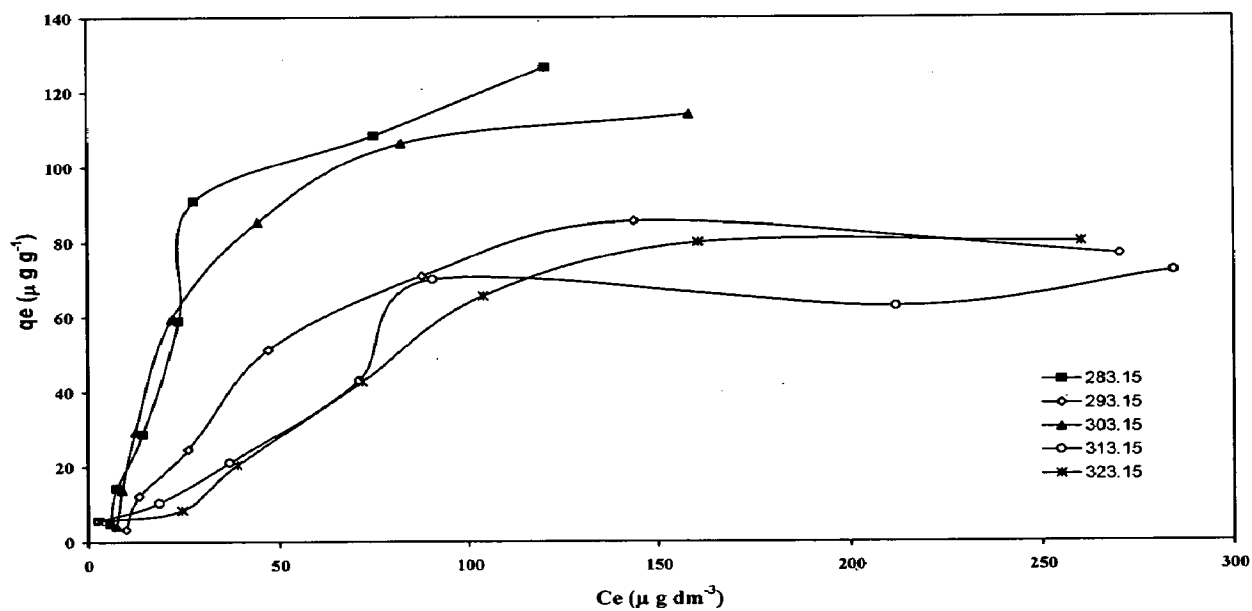


Fig. 5.3.15. Equilibrium adsorption isotherms at different temperatures for adsorption of As(V) onto RHA-Fe. ($pH_0 = 6.5$, $C_0 = 20-500 \mu\text{g dm}^{-3}$, $m = 3 \text{ g dm}^{-3}$).

5.3.6 Adsorption Kinetic Study

Pseudo-first-order, pseudo-second-order, intraparticle diffusion models and Bangham models are the frequently used models, for the kinetic study. So, these models are used to explain the sorption kinetics of As onto BFA-Fe and RHA-Fe.

5.3.6.1 Pseudo-first-order model

The pseudo-first-order equation is:

$$\frac{dq_t}{dt} = k_f (q_e - q_t) \quad (5.3.1)$$

Where, q_t is the amount of adsorbate adsorbed at time t ($\mu\text{g g}^{-1}$),

q_e is the adsorption capacity in equilibrium ($\mu\text{g g}^{-1}$),

k_f is the rate constant of pseudo-first-order model (min^{-1}), and

t is the time (min).

After definite integration by applying the initial conditions $q_t = 0$ at $t = 0$ and $q_t = q_t$ at $t = t$, the equation becomes,

$$\log(q_e - q_t) = \log q_e - \frac{k_f}{2.303} t \quad (5.3.2)$$

Values of adsorption rate constant (k_f) for arsenic adsorption onto BFA-Fe and RHA-Fe were determined from the plot $\log(q_e - q_t)$ vs. time. The values in the (Table 5.3.2) were determined from Eq. (5.3.2) by plotting $\log(q_e - q_t)$ against t for As onto BFA-Fe and RHA-Fe. There is a slight mismatch between the experimental results and that of the values calculated using the constants of the first order model. Experimental results did not follow first-order kinetics given by Eq. (5.3.1) as there was difference in two important aspects: (i) $k_f(q_e - q_t)$ does not represent the number of available sites, and (ii) $\log q_e$ was not equal to the intercept of the plot of $\log(q_e - q_t)$ against t .

5.3.6.2 Pseudo-second-order model

The pseudo-second-order model can be represented in the following form:

$$q_t = \frac{k_s q_e^2 t}{1 + k_s q_e t} \quad (5.3.3)$$

This equation has been solved by using non linear technique using Microsoft Excel's solver-add-in function constants k_s and q_e were obtained. Fig. 5.3.16- 5.3.17 shows a representative plot of q_t versus t (experimental and calculated) for adsorption of

As(III) and As(V) onto BFA-Fe and RHA-Fe, respectively. ($C_0 = 100 \mu\text{g dm}^{-3}$ at 30°C and at $pH_0 : 6.3-6.5$, $m = 3 \text{ g dm}^{-3}$). The values of the pseudo-first order and pseudo-second order correlation coefficients are tabulated in Table 5.3.2. The $q_{e,exp}$ and the $q_{e,cal}$ values for the pseudo-first-order model and pseudo-second-order models are also shown in Table 5.3.2. The $q_{e,exp}$ and the $q_{e,cal}$ values from the pseudo-second-order kinetic model are very close to each other. The calculated correlation coefficients are equal to unity for pseudo-second-order kinetics than that for the pseudo-first-order kinetic model. Therefore, the sorption can be approximated more appropriately by pseudo-second-order kinetic model than the other kinetic models for the adsorption of As(III) and As(V) onto BFA-Fe and RHA-Fe.

5.3.6.3 Intra-particle Diffusion model

Even though there are many resistances for the sorption process to take place, as discussed in the Chapter III, the overall adsorption process may be controlled by the slowest step, which is affecting more. That slowest step can be any one of the following: film or external diffusion, pore diffusion, surface diffusion and adsorption on the pore surface, or a combination of more than one step. Generally, a process is diffusion controlled if its rate is dependent upon the rate at which components diffuse towards one another. The possibility of intra-particle diffusion was explored by using the intra-particle diffusion model (Weber and Morris, 1953).

$$q_t = k_{int} t^{0.5} + C \quad (5.3.4)$$

where, k_{int} is the intra-particle diffusion rate constant ($\mu\text{g g}^{-1} \text{min}^{0.5}$) and C ($\mu\text{g g}^{-1}$) is a constant that gives idea about the thickness of the boundary layer, i.e., larger the value of C the greater is the boundary layer effect (Kannan and Sundaram, 2001). If the Weber-Morris plot of q_t versus $t^{0.5}$ satisfies the linear relationship with the experimental data, then the sorption process is found be controlled by intra-particle diffusion only. However, if the data exhibit multi-linear plots, then two or more steps influence the sorption process.

Fig. 5.3.18 shows a representative q_t versus $t^{0.5}$ plot for AS(III) and As(V) onto BFA-Fe for $C_0 = 100 \mu\text{g dm}^{-3}$ at 303 K and pH_0 6.3-6.5. Fig. 5.3.19 shows a representative q_t versus $t^{0.5}$ plot for AS(III) and As(V) onto RHA-Fe for $C_0 = 100 \mu\text{g dm}^{-3}$ at 303 K and $pH_0 = 6.3-6.5$.

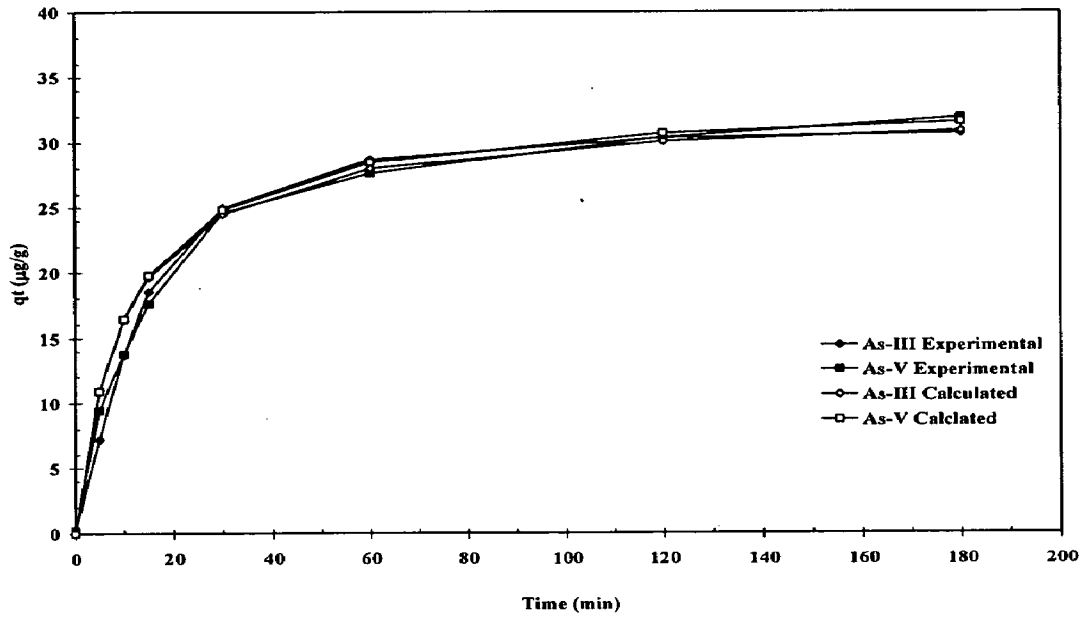


Fig. 5.3.16. Time versus q_t (Experimental and Calculated) plot for the removal of As(III) and As(V) by BFA-Fe. $T = 303 \text{ K}$, $C_0 = 100 \text{ } \mu\text{g dm}^{-3}$, $m = 3 \text{ g dm}^{-3}$.

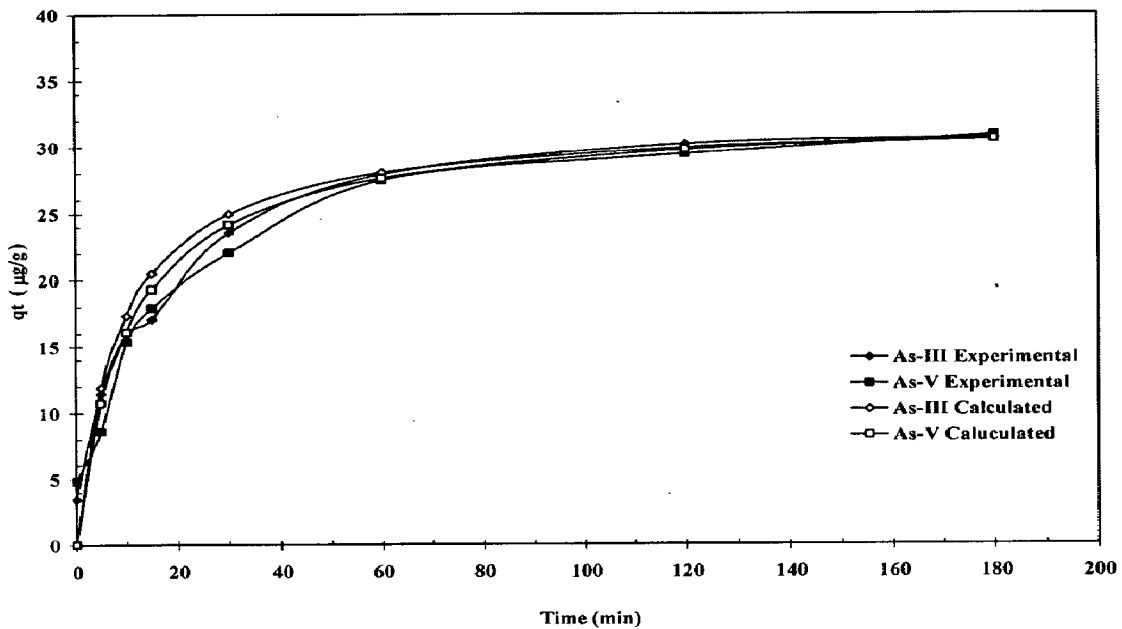


Fig. 5.3.17. Time versus q_t (Experimental and Calculated) plot for the removal of As(III) and As(V) by RHA-Fe. $T = 303 \text{ K}$, $C_0 = 100 \text{ } \mu\text{g dm}^{-3}$, $m = 3 \text{ g dm}^{-3}$.

Table 5.3.2. Kinetic parameters for the removal of As(III) and As(V) by BFA-Fe and RHA-Fe

Models	BFA-Fe		RHA-Fe	
	As(III)	As(V)	As(III)	As(V)
Pseudo-first-order				
Constants				
$q_{e,exp}$ ($\mu\text{g g}^{-1}$)	30.7030	31.8807	30.5227	30.8123
$q_{e,calc}$ ($\mu\text{g g}^{-1}$)	32.5503	28.2833	22.0515	28.1954
k_f (min^{-1})	0.0555	0.0453	0.0345	0.0540
R^2	0.9908	0.9995	0.9982	0.9819
Pseudo-second-order				
$q_{e,calc}$ ($\mu\text{g g}^{-1}$)	32.5773	33.3578	31.9911	32.1998
h ($\mu\text{g g}^{-1} \text{min}^{-1}$)	3.2500	3.1900	3.8225	3.2070
k_s ($\text{g } \mu\text{g}^{-1} \text{min}^{-1}$)	0.0031	0.0029	0.0037	0.0031
R^2	0.9970	0.9975	0.9983	0.9977
Intra particle diffusion				
k_{int1} ($\mu\text{g g}^{-1} \text{min}^{-1/2}$)	5.9014	4.9797	5.7335	5.7335
C_1 ($\mu\text{g g}^{-1}$)	-8.199	-1.8055	-3.7537	-3.7537
R^2	1	0.9991	0.9841	0.9841
k_{int2} ($\mu\text{g g}^{-1} \text{min}^{-1/2}$)	0.5912	0.9048	1.0321	1.0321
C_2 ($\mu\text{g g}^{-1}$)	22.174	20.1290	17.7250	17.7250
R^2	0.9181	0.9880	0.9355	0.9355
Bangham				
α	0.5395	1.3422	5.3944	1.4819
k_0 ($\mu\text{g}^{-1} \text{dm}^{-3}$)	3.9907	0.5195	0.5193	0.5708
R^2	0.553	0.724	0.8914	0.8955

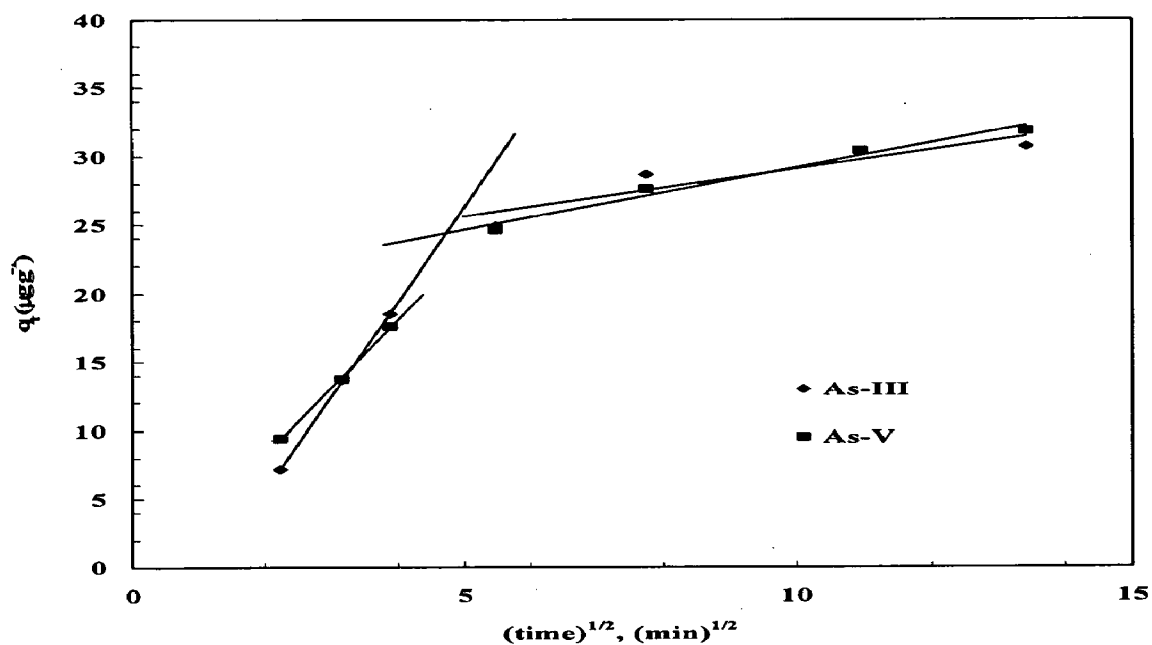


Fig. 5.3.18. Weber and Morris intra-particle diffusion plot for the removal of As(III) and As(V) by BFA-Fe. $T = 303 \text{ K}$, $C_0 = 100 \mu\text{g dm}^{-3}$, $m = 3 \text{ g dm}^{-3}$.

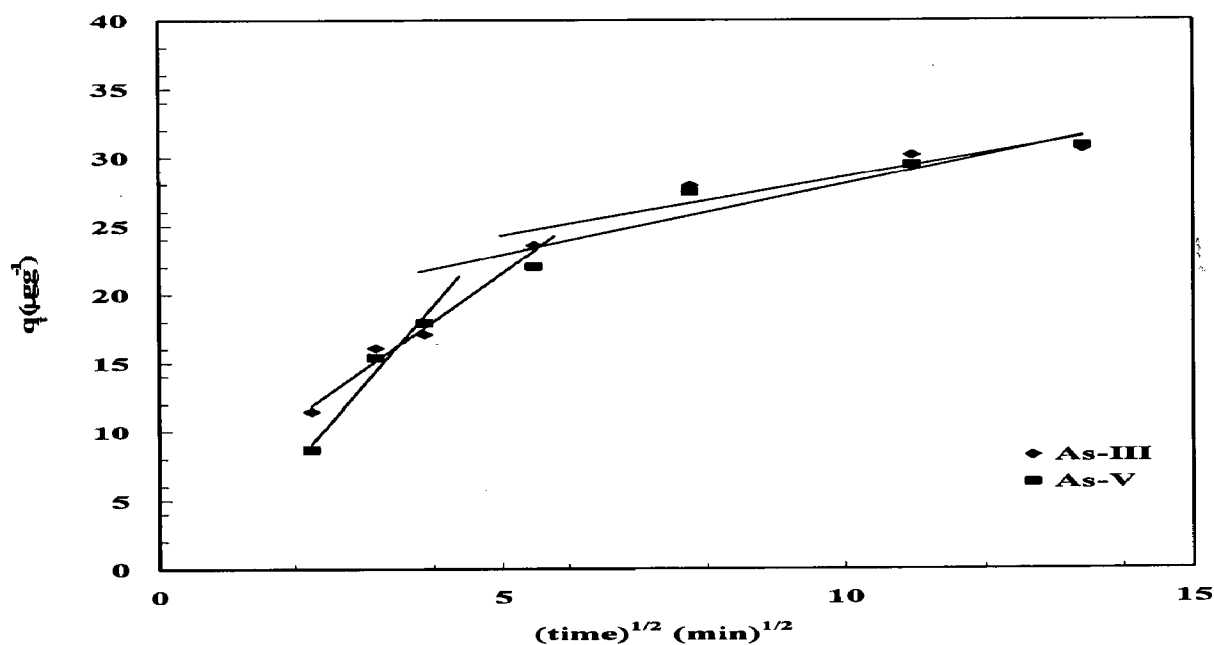


Fig. 5.3.19. Weber and Morris intra-particle diffusion plot for the removal of As(III) and As(V) by RHA-Fe. $T = 303 \text{ K}$, $C_0 = 100 \mu\text{g dm}^{-3}$, $m = 3 \text{ g dm}^{-3}$.

Extrapolation of the linear portions of the plots back to the y-axis gives the intercepts, which provide the measure of the boundary layer thickness. If the intercept is large, the boundary layer effect will also be large. The slope of the Weber-Morris plots - q_t versus $t^{0.5}$ - are defined as a rate parameter, characteristic of the rate of adsorption in the region where intra-particle diffusion is rate controlling. The values of rate parameters are given in Table 5.3.2. From the Fig. 5.3.18-5.3.19 it can be seen that the diffusion of ions into the pores of the adsorbent is the controlling-step during the sorption process.

5.3.6.4 Bangham's equation

Bangham's equation can be used to check the whether pore-diffusion is the only rate-controlling step or not in the adsorption system.

$$\log \log \left(\frac{C_0}{C_0 - q_t m} \right) = \log \left(\frac{k_{0B} m}{2.303V} \right) + \alpha \log(t) \quad (5.3.5)$$

where, $\alpha (<1)$ and k_{0B} are constants. If the experimental data are represented by Eq. (5.3.11), then it is an indication that the adsorption kinetics is limited by the pore diffusion. Fig. 5.3.20- Fig. 5.3.21 shows a representative plots of $\log \log(C_0/(C_0 - q_t m))$ versus $\log(t)$ plot for As adsorption onto BFA-Fe and RHA-Fe for $C_0 = 100 \mu\text{g dm}^{-3}$ at 303 K and at pH_0 6.3-6.5. However, the plots (Fig. 5.3.20 - Fig. 5.3.21) according to above equation did not yield linear curves and the values of R^2 are far from one. This shows that the diffusion of As into the pores of adsorbent is not the only rate-controlling step. Similar trend was observed for adsorption of As onto RHA-Fe. Values of the Bangham parameters and the correlation coefficients are given in Tables 5.3.2.

5.3.7 Determination of Diffusivity

Kinetic data could be treated by simplified form of Vermeulen's approximation (Vermeulen, 1953) to the model given by (Boyd et al., 1947), as discussed in Chapter III, for the calculation of effective particle diffusivity of adsorbates onto BFA-Fe and RHA-Fe.

$$F(t) = \left[1 - \exp \left(\frac{-\pi^2 D_e t}{R_a^2} \right) \right]^{1/2} \quad (5.3.6)$$

Thus, the slope of the plot of $\ln[1/(1 - F^2(t))]$ versus t gives D_e . The plots are shown in Fig. 5.3.22 - Fig.5.3.23. The values of effective diffusivity coefficient (D_e) of various

adsorbate-adsorbent system (as calculated from Eq. (5.3.14)) are tabulated in Table 5.3.3. This shows that As(III) have highest overall pore diffusion rate.

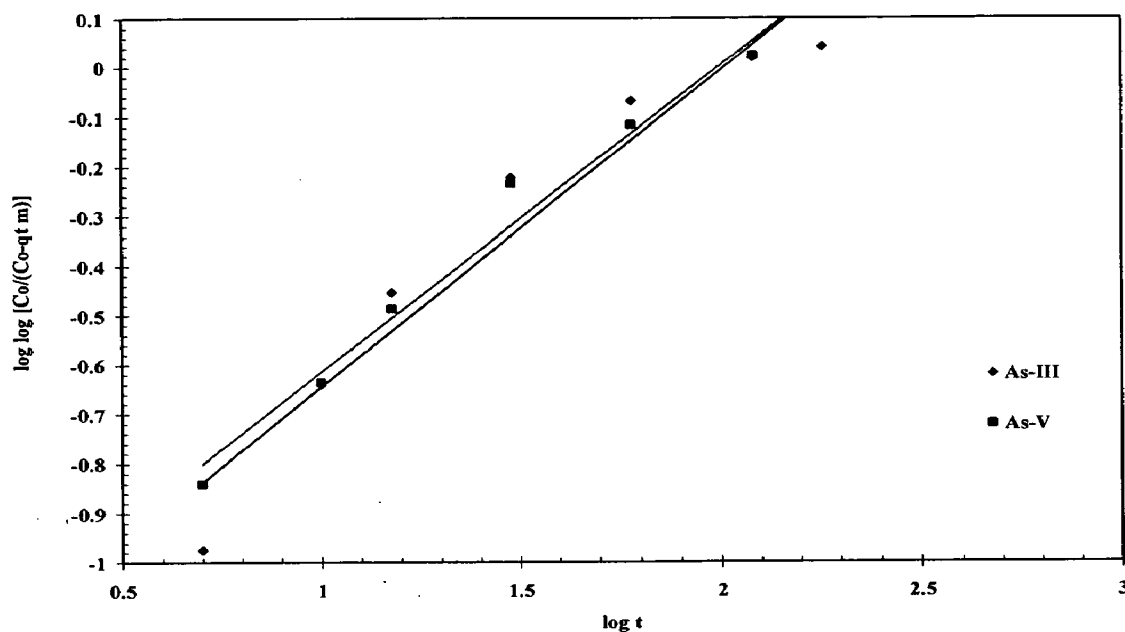


Fig. 5.3.20. Bangham plot for the removal of As(III) and As(V) by BFA-Fe.
 $T = 303 \text{ K}$, $C_0 = 100 \mu\text{g dm}^{-3}$, $m = 3 \text{ g dm}^{-3}$.

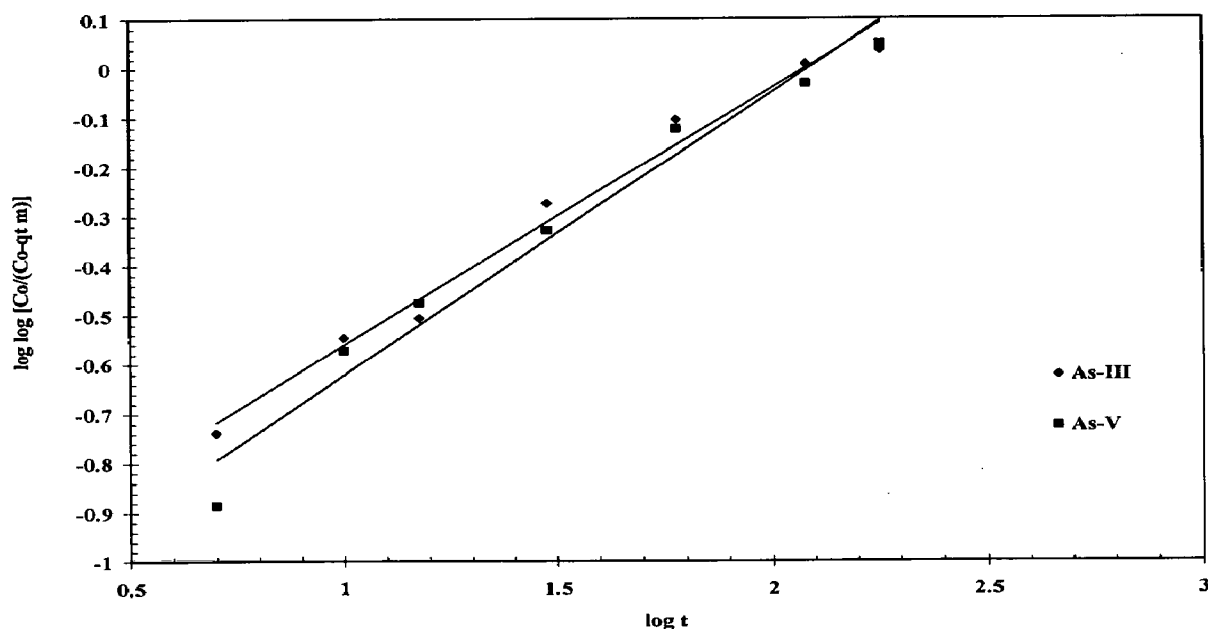


Fig. 5.3.21. Bangham plot for the removal of As(III) and As(V) by RHA-Fe.
 $T = 303 \text{ K}$, $C_0 = 100 \mu\text{g dm}^{-3}$, $m = 3 \text{ g dm}^{-3}$.

Table 5.3.3 Comparison of effective pore diffusivities of As(III) and As(V) for BFA-Fe and RHA-Fe.

		$D_e \text{ (m}^2 \text{ s}^{-1}) \times 10^{12}$	
BFA-Fe			
$C_o \text{ (}\mu\text{g dm}^{-3}\text{)}$	As(III)	As(V)	
100	7.95	4.89	
RHA-Fe			
$C_o \text{ (}\mu\text{g dm}^{-3}\text{)}$	As(III)	As(V)	
100	8.4	5.84	

5.4 ADSORPTION EQUILIBRIUM STUDY

The experimental equilibrium adsorption data of As(III) and As(V) onto BFA-Fe and RHA-Fe have been tested by using the three two-parameter Freundlich, Langmuir, and Temkin isotherm equations and a three parameter Redlich-Peterson (R-P) equation. As discussed in Chapter III, following equations represents these isotherms:

$$\text{Freundlich} \quad q_e = K_F C_e^{1/n} \quad (5.3.7)$$

$$\text{Langmuir} \quad q_e = \frac{q_m K_L C_e}{1 + K_L C_e} \quad (5.3.8)$$

$$\text{Temkin} \quad q_e = B_T \ln K_T + B_T \ln C_e \quad (5.3.9)$$

$$\text{Redlich-Peterson} \quad q_e = \frac{K_R C_e}{1 + a_R C_e^\beta} \quad (5.3.10)$$

The Freundlich isotherm is valid for a heterogeneous adsorbent surface with a non-uniform distribution of heat of adsorption over the surface. The Langmuir isotherm, however, assumes that the sorption takes place at specific homogeneous sites within the adsorbent. The Redlich-Peterson isotherm can, however be applied in homogenous as well as heterogeneous systems. Non-linear regression analysis was carried out using the solver-add-in function of Ms Excel to find out the isotherm parameters by fitting the experimental data.

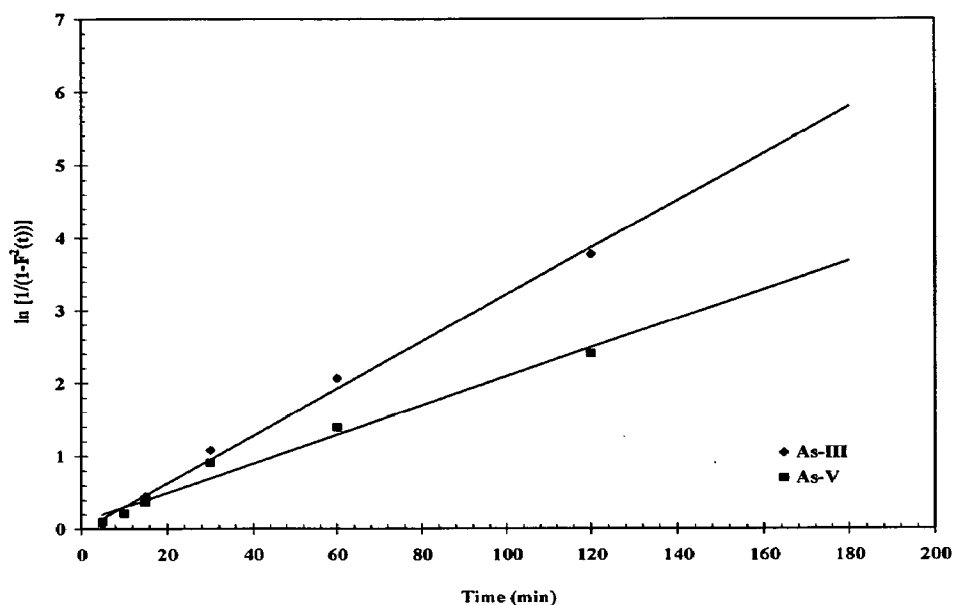


Fig. 5.3.22. $F(t)$ plot for the determination of effective pore diffusivity (D_e) of As(III) and As(V) by BFA-Fe. $T = 303$ K, $C_0 = 100 \mu\text{g dm}^{-3}$, $m = 3 \text{ g dm}^{-3}$

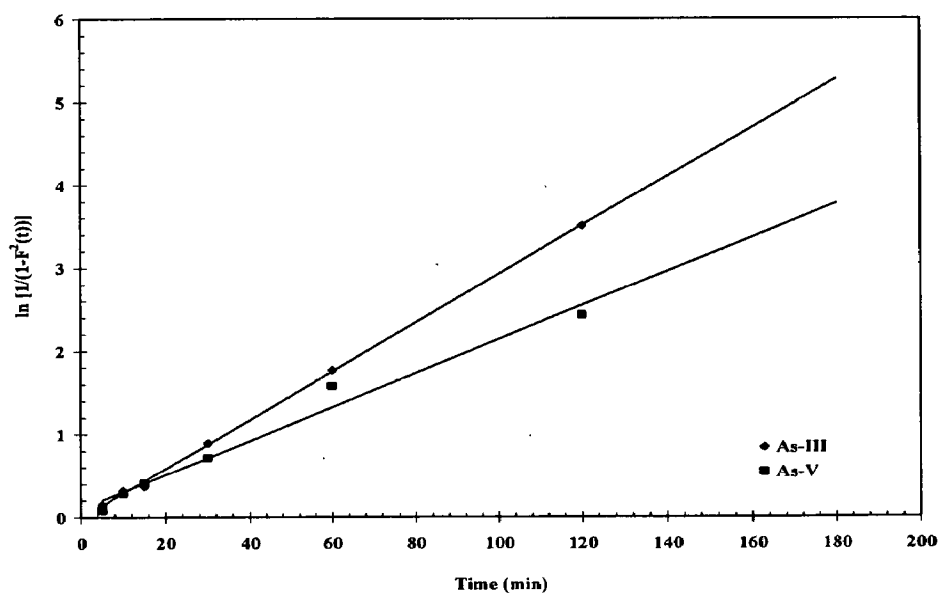


Fig. 5.3.23. $F(t)$ plot for the determination of effective pore diffusivity (D_e) of As(III) and As(V) by RHA-Fe. $T = 303$ K, $C_0 = 100 \mu\text{g dm}^{-3}$, $m = 3 \text{ g dm}^{-3}$

Two different error functions of non-linear regression basin were employed in this study to find out the most suitable kinetic and isotherm models to represent the experimental data. The hybrid fractional error function (HYBRID) (Porter et al., 1999) and

the Marquardt's percent standard deviation (MPSD) error function (Marquardt, 1953) have been used previously by a number of researchers in the field. These error functions are given as

$$HYBRID = \frac{100}{n-p} \sum_{i=1}^n \left| \frac{(q_{e,exp} - q_{e,calc})}{q_{e,exp}} \right|_i \quad (5.3.11)$$

$$MPSD = 100 \sqrt{\frac{1}{n-p} \sum_{i=1}^n \left(\frac{(q_{e,exp} - q_{e,calc})}{q_{e,exp}} \right)_i^2} \quad (5.3.12)$$

where, n is number of data points, P is number of unknown parameters, $q_{e,exp}$ is the experimental adsorption capacity ($\mu\text{g g}^{-1}$) and $q_{e,calc}$ is the adsorption capacity calculated by isotherm model ($\mu\text{g g}^{-1}$).

HYBRID was developed to improve the fit of the square of errors function at low concentration values. The MPSD is similar in some respects to a geometric mean error distribution modified according to the number of degrees of freedom of the system.

The parameters of the isotherm, and the correlation coefficient, R^2 for the fitting of the experimental data are listed in Tables 5.4.1 - 5.4.4. By comparing the results of the values for the error functions (Table 5.4.5 - Table 5.4.6) and correlation coefficients (Tables 5.4.1 to 5.4.4), it is found that for the As(III)- BFA-Fe system, Langmuir isotherms best represents the adsorption data at all temperatures for the As(V)-BFA-Fe, As(III)- RHA-Fe, As(V)-RHA-Fe, systems, Freundlich isotherm best-fit at all temperatures. For Freundlich isotherm, K_F and $1/n$ indicate the adsorption capacity and adsorption intensity, respectively. Higher the value of $1/n$, the higher will be the affinity between the adsorbate and the adsorbent, and the heterogeneity of the adsorbent sites. It is found from Tables 5.4.1 - 5.4.4 that the BFA-Fe showed greater heterogeneity for As(III) than that of for other adsorbate-adsorbent systems. Since for all the adsorbates, $1/n < 1$, the adsorbates are favourably adsorbed by BFA-Fe and RHA-Fe. BFA-Fe generally showed greater heterogeneity than RHA-Fe for As(III). For Langmuir isotherms, q_m is the monolayer saturation at equilibrium, whereas, K_L corresponds to the concentration at which the amount of adsorbates bound to the adsorbent. A high K_L value indicates a higher affinity. The data in Tables 5.4.1 - 5.4.4 also indicate that the q_m value for As(III) and As(V) of BFA-Fe were higher than that of for RHA-Fe.

Table 5.4.1. Isotherm parameters for the adsorption of As(III) onto BFA-Fe at different temperatures.

Isotherms	Constants	Temperatures (Kelvin, K)					
		283	293	303	313	323	
Langmuir	$K_L, \text{dm}^3 \mu\text{g}^{-1}$	0.034	0.008	0.245	0.018	0.002	
	$q_{\text{lim}}, \mu\text{g g}^{-1}$	109.890	144.928	13.514	217.391	553.595	
	R^2 (dm ³ linear)	0.932	0.951	0.991	0.997	0.993	
	R^2 (Non-Linear)	0.984	0.997	0.999	0.998	0.997	
	HYBRID	-1.885	-3.029	93.757	-0.218	-123.732	
	MPSD	12.153	5.025	81.154	4.092	150.113	
	$K_F, \text{dm}^3 \mu\text{g}^{-1}$	8.209	1.833	5.948	7.050	3.248	
Freundlich	n	1.883	1.314	1.511	1.513	1.802	
	1/n	0.531	0.751	0.521	0.551	0.555	
	R^2 (Linear)	0.891	0.984	0.952	0.953	0.955	
	R^2 (Non-Linear)	0.944	0.992	0.981	0.981	0.978	
	HYBRID	-1.545	-0.933	-1.571	-1.570	5.724	
	MPSD	19.045	13.718	17.199	18.232	20.277	
	B	25.475	23.579	25.139	39.938	11.857	
Temkin	$K_T, \text{dm}^3 \mu\text{g}^{-1}$	0.275	0.152	0.323	0.253	0.394	
	R^2 (Linear)	0.913	0.957	0.977	0.953	0.971	
	R^2 (Non-Linear)	0.955	0.978	0.989	0.981	0.985	
	HYBRID	-2.353	20.414	7.047	13.215	22.194	
	MPSD	10.855	75.181	33.357	50.847	58.844	
	$a_R, \text{dm}^3 \mu\text{g}^{-1}$	1.742	5.758	1.410	1.573	20.547	
	$K_R, \text{dm}^3 \mu\text{g}^{-1}$	8.400	12.000	12.292	15.805	58.723	
Redlich-Peterson	B	0.559	0.255	0.415	0.394	0.450	
	R^2 (Linear)	0.887	0.853	0.782	0.889	0.934	
	R^2 (Non-Linear)	0.942	0.877	0.884	0.942	0.955	
	HYBRID	108.144	-1.001	-1.405	-1.551	2.239	
	MPSD	82.139	14.977	22.324	18.315	33.301	

Table 5.4.2. Isotherm parameters for the adsorption of As(V) onto BFA-Fe at different temperatures.

Isotherms	Constants	Temperatures (Kelvin, K)					
		283	293	303	313	323	
Langmuir	$K_L, \text{dm}^3 \mu\text{g}^{-1}$	0.005	0.007	0.011	0.014	0.011	
	$q_{\text{max}}, \mu\text{g.g}^{-1}$	555.555	133.333	357.143	81.957	115.279	
	R^2 (Linear)	0.701	0.904	0.845	0.978	0.872	
	R^2 (Non-Linear)	0.837	0.951	0.921	0.989	0.934	
	HYBRID	-53.388	58.381	-2.371	4.148	5.250	
	MPSD	47.282	50.771	19.200	15.785	28.029	
Freundlich	$K_F, \text{dm}^3 \mu\text{g}^{-1}$	2.121	3.255	4.495	2.527	2.940	
	n	1.059	1.405	1.172	1.504	1.542	
	$1/n$	0.935	0.712	0.853	0.524	0.548	
	R^2 (Linear)	0.987	0.981	0.955	0.987	0.999	
	R^2 (Non-Linear)	0.993	0.990	0.978	0.994	1.000	
	HYBRID	-0.884	-0.928	-3.721	-0.905	3.138	
Temkin	MPSD	12.378	13.595	27.511	11.772	23.757	
	B	45.278	22.252	48.904	13.810	15.800	
	$K_T, \text{dm}^3 \mu\text{g}^{-1}$	0.154	0.271	0.314	0.305	0.280	
	R^2 (Linear)	0.908	0.889	0.945	0.919	0.833	
	R^2 (Non-Linear)	0.953	0.943	0.973	0.959	0.913	
	HYBRID	25.703	15.775	53.709	-385.128	25.534	
Redlich-Peterson	MPSD	80.909	85.552	170.095	485.235	83.789	
	$a_R, \text{dm}^3 \mu\text{g}^{-1}$	20.359	0.851	3.020	11.830	251.548	
	$K_R, \text{dm}^3 \mu\text{g}^{-1}$	45.233	5.375	15.745	31.712	759.723	
	B	0.057	0.911	0.138	0.385	0.352	
	R^2 (Linear)	0.251	0.757	0.254	0.958	0.998	
	R^2 (Non-Linear)	0.510	0.941	0.504	0.990	0.999	
HYBRID		-0.737	49.402	-8.184	-0.755	4.014	
	MPSD	13.780	40.392	32.584	12.771	25.559	

Table 5.4.3. Isotherm parameters for the adsorption of As(III) onto RHA-Fe at different temperatures.

Isotherms	Constants	Temperatures (Kelvin, K)				
		283	293	303	313	323
Langmuir	$K_L, \text{dm}^3 \mu\text{g}^{-1}$	0.071	0.009	0.128	0.007	0.052
	$q_m, \mu\text{g g}^{-1}$	37.037	92.593	23.810	294.118	112.350
	R^2 (Linear)	0.932	0.951	0.991	0.979	0.997
	R^2 (Non-Linear)	0.955	0.980	0.995	0.989	0.998
	HYBRID	73.934	38.571	91.254	-5.195	-2.505
	MPSD	58.120	40.235	79.471	5.572	35.827
Freundlich	$K_F, \text{dm}^3 \mu\text{g}^{-1}$	3.572	1.131	3.015	2.912	13.700
	n	1.205	1.039	1.434	1.235	2.581
	$1/n$	0.830	0.952	0.597	0.809	0.387
	R^2 (Linear)	0.975	1.000	0.978	0.988	0.950
	R^2 (Non-Linear)	0.987	1.000	0.989	0.994	0.980
	HYBRID	-1.485	-38.994	52.739	-0.485	-12.855
Temkin	MPSD	17.805	33.142	53.517	10.894	43.712
	B	53.347	45.189	45.257	42.891	17.425
	$K_T, \text{dm}^3 \mu\text{g}^{-1}$	0.157	0.073	0.175	0.141	1.027
	R^2 (Linear)	0.955	0.882	0.985	0.952	0.955
	R^2 (Non-Linear)	0.982	0.939	0.993	0.981	0.983
	HYBRID	17.513	39.532	3.207	9.551	-0.937
Redlich-Peterson	MPSD	50.198	147.483	22.535	32.718	43.919
	$a_R, \text{dm}^3 \mu\text{g}^{-1}$	5.535	5.090	2.214	10.045	55.552
	$K_R, \text{dm}^3 \mu\text{g}^{-1}$	23.200	5.375	15.745	31.712	759.723
	B	0.184	0.044	0.345	0.200	0.515
	R^2 (Linear)	0.517	0.745	0.848	0.824	0.984
	R^2 (Non-Linear)	0.785	0.584	0.921	0.841	0.992
HYBRID		-2.050	-0.070	-7.727	-0.511	-15.079
	MPSD	19.784	3.058	15.783	12.089	48.594

Table 5.4.4. Isotherm parameters for the adsorption of AS(V) onto RHA-Fe at different temperatures.

Isotherms	Constants	Temperatures (Kelvin, K)				
		283	293	303	313	323
Langmuir	$K_L, \text{dm}^3 \mu\text{g}^{-1}$	0.059	0.013	0.110	0.014	0.024
	$q_m, \mu\text{g g}^{-1}$	47.519	74.527	35.714	81.957	53.753
	R^2 (Linear)	0.859	0.978	0.845	0.978	0.872
	R^2 (Non-Linear)	0.932	0.989	0.919	0.989	0.934
	HYBRID	50.935	44.215	-24.835	4.148	44.301
	MPSD	59.292	43.417	72.595	15.785	41.028
Freundlich	$K_F, \text{dm}^3 \mu\text{g}^{-1}$	3.891	1.448	4.500	5.859	2.940
	n	1.250	1.185	1.172	1.504	1.542
	$1/n$	0.794	0.843	0.853	0.524	0.548
	R^2 (Linear)	0.940	0.989	0.949	0.958	0.999
	R^2 (Non-Linear)	0.970	0.994	0.972	0.994	1.000
	HYBRID	-3.141	-0.751	-4.050	-243.015	3.138
Temkin	MPSD	24.508	12.398	29.422	207.853	23.757
	B	41.945	38.158	49.991	13.810	15.800
	$K_T, \text{dm}^3 \mu\text{g}^{-1}$	0.200	0.092	0.299	0.305	0.280
	R^2 (Linear)	0.987	0.945	0.931	0.919	0.833
	R^2 (Non-Linear)	0.993	0.973	0.955	0.959	0.913
	HYBRID	5.509	19.591	52.587	-385.128	25.534
Redlich-Peterson	MPSD	28.105	58.527	189.217	485.235	83.789
	$a_R, \text{dm}^3 \mu\text{g}^{-1}$	5.137	2.859	2.857	11.830	251.548
	$K_R, \text{dm}^3 \mu\text{g}^{-1}$	21.850	15.75	5.45	51.18	95.745
	B	0.223	0.182	0.145	0.385	0.352
	R^2 (Linear)	0.507	0.757	0.249	0.958	0.998
	R^2 (Non-Linear)	0.712	0.811	0.499	0.990	0.999
HYBRID		-4.083	-0.758	-0.905	-0.755	-4.014
	MPSD	27.319	13.580	88.354	12.771	25.559

Table 5.4.5. Error analyses functions for adsorption of As(III) and AS(V) onto BFA-Fe.

Temperature(K)/ Isotherms	As(III)					As(V)				
	HYBRID	MPSD	SSE	SAE	ARE	HYBRID	MPSD	SSE	SAE	ARE
Langmuir										
283	-1.89	12.15	229.41	31.05	57.79	-53.39	47.28	351.54	123.55	38.14
293	-3.03	5.03	219.89	5.35	42.99	58.38	50.77	253.40	115.18	41.7
303	93.75	81.15	192.53	22.30	55.97	-2.37	19.20	291.84	30.17	12.57
313	-0.22	4.09	379.58	13.19	42.95	4.15	15.78	25.12	12.37	9.05
323	-123.73	150.11	398.98	350.92	95.11	5.25	28.03	853.55	52.75	19.19
Freundlich										
283	-1.55	19.04	959.93	59.53	13.21	-0.88	12.38	931.39	48.77	9.12
293	-0.94	13.72	147.50	25.44	10.20	-0.92	13.59	407.95	39.45	10.22
303	-1.57	17.20	778.74	47.72	12.51	-3.72	27.51	445.00	100.10	19.00
313	-1.57	18.23	977.48	72.42	72.42	-0.90	11.77	155.20	24.24	8.40
323	5.72	20.27	87.50	19.93	13.45	3.14	23.75	172.95	48.08	11.35
Temkin										
283	-2.37	10.85	317.15	33.81	7.34	25.70	80.90	1345.22	90.32	47.34
293	20.41	75.18	245.85	38.75	35.91	15.77	85.55	559.73	55.38	44.99
303	7.05	33.35	145.50	25.37	15.59	53.71	170.09	1545.40	90.77	71.75
313	13.21	50.85	555.53	55.95	24.40	-385.12	485.23	1588.80	340.37	75.80
323	22.19	58.84	320.40	37.58	30.12	25.53	83.79	801.05	59.39	42.52
Redlich-Peterson										
283	8.14	82.14	128.90	275.41	51.80	-0.73	13.78	905.05	48.51	48.51
293	-1.00	14.98	143.72	25.05	9.99	49.40	40.39	1287.90	74.52	28.23
303	-1.40	22.32	177.30	53.05	12.02	-8.18	32.58	8314.44	122.51	19.35
313	-1.55	18.31	159.85	57.13	12.03	-0.77	12.77	145.70	23.57	8.15
323	2.24	33.30	755.41	50.32	24.45	4.01	25.57	1173.57	48.10	11.37

Table 5.4.6. Error analyses functions for adsorption of As(III) and As(V) onto RHA-Fe.

Temperature(K)/ Isotherms	As(III)					As(V)				
	HYBRID	MPSD	SSE	SAE	ARE	HYBRID	MPSD	SSE	SAE	ARE
Langmuir										
283	73.93	58.12	37422.52	355.84	52.81	50.93	59.29	1914.92	253.29	43.53
293	38.57	40.24	12051.7	175.38	27.55	44.21	43.42	9891.87	180.15	31.58
303	91.25	79.47	35991.0	382.89	55.19	-24.83	72.59	15951.9	181.47	49.14
313	-5.19	5.57	53.32	13.90	4.07	4.15	15.78	25.12	12.37	9.05
323	-2.50	35.82	1595.07	58.57	20.25	44.30	41.03	2424.5	101.22	31.54
Freundlich										
283	-1.48	17.80	2218.88	81.15	13.52	-3.14	24.51	1703.34	82.04	19.58
293	-38.99	33.14	3545.03	111.50	27.85	-0.75	12.40	730.23	43.33	9.21
303	52.74	53.52	10275.7	223.92	44.81	-4.05	29.42	5247.35	109.15	21.91
313	-0.48	10.89	525.18	39.80	8.012	-243.01	207.85	41755.5	450.55	173.58
323	-12.85	43.71	3792.93	90.55	24.85	3.14	23.75	1172.95	48.08	11.35
Temkin										
283	17.51	50.20	895.45	72.70	34.81	5.51	28.11	1734.1	27.98	13.59
293	39.53	147.48	2171.9	103.38	59.89	19.59	58.53	753.08	54.52	38.72
303	3.21	22.54	250.97	32.79	13.58	52.59	189.22	1788.12	95.04	79.49
313	9.55	32.71	525.18	54.13	21.84	-385.13	485.23	15788.8	340.37	275.8
323	-0.94	43.92	1348.30	50.94	25.55	25.53	83.79	801.05	59.39	42.52
Redlich-Peterson										
283	-2.05	19.78	2517.93	80.95	13.34	-4.08	27.32	1734.11	82.47	19.57
293	-0.07	3.05	37.75	9.59	2.12	-0.77	13.58	719.47	42.74	8.97
303	-7.73	15.78	1504.1	59.03	9.72	-0.90	88.35	23551.1	232.78	55.31
313	-0.51	12.09	523.22	39.51	7.93	-0.77	12.77	145.7	23.57	8.15
323	-15.08	48.70	3775.55	90.18	24.55	4.01	25.57	1173.57	48.1	11.37

5.5 ESTIMATION OF THERMODYNAMIC PARAMETERS

The Gibbs free energy change of the adsorption process is related to the adsorption equilibrium constant by the classical Van't Hoff equation:

$$\Delta G_{ads}^0 = -RT \ln K_{ads} \quad (5.5.1)$$

The Gibbs free energy change is also related to the change in entropy and heat of adsorption at a constant temperature as given by the equation:

$$\Delta G_{ads}^0 = \Delta H^0 - T \Delta S^0 \quad (5.5.2)$$

The above two equations give,

$$\ln K_{ads} = \frac{-\Delta G_{ads}^0}{RT} = \frac{\Delta S^0}{R} - \frac{\Delta H^0}{R} \frac{1}{T} \quad (5.5.3)$$

where, ΔG_{ads}^0 is the free energy change (kJ mol^{-1}), ΔH^0 is the change in enthalpy (kJ mol^{-1}), ΔS^0 is the entropy change ($\text{kJ mol}^{-1} \text{K}^{-1}$), K_{ads} is the equilibrium constant of interaction between the adsorbate and the adsorbent surface, T is the absolute temperature (K) and R is the universal gas constant ($8.314 \text{ J mol}^{-1} \text{K}^{-1}$). Thus, ΔH^0 can be determined by the slope of the linear Van't Hoff plot i.e. as $\ln(K_{ads})$ versus $(1/T)$, using the equation:

$$\Delta H^0 = \left[R \frac{d \ln K_{ads}}{d(1/T)} \right] \quad (5.5.4)$$

This ΔH^0 is the isosteric heat of adsorption ($\Delta H_{st,0}$) with zero surface coverage (i.e. $q_e = 0$). K_{ad} at $q_e = 0$ was obtained from the intercept of the $\ln(q_e/C_e)$ versus q_e plot. Fig. 5.5.1 – Fig. 5.5.4 shows the Van't Hoff's plot for $\ln(q_e/C_e)$ versus q_e , from which ΔH^0 and ΔS^0 values have been estimated (Table 5.5.1 to Table 5.5.2).

Table 5.5.1 Thermodynamic parameters for the sorption of As(III) and As(V) onto BFA-Fe

Compounds	ΔG_{ads}^0 (KJ mol ⁻¹)					ΔH^0 (KJ mol ⁻¹)	ΔS^0 (KJ mol ⁻¹ K ⁻¹)
	283 K	293 K	303 K	313 K	323 K		
Langmuir							
As(III)	-35.47	-35.57	-35.57	-35.78	-35.88	-32.55	0.01
As(V)	-30.53	-32.21	-33.9	-35.58	-37.27	-17.19	0.17
Freundlich							
As(III)	-45.14	-48.04	-49.93	-51.82	-53.71	-7.39	0.19
As(V)	-44.72	-47.01	-49.31	-51.5	-53.89	-20.12	0.23
Temkin							
As(III)	-38.97	-40.58	-42.39	-44.09	-45.08	-9.35	0.17
As(V)	-38.81	-40.54	-42.28	-44.01	-45.75	-10.328	0.17
Redilich-Peterson							
As(III)	-43.85	-45.34	-48.82	-51.31	-53.8	-25.58	0.25
As(V)	-44.75	-48.3	-51.84	-55.39	-58.93	-55.57	0.35

Table 5.5.2 Thermodynamic parameters for the sorption of As(III) and As(V) onto RHA-Fe.

Compounds	ΔG_{ads}^0 (KJ mol ⁻¹)					ΔH^0 (kJ mol ⁻¹)	ΔS^0 (kJ mol ⁻¹ K ⁻¹)
	283 K	293 K	303 K	313 K	323 K		
Langmuir							
As(III)	-20.13	-21.10	-22.07	-23.05	-24.02	-7.41	0.09
As(V)	-9.07	-9.85	-10.53	-11.41	-12.20	-13.14	0.08
Freundlich							
As(III)	-44.51	-45.32	-48.02	-49.73	-51.44	-3.73	0.17
As(V)	-54.72	-48.01	49.30	-49.35	-52.45	-22.11	0.31
Temkin							
As(III)	-35.85	-39.25	-41.58	-44.09	-45.51	-31.47	0.241
As(V)	-38.15	-40.00	-41.85	-43.7	-45.55	-14.22	0.185
Redilich-Peterson							
As(III)	-47.53	-50.58	-53.54	-55.49	-59.44	-35.93	0.295
As(V)	-43.84	-47.8	-51.75	-55.72	-59.59	-58.25	0.400

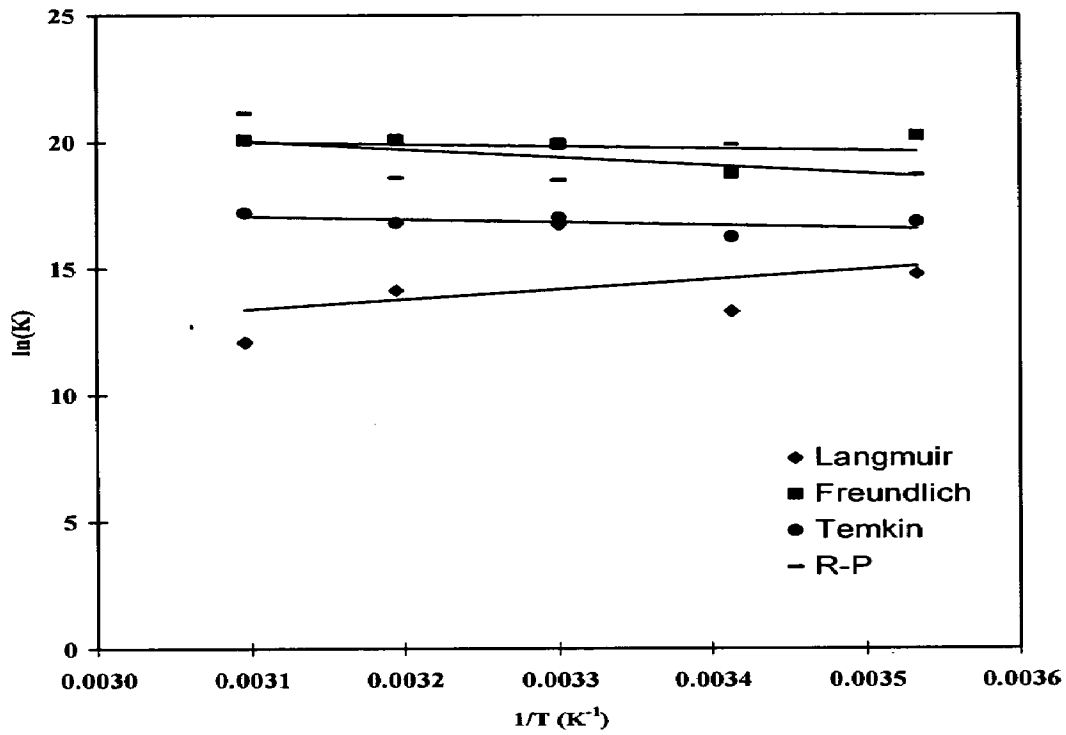


Fig. 5.5.1. Van't Hoff plot for the adsorption of As(III) onto BFA-Fe.

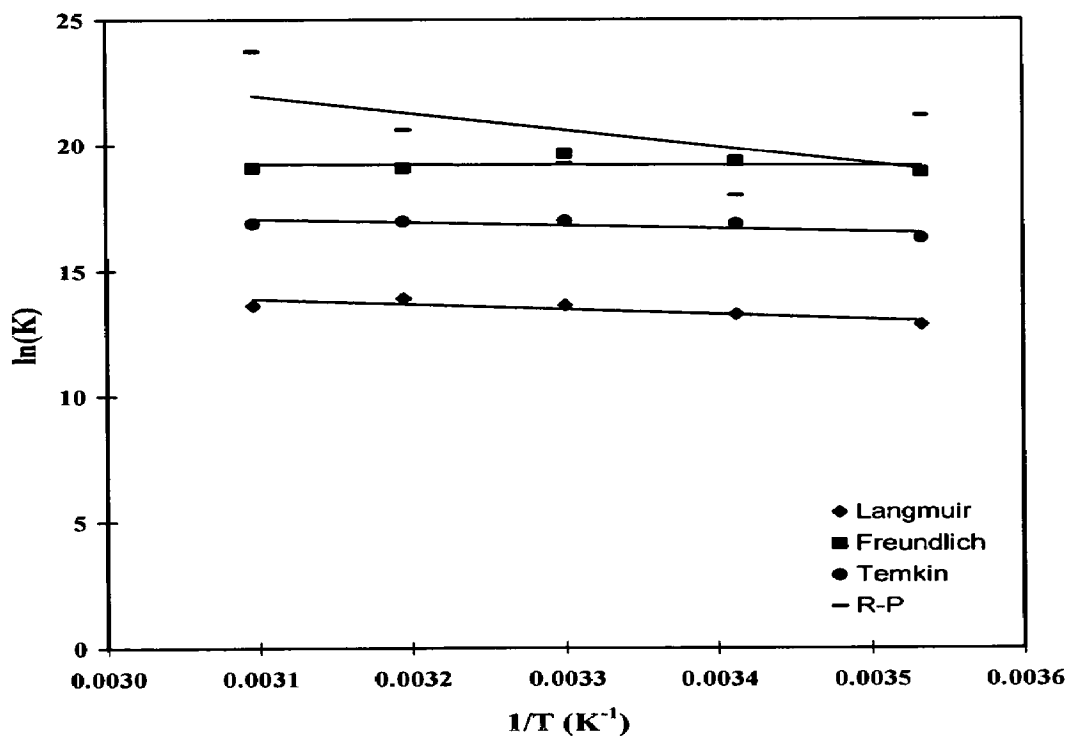


Fig. 5.5.2. Van't Hoff plot for the adsorption of As(V) onto BFA-Fe.

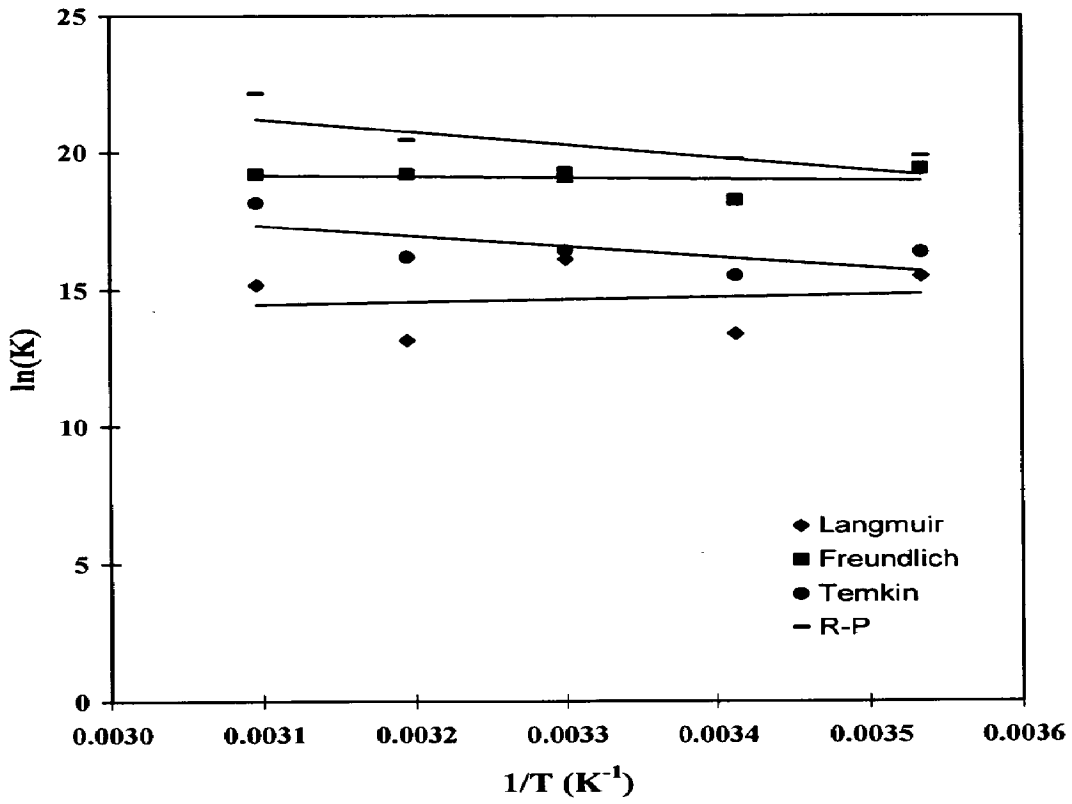


Fig. 5.5.3. Van't Hoff plot for the adsorption of As(III) onto RHA-Fe.

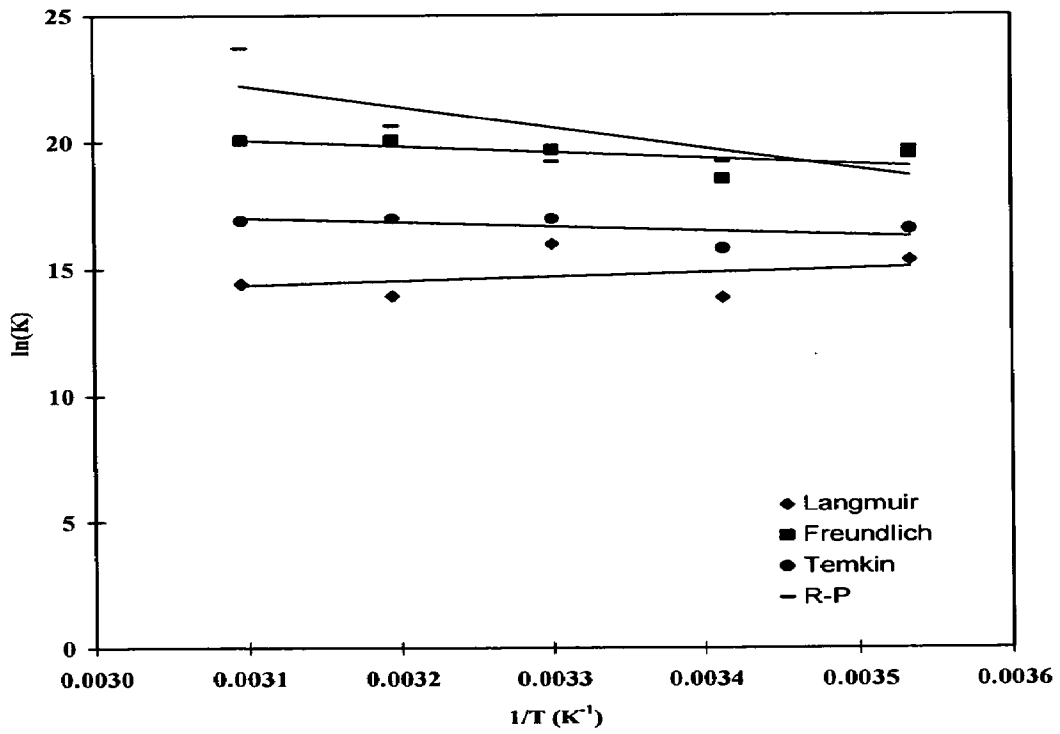


Fig. 5.5.4. Van't Hoff plot for the adsorption of As(V) onto RHA-Fe.

For adsorption to occur, ΔG_{ads}^0 the free energy change of adsorption must be negative. The adsorption of As onto BFA-Fe and RHA-Fe is exothermic in nature, giving a negative value of ΔH^0 . The positive value of ΔS^0 suggests increased randomness at the solid-solution interface with some structural changes in the adsorbate and adsorbent and an affinity of the BFA-Fe and RHA-Fe towards As. Also, positive ΔS^0 value corresponds to an increase in the degree of freedom of the adsorbed species. ΔG_{ads}^0 values are negative indicating that the sorption process led to a decrease in Gibbs free energy.

5.6. THERMAL DEGRADATION KINETICS OF THE SPENT ADSORBENTS

The disposal of spent adsorbents is a major environmental problem. The use of low-cost adsorbents for the process of adsorption generates large volumes of solid waste. These solid wastes have great potential for energy recovery. However, the separation of the adsorbents from the solvents by sedimentation, filtration, centrifugation, dewatering and drying is very important. The dried As(III)- or As(V)-loaded spent BFA-Fe and RHA-Fe can be regenerated by desorption either with alkalis or by thermal means. The BFA-Fe can be fired either directly or by making briquettes in the combustors/incinerators to recover its energy value. The blank and As(III) or As(V) loaded adsorbents were studied for their thermal degradation characteristics by thermogravimetric (TG) instrument.

5.6.1 Results of TGA, DTA and DTG

Thermal stability of BFA-Fe and RHA-Fe is dependent on the decomposition temperature of its oxides and functional groups present. The carbons when heated to higher temperatures ($> 200^\circ\text{C}$), the surface groups decompose, producing CO (150-500 $^\circ\text{C}$), CO₂ (350-1000 $^\circ\text{C}$), water vapour and free hydrogen (500-1000 $^\circ\text{C}$) (Mall et al., 2006). In the present study, the operating pressure was kept slightly positive, the purge gas (air) and (nitrogen) flow rate was maintained at 200 ml min⁻¹ and the heating rate was maintained at 100 $^\circ\text{C}$ min⁻¹.

The thermogravimetric analysis (TGA), differential thermal analysis (DTA) and differential thermo gravimetry (DTG) curves of the blank and As(III) and As(V) loaded BFA-Fe and RHA-Fe are shown in Figs. 5.6.1 through 5.6.4, respectively, both in air as well as in nitrogen medium. Three different zones can be seen in Figs. 5.6.1 through 5.6.2 for the air atmosphere for all the blank and loaded adsorbent.

For BFA-Fe (Fig. 5.6.1 (a)), the first zone ranges room temperature to 400°C , the second zone from 400°C to 750°C , and the third zone from 750°C to 1000°C . The maximum weight loss of $\sim 35\%$ was recorded in the second zone, while the first zone corresponds to comparatively much smaller weight loss of $\sim 19\%$. The third zone shows almost no weight loss ($\sim 1.55\%$) and, therefore, no degradation.

For RHA-Fe in air atmosphere (Fig. 5.6.2 (a)), $\sim 5.5\%$ weight loss is observed in the first zone, from room temperature to 400°C , $\sim 13.5\%$ weight loss in the second zone, from 400°C to 590°C , and a weight loss of $\sim 1.31\%$ in the third zone, from 590°C to 1000°C . Under oxidizing atmosphere, the first zone corresponds to removal of moisture and light volatiles. The weight loss has been reported to be associated in part with the evolution of H_2O , CO_2 and CO . The second zone for RHA-Fe is smaller than BFA-Fe with the maximum rate of weight loss for BFA-Fe being 2.14 mg min^{-1} and 1.28 mg min^{-1} for RHA-Fe. Subsequently, the sample weight remains almost constant in the third zone with the ash remaining at 1000°C .

Thermal degradation characteristics in nitrogen atmosphere show the removal of moisture of $\sim 4\%$ and 3.5% at a temperature of 100°C , for BFA-Fe and RHA-Fe, respectively. The rate of weight loss upto 500°C gives the percentage removal of volatiles.

The total weight loss of BFA-Fe and RHA-Fe under nitrogen atmosphere in the temperature range of 100°C - 1000°C is $\sim 42\%$ and 25% , respectively. The maximum rate of weight loss in air atmosphere were obtained as 2.14 , 1.282 mg min^{-1} and in the nitrogen atmosphere 0.855 and 0.558 for blank BFA-Fe and RHA-Fe, respectively.

Table 5.6.1. DTA for the blank and loaded adsorbents in the air and nitrogen atmosphere at flow rate 200 ml min⁻¹

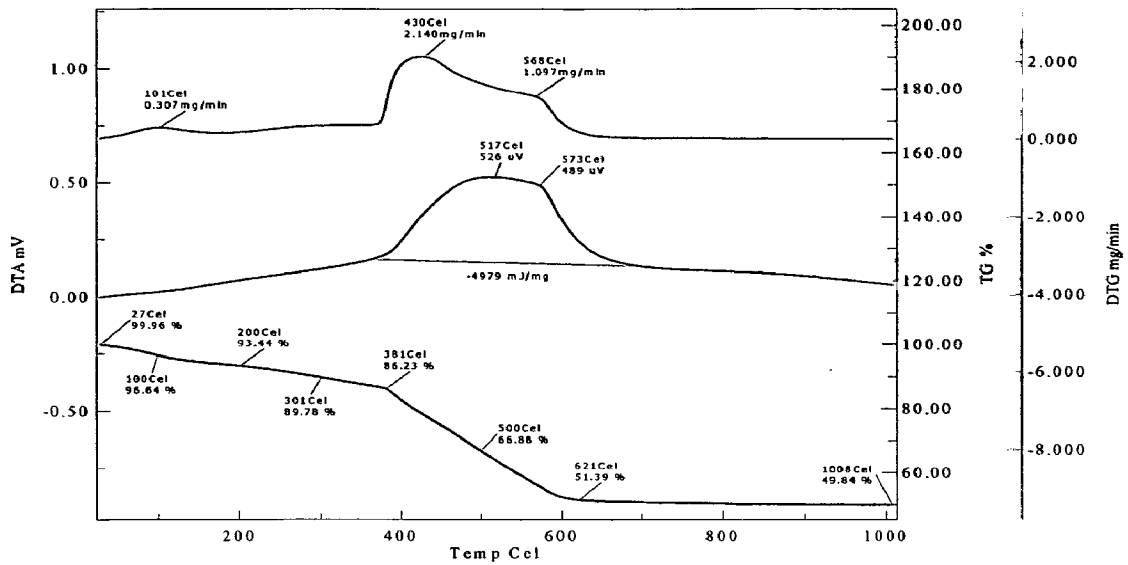
Adsorbent (Blank/loaded)	ΔH_1 mJ kg ⁻¹	T _{1i} °C	T _{2f} °C
BFA-Fe	-4979	390	700
BFA-Fe-As(III)	-4897	385	715
BFA-Fe-As(V)	-4728	400	590
RHA-Fe	-1703	385	570
RHA-Fe-As(III)	-1475	395	580
RHA-Fe-As(V)	-1525	400	700

Table 5.6.2 Thermal degradation characteristics of blank and loaded adsorbents in air and nitrogen atmosphere at a flow rate of 200 ml min⁻¹

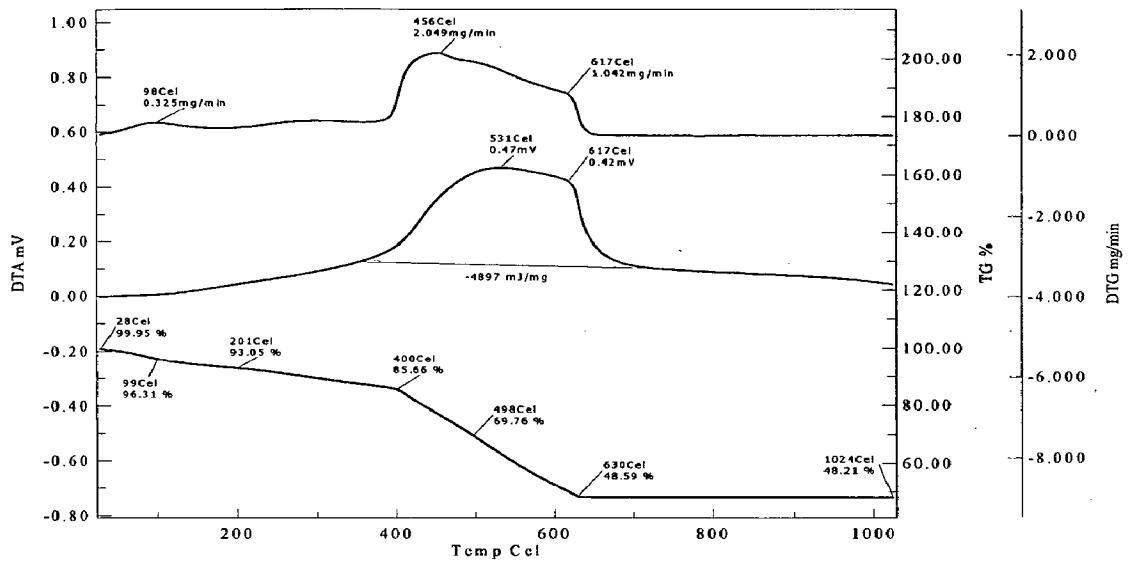
Adsorbent	Air atmosphere						Nitrogen atmosphere					
	Drying Range	Moisture (%)	Degradation Range (°C)	T _{max} (°C)	Max. Rate of Weight		Drying Range	Moisture (%)	Degradation Range (°C)	T _{max} (°C)	Max. Rate of Weight	
BFA-Fe	27-100	3.32	>200	430	2.14		28-100	4.14	>200	805	0.855	
As(III)-BFA-Fe	28-99	3.54	>200	455	2.049		28-99	3.42	>200	808	0.948	
As(V)-BFA-Fe	28-100	3.91	>200	439	2.27		27-101	3.72	>200	795	0.559	
RHA-Fe	28-99	4.05	>200	445	1.282		27-98	3.45	>200	825	0.558	
As(III)-RHA-Fe	28-100	2.17	>200	519	1.1		28-100	1.75	>200	881	0.178	
As(V)-RHA-Fe	27-102	2.37	>200	473	1.249		23-97	2.48	>200	870	0.325	

Table 5.6.3. Distribution of volatiles released during thermal degradation of blank and loaded adsorbents in an air and nitrogen atmosphere at a flow rate of 200 ml min⁻¹.

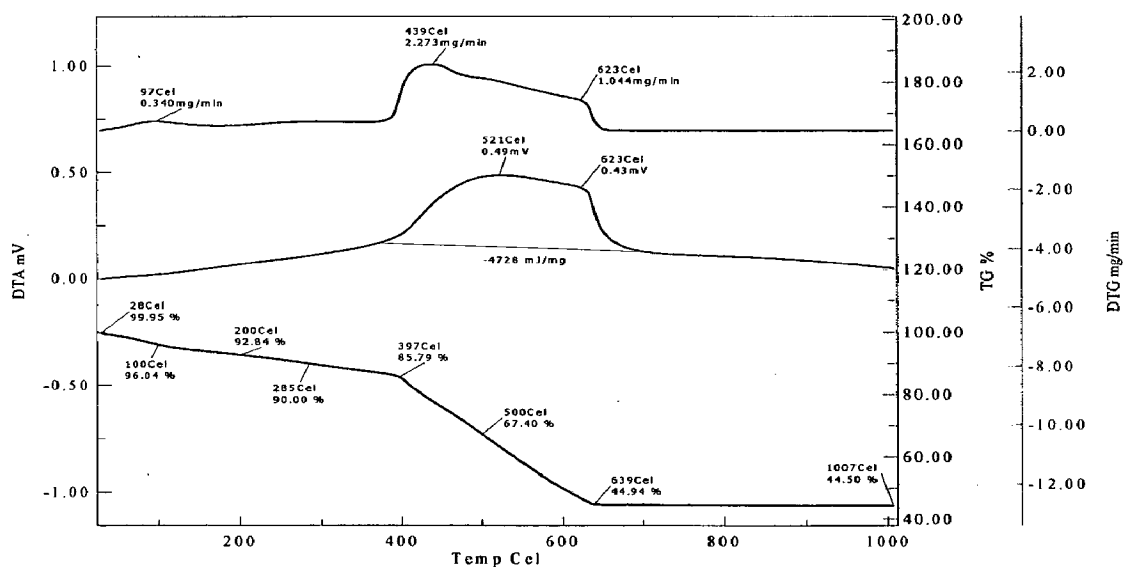
Adsorbent (Blank/ loaded)	%Weight loss in air atmosphere (approximate)				%Weight loss in nitrogen atmosphere (approximate)		Total Volatile matter including moisture	Total Volatile matter including moisture
	<200°C	200-400 °C	400-700 °C	>700°C	<200°C	200-975 °C		
BFA-Fe	5.95	7.21	34.84	1.55	7.51	34.45	50.55	41.95
As(III)- BFA-Fe	5.9	7.39	37.07	0.38	5.9	30.59	51.74	37.59
As(V)- BFA-Fe	7.11	7.05	40.85	0.44	5.75	27.59	55.45	34.35
RHA-Fe	5.34	4.29	13.5	1.31	5.83	20.23	25.44	25.05
As(III)- RHA-Fe	4.25	4.22	13.01	0.39	3.57	11.21	21.88	14.88
As(V)- RHA-Fe	4.5	4.37	13.12	0.21	5.11	18.13	22.2	23.24



(a)

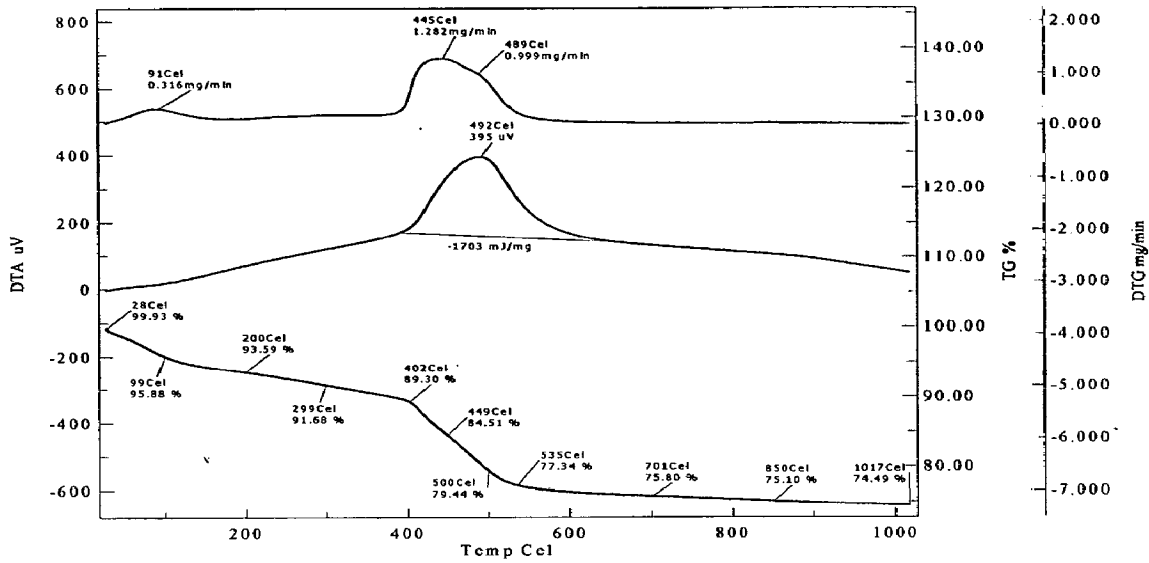


(b)

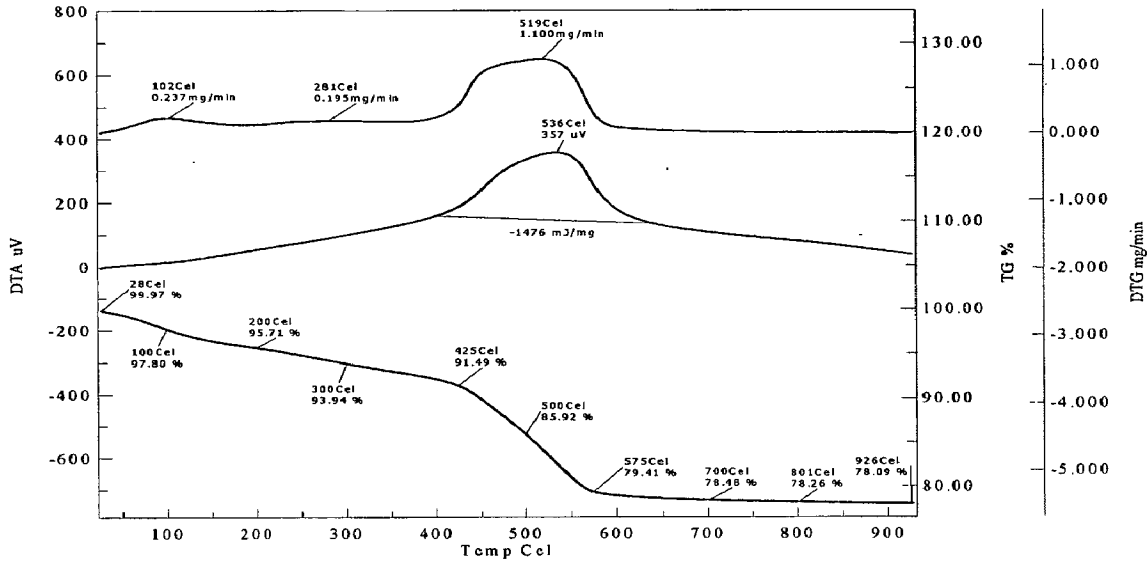


(c)

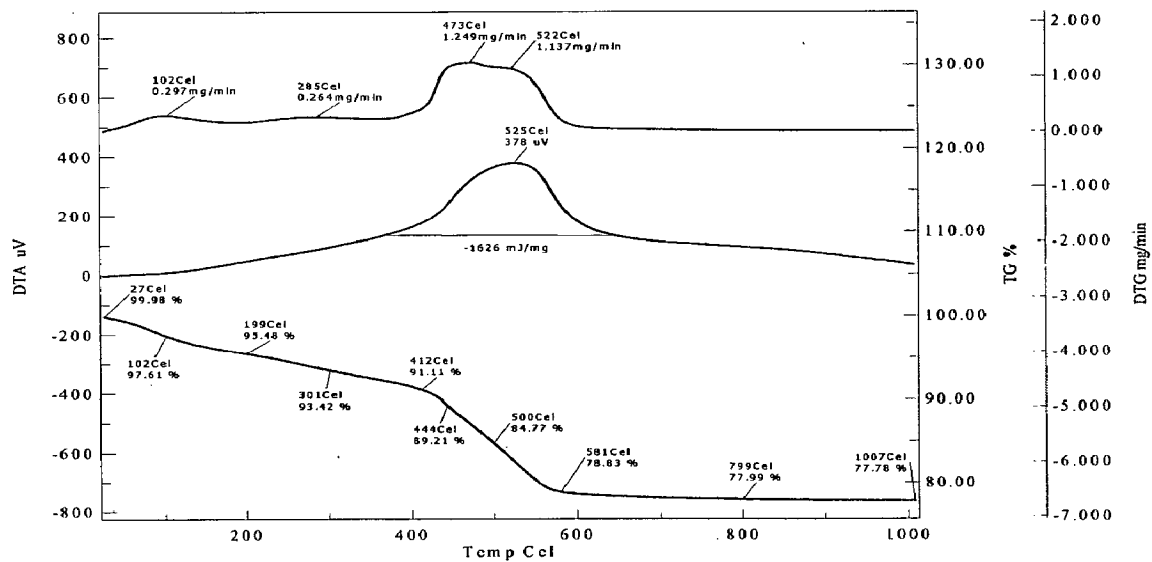
Fig. 5.6.1 TGA analysis of (a) Blank, (b) As-III and (c) As-V loaded BFA-Fe in the air atmosphere



(a)

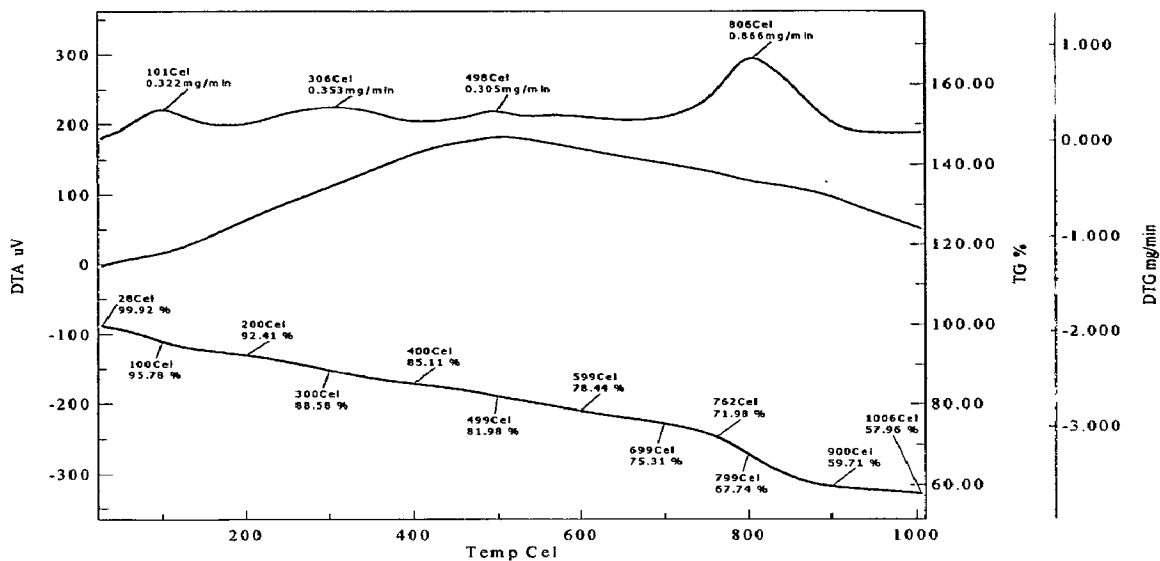


(b)

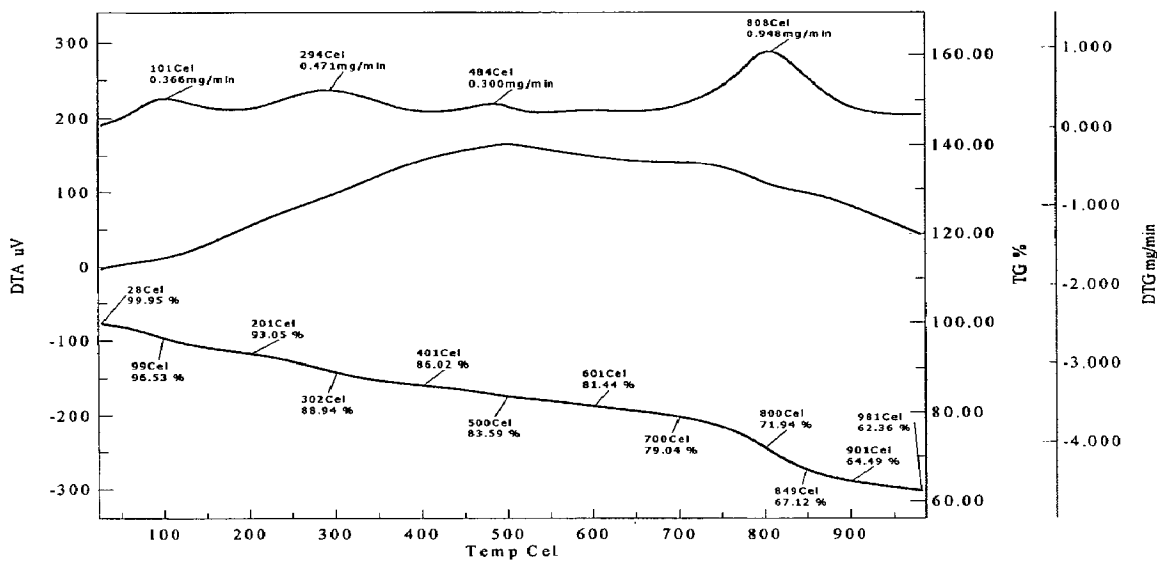


(c)

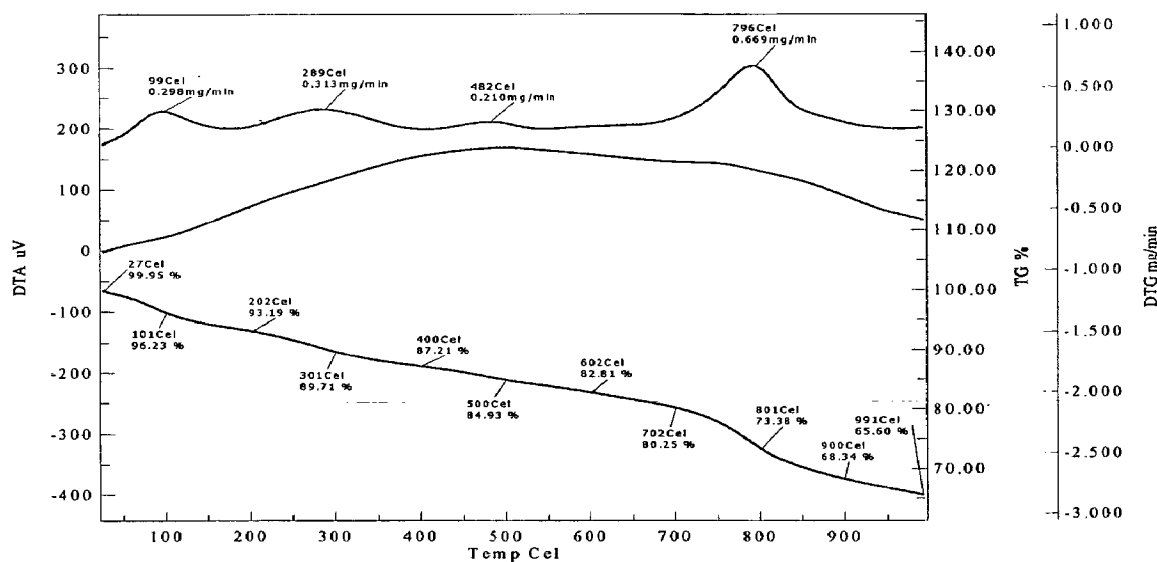
Fig. 5.6.2. TGA analysis of (a) Blank, (b) As-III and (c) As-V loaded RHA-Fe in the air atmosphere



(a)

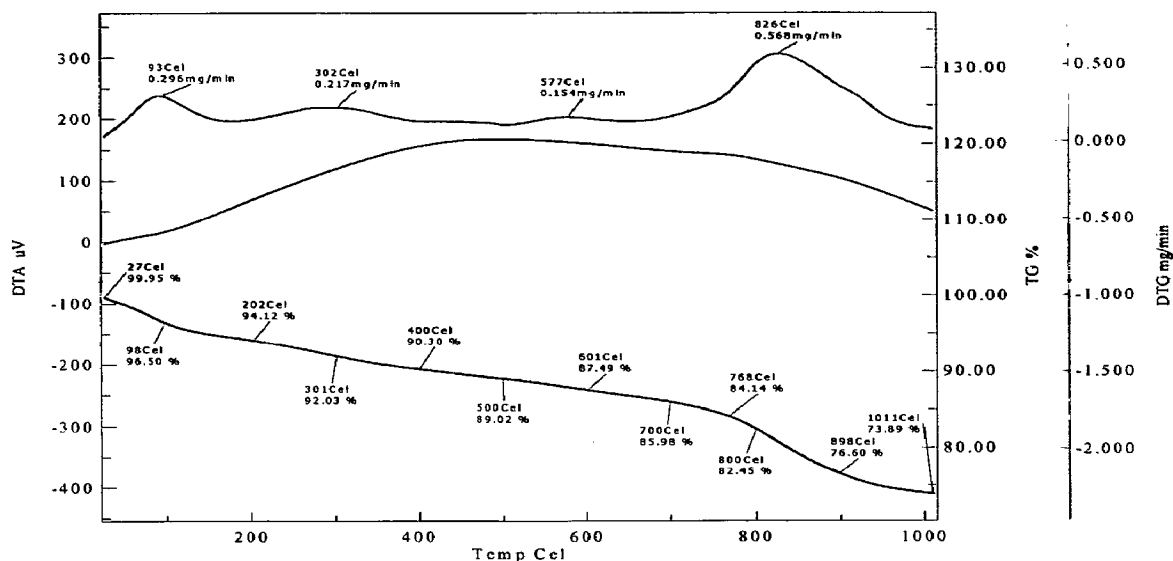


(b)

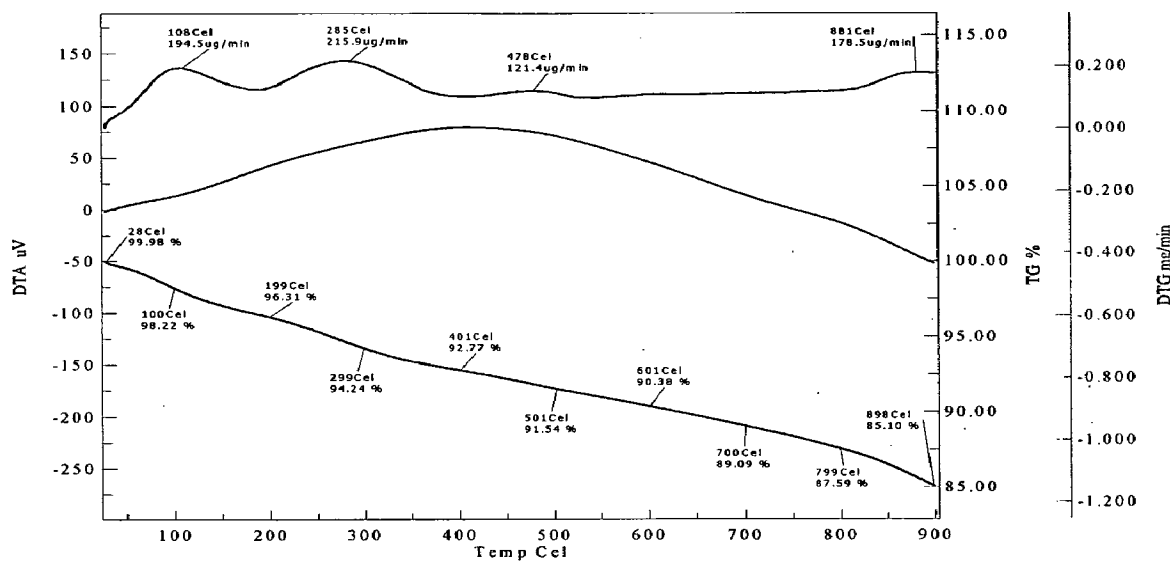


(c)

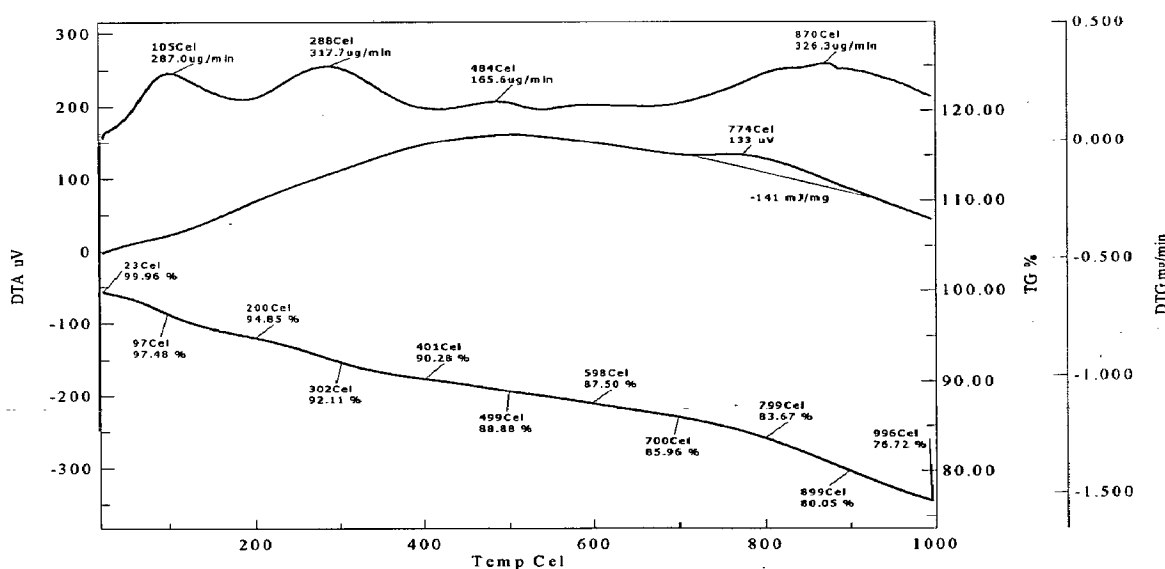
Fig. 5.6.3. TGA analysis of (a) Blank, (b) As-III and (c) As-V loaded BFA-Fe in the Nitrogen atmosphere



(a)



(b)



(c)

Fig. 5.6.4. TGA analysis of (a) Blank, (b) As-III and (c) As-V loaded RHA-Fe in the Nitrogen atmosphere

CONCLUSIONS AND RECOMMENDATIONS

6.1 CONCLUSIONS

From the present study, the following conclusions can be drawn:

- 1 The adsorbents, BFA-Fe and RHA-Fe are low density and low cost materials.
- 2 BFA-Fe has larger BET surface area as compared to that of RHA-Fe.
- 3 The SEM figures of FeCl₃ coated BFA and RHA showed fibrous structure with pores of varying sizes.
- 4 The EDAX analysis of BFA-Fe and RHA-Fe showed that BFA-Fe has higher carbon and iron content as compared to that of RHA-Fe.
- 5 The FTIR spectra of the adsorbents indicated presence of various types of functional groups e.g. free and hydrogen bonded OH group, the silanol groups (Si-OH), CO group stretching from aldehydes and ketones on the surface of adsorbents.
- 6 Thermogravimetric analysis exhibited the thermal stability of the adsorbents upto 400 °C.
- 7 Optimum BFA-Fe and RHA-Fe dosages were found to be 3 g dm⁻³ for C₀=100 µg dm⁻³ of As-III and As-V, and 3 h was the equilibrium contact time for adsorption of As onto BFA-Fe and RHA-Fe.
- 8 The sorption kinetics was well represented by the pseudo-second-order kinetic model.

- 9 Freundlich isotherms, generally, well-represented the equilibrium adsorption of As onto BFA-Fe and RHA-Fe.
- 10 An increase in temperature induced a negative effect on the sorption process. The values of change in Gibbs free energy (ΔG_{ads}^0) were found in the range of 30-58 kJ mol⁻¹, 9-59 kJ mol⁻¹ for BFA-Fe and RHA-Fe, respectively. The negative value of change in ΔG_{ads}^0 indicated the feasibility and spontaneity of adsorption on the adsorbents.

6.2 RECOMMENDATIONS

On the basis of the present studies, the following recommendations may be made for future studies:

- 1 BFA and RHA from different sources and different particle size should be characterized for their physico-chemical parameters and surface characteristics.
- 2 Other types of iron coating procedures may be used on BFA and RHA and various other low cost adsorbents to check the As removal efficiency.
- 3 Column and scale-up studies should be conducted to evaluate the suitability of BFA-Fe and RHA-Fe as adsorbents for the removal of As from drinking water.

LITERATURE CITED

- Ahmed MF, An Overview of Arsenic Removal Technologies in Bangladesh and India, Department of Civil Engineering, Bangladesh University of Engineering & Technology, Dhaka-1000, Bangladesh.
- Amirbahman A, Kent DB, Curtis GP, Davis JA, Kinetics of sorption and abiotic oxidation of arsenic(III) by aquifer materials, *Geochimica et Cosmochimica Acta*, 70, 533–547 (2006).
- Aharoni C, Sideman S, Hoffer E, Adsorption of phosphate ions by colloid ion-coated alumina, *Journal of Chemical Technology and Biotechnology*, 29, 404-412, (1979).
- Ayoob S, Gupta AK, Bhakat PB, Performance evaluation of modified calcined bauxite in the sorptive removal of arsenic(III) from aqueous environment, *Colloids and Surfaces A: Physicochemical and Engineering Aspects* 293, 247–254, (2007).
- Balarama Krishna MV, Chandrasekaran K, Karunasagar D, Arunachalam J, A combined treatment approach using Fenton's reagent and zero valent iron for the removal of arsenic from drinking water, *Journal of Hazardous Materials*, B84, 229–240 (2001).
- Ballinas ML, Miguel ERDS, Rodriguez MTJ, Silva O, Munoz M, Gyves JD, Arsenic(V) removal with polymer inclusion membranes from sulfuric acid media using DBBP as carrier, *Environmental science and technology*, 38, (3) 886–891 (2004).
- Basha CA, Selvi SJ, Ramasamy E, Chellammal S, Removal of arsenic and sulphate from the copper smelting industrial effluent, *Chemical Engineering Journal*, 141, 89–98, (2008).
- Bhakat PB, Gupta AK, Ayoob S, Kundu S, Investigations on arsenic(V) removal by modified calcined bauxite, *Colloids and Surfaces A: Physicochemical and Engineering Aspects*, 281, 237–245 (2006).
- Biswas BK, Inoue J, Inoue K, Ghimire KN, Harada H, Ohto K, Kawakita H, Adsorptive removal of As(V) and As(III) from water by a Zr(IV)-loaded orange waste gel, *Journal of Hazardous Materials*, 154, 1066–1074 (2008).

- Borho M and Wilderer P, Optimized removal of arsenate(III) by adaptation of oxidation and precipitation processes to the filtration step, *Water science technology*, 34 (9), 25-31 (1996).
- Boyd GE, Adamson AW, Meyers LS, The exchange adsorption of ions from aqueous solution by organic zeolites II Kinetics, *Journal of American Chemical Society*, 69, 2836-2848 (1947).
- Chang YY, Song K, Yang Y, Removal of As(III) in a column reactor packed with iron-coated sand and manganese-coated sand, *Journal of Hazardous Materials*, 150, 565–572 (2008).
- Chutia P, Kato S, Kojima T, Satokawa S, Adsorption of As(V) on surfactant-modified natural zeolites, *Journal of Hazardous Materials*, doi:10.1016/j.jhazmat. 2008.05.024 2008.
- Diamadopoulos E, Ioannidis S and Sakellaropoulos GP, As(V) removal from aqueous solutions by fly ash, *Water Research*, 27 (12), 1773-1777 (1993).
- Directive 1999/45/ec of the european parliament and of the council, *Official Journal of the European Communities*, 200, 1-68 (1999).
- Dutta PK, Pehoen So, Sharma VK and Ray AK, Photocatalytic Oxidation of Arsenic(III): Evidence of Hydroxyl Radicals, *Environmental Science and Technology*, 39, 1827-1834 (2005).
- Ferreccio C, Sancha AM, Arsenic exposure and its impact on health in Chile. *Journal of health population and nutrition*, 24 (2), 164–175 (2006).
- Fogler HS, *Elements of Chemical Reaction Engineering*, Prentice-Hall PTR, 3 (1998).
- Ghimirea KN, Inouea K, Yamaguchia H, Makinob K, Miyajima T, Adsorptive separation of arsenate and arsenite anions from aqueous medium by using orange waste, *Water Research*, 37, 4945–4953 (2003).
- Gholami MM, Mokhtari MA, Aameri A, Fard MRA, Application of reverse osmosis technology for arsenic removal from drinking water, *Desalination*, 200, (1–3)–725–727 (2006).

- Guo H, Stüben D, Berner Z, Adsorption of arsenic(III) and arsenic(V) from groundwater using natural siderite as the adsorbent, *Journal of Colloid and Interface Science*, 315, 47–53 (2007).
- Ho YS., Mckay G, The kinetics of sorption of divalent metal ions onto sphagnum mass peat, *Water Research*. 34(3), 735-742 (2000).
- Ho YS., Mckay G, Kinetic model for lead(II) sorption onto peat, *Adsorption Science Technology*, 16(4), 243-255, (1998).
- Ho YS., Mckay G, Pseudo-second order model for sorption processes, *Process Biochemical*, 34 (5), 415-465 (1999).
- Han B, Runnells T, Zimbron J, Wickramasinghe R, Arsenic removal from drinking water by flocculation and microfiltration, *Desalination* 145 (1–3) 293–298 (2002).
- Huang X, Jiao L, Liao X and Shi B, Adsorptive Removal of As(III) from Aqueous Solution by Zr(IV)-Loaded Collagen Fiber, *Industrial Engineering and Chemistry Research*, doi: 10.1021/ie071608k.
- Jalil AF, Ali MA, Hossain MA, M.D., Badruzzaman ABM., An overview of arsenic removal technologies in BUET, In *Bangladesh Environment- M.F.Ahmed (Ed.)*, Bangladesh Poribesh Andolon, 177-188 (2000).
- Kannan N, Sundaram MM, Kinetics and mechanism of removal of methylene blue by adsorption on various carbons - a comparative study, *Dyes Pigments*, 51(1), 25-40 (2001).
- Lagergren S., About the theory of so called adsorption of soluble substances, *Ksver Veterskapsakad Handl*, 24, 1-6 (1898).
- Lakshmi UR, Srivastava VC, Mall ID, Lataye DH, Rice husk ash as an effective adsorbent: Evaluation of adsorptive characteristics for Indigo Carmine dye, *Journal of Environmental Management*, doi:10.1016/j.jenvman 2008.01.002.
- Lakshmipathiraj P, Narasimhan BRV, Prabhakar S, Raju GB, Adsorption of arsenate on synthetic goethite from aqueous solutions, *Journal of Hazardous Materials*, 136 (2), 281-287 (2006).
- Lagergren S, About the theory of so called adsorption of soluble substances, *Ksver Veterskapsakad Handl*, 24, 1-6 (1898).

- Lataye DH, Adsorptive treatment of pyridine and its derivatives from wastewaters, Ph.D Thesis, Department Of Chemical Engineering, Indian Institute Of Technology Roorkee, June (2007).
- Lataye DH, Mishra IM, Mall ID, Pyridine sorption from aqueous solution by rice husk ash (RHA) and granular activated carbon (GAC): Parametric, kinetic, equilibrium and thermodynamic aspects, *Journal of Hazardous Materials*, 154, (1-3), 858-870 (2008).
- Lataye DH, Mishra IM, Mall ID, Removal of pyridine from aqueous solution by adsorption on bagasse fly ash, *Industrial engineering and chemistry research*, 45(11), 3934-3943 (2006).
- Lin T and Wu J, Adsorption of arsenite and arsenate within Activated alumina grains: equilibrium and Kinetics, *Water research*, 35(8), 2049–2057 (2001).
- Lorenzen L, Deventer JSJV, Landi WM, Factors affecting the mechanism of the adsorption of arsenic species on activated carbon, *Minerals Engineering*, 8, (4/5), 557-569 (1995).
- Maitya S, Chakravarty, Bhattacharjee S, Roy BC, A study on arsenic adsorption on polymetallic sea nodule in aqueous medium, *Water Research*, 39, 2579–2590 (2005).
- Maji SK, Pal A, Pal T, Arsenic removal from real-life groundwater by adsorption on laterite soil, *Journal of Hazardous Materials*, 151, 811–820 (2008).
- Mall ID, Srivastava VC, Agarwal NK, Adsorptive removal of Auramine-O: Kinetic and equilibrium study, *Journal of Hazardous Materials*, 143, 386–395 (2007).
- Mall ID, Srivastava VC, Agarwal NK, Mishra IM, Removal of congo red from aqueous solution by bagasse fly ash and activated carbon: Kinetic study and equilibrium isotherm analyses, *Chemosphere*, 61, 492–501, (2005a).
- Mall ID, Srivastava VC, Agarwal NK, Mishra IM, Adsorptive removal of malachite green dye from aqueous solution by bagasse fly ash and activated carbon-kinetic study and equilibrium isotherm analyses, *Colloids and Surfaces A: Physicochemical Engineering Aspects* 264, 17–28 (2005b).
- Mall ID, Srivastava VC, Kumar GVA, Mishra IM, Characterization and utilization of mesoporous fertilizer plant waste carbon for adsorptive removal of dyes from aqueous solution. *Colloids and Surfaces A: Physicochemical and Engineering Aspects*, 278(1-3), 175-187, (2006).

- Marquardt DW, An algorithm for least-squares estimation of nonlinear parameters, *Journal of Society and Industrial and Applied Mathematics*, 11, 431-441 (1963).
- Mohan D, Pittman Jr. CU, Arsenic removal from water/wastewater using adsorbents—A critical review, *Journal of Hazardous Materials*, 142, 1–53 (2007)
- Parga JR, Cocke DL, Valenzuela JL, Gomes JA, Kesmez M, Irwin G, Moreno H, Weir M, Arsenic removal via electrocoagulation from heavy metal contaminated groundwater in La Comarca Lagunera Mexico, *Journal of Hazardous Materials*, B124, 247–254 (2005).
- Porter JF., McKay G, Choy KH, The prediction of sorption from a binary mixture of acidic dyes using single- and mixed isotherm variants of the ideal adsorbed solute theory, *Chemical Engineering Science*, 54, 5863-85 (1999).
- Ratna Kumar P, Chaudhari S, Khilar KC, Mahajan SP, Removal of arsenic from water by electrocoagulation, *Chemosphere*, 55, 1245–1252 (2004).
- Selvakumar R, Kavitha S, Sathishkumar M, Swaminathan K, Arsenic adsorption by polyvinyl pyrrolidone K25 coated cassava peel carbon from aqueous solution, *Journal of Hazardous Materials*, 153, 67–74 (2008).
- Shao W, Li X, Cao Q, Luo F, Li J, Du Y, Adsorption of arsenate and arsenite anions from aqueous medium by using metal(III)-loaded amberlite resins, *Hydrometallurgy*, 91, 138–143 (2008).
- Singh TS, Pant KK, Equilibrium, kinetics and thermodynamic studies for adsorption of As(III) on activated alumina, *Separation and Purification Technology*, 36, 139-147 (2004).
- Singh TS, Pant KK, Experimental and modelling studies on fixed bed adsorption of As(III) ions from aqueous solution, *Separation and Purification Technology*, 48, 288–296 (2006).
- Srivastava VC, Mall ID, Mishra IM, Removal of cadmium(II) and zinc(II) metal ions from binary aqueous solution by rice husk ash, *Colloids and Surfaces A: Physicochemical Engineering Aspects*, 312, 172–184 (2008).
- Srivastava VC, Swamy MM, Mall ID, Prasad B, Mishra IM, Adsorptive removal of phenol by bagasse fly ash and activated carbon: Equilibrium, kinetics and thermodynamics, *Colloids and Surfaces A: Physicochemical Engineering. Aspects* 272, 89–104 (2006).

Srivastava VC, Heavy metals removal from aqueous solution using low-cost adsorbents, Ph.D Thesis, Department of Chemical Engineering, Indian institute of technology, Roorkee, 2006

Technologies and Costs for Removal of Arsenic from Drinking Water, United States Environmental Protection Agency, Office of Water, 4606 (2000).

Tripathy SS, Raichur AM, Enhanced adsorption capacity of activated alumina by impregnation with alum for removal of As(V) from water, Chemical Engineering Journal, 138, 179–186 (2008).

Vaughan Jr. RL, Reed BE, Modeling As(V) removal by iron oxide impregnated activated carbon using the surface complexation approach, Water Research, 39, 1005–1014 (2005).

Vermeulen T, Theory for irreversible and constant pattern solid diffusion, Industrial Engineering and Chemistry research, 45(8), 1664-1670 (1953).

Wang J, Wang T, Burken JG, Chusuei CC, Ban H, Ladwig K, Huang CP, Adsorption of arsenic(V) onto fly ash: A speciation-based approach, Chemosphere, 72, 381–388 (2008).

Weber WJ Jr., Morris JC, Kinetics of adsorption on carbon from solution, Journal of Sanit Engineering. Div. ASCE, 89 (SA2), 31-59 (1963).

Zhang W, Singh P, Paling E, Delides S, Arsenic removal from contaminated water by natural iron ores, Minerals Engineering, 17, 517–524 (2004).

WEBSITES CITED

1. Safe Drinking Water, UNICEF report, http://www.unicef.org/specialsession/about/sgreport.pdf/03_SafeDrinkingWater D7341 Insert_English. pdf, cited on 10th June 10, 2008.
2. http://en.wikipedia.org/wiki/Drinking_water#cite_note-, cited on 19th April 2008.
3. http://en.wikipedia.org/wiki/Water_borne_diseases, cited on 19th April 2008.
4. http://www.niehs.nih.gov/news/events/pastmtg/2006/arsenicland/docs/arsenic_cycle_large.pdf, cited on 19th April 2008.
5. http://en.wikipedia.org/wiki/Arsenic_poisoning, cited on 23rd April 2008.

6. Arsenic in Drinking Water (Free Executive Summary) ISBN:, 330 pages, 6 x 9, (1999)
<http://www.nap.edu/catalog/6444.html>.
7. <http://phys4.harvard.edu/wilson/arsenic-conf.html>. Dt.06th June 2007.
8. http://en.wikipedia.org/wiki/Arsenic#Notable_characteristics, cited on 23rd June, 2008.